



**British
Geological Survey**

NATURAL ENVIRONMENT RESEARCH COUNCIL

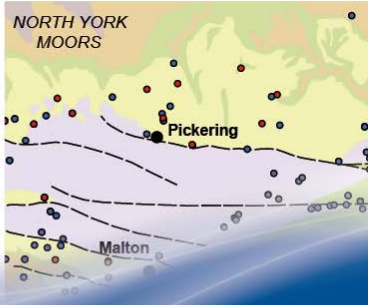


Environmental Baseline Monitoring - Vale of Pickering: Phase I - Final Report (2015/16)

Groundwater Science Programme

Open Report OR/16/002

A BGS led project with the following partners:

- University of Birmingham
- University of Bristol
- University of Liverpool
- The University of Manchester
- University of York (National Centre for Atmospheric Science)
- Public Health England



www.bgs.ac.uk/valeofpickering

Environmental Baseline Monitoring - Vale of Pickering: Phase I - Final Report (2015/16)

The National Grid and other
Ordnance Survey data © Crown
Copyright and database rights
2016. Ordnance Survey Licence
No. 100021290 EUL.

Keywords

Baseline, monitoring, shale gas,
groundwater, water quality,
seismicity, air quality,
greenhouse gases, soil gas,
radon.

Bibliographical reference

R S WARD, G ALLEN, B J
BAPTIE, Z DARAKTCHIEVA, D G
JONES, C J JORDAN, R M PURVIS
AND P L SMEDLEY. 2016.
Environmental Baseline
Monitoring - Vale of Pickering:
Phase I - Final Report (2015/16).
*British Geological Survey Open
Report*, OR/16/002. 96pp.

Copyright in materials derived
from the British Geological
Survey's work is owned by the
Natural Environment Research
Council (NERC) and/or the
authority that commissioned the
work. Copyright in figures
contributed by co-authors is
retained by them. You may not
copy or adapt this publication
without first obtaining
permission. Contact the BGS
Intellectual Property Rights
Section, British Geological
Survey, Keyworth,
e-mail ipr@bgs.ac.uk. You may
quote extracts of a reasonable
length without prior permission,
provided a full acknowledgement
is given of the source of the
extract.

Maps and diagrams in this book
use topography based on
Ordnance Survey mapping.

R S Ward, G Allen, B J Baptie, Z Daraktchieva, D G Jones,
C J Jordan, R M Purvis and P L Smedley

Contributors

J Bearcock, J Bradley, S Burke, A Butcher, F Cigna, R Dunmore,
A Horleston, M Kendall, A Lewis, R Lister, R Lockett, M I Mead,
C Milne, S Nice, J Pitt, A Rietbrock, M Rivett and J Tellam

BRITISH GEOLOGICAL SURVEY

The full range of our publications is available from BGS shops at Nottingham, Edinburgh, London and Cardiff (Welsh publications only) see contact details below or shop online at www.geologyshop.com

The London Information Office also maintains a reference collection of BGS publications, including maps, for consultation.

We publish an annual catalogue of our maps and other publications; this catalogue is available online or from any of the BGS shops.

The British Geological Survey carries out the geological survey of Great Britain and Northern Ireland (the latter as an agency service for the government of Northern Ireland), and of the surrounding continental shelf, as well as basic research projects. It also undertakes programmes of technical aid in geology in developing countries.

The British Geological Survey is a component body of the Natural Environment Research Council.

British Geological Survey offices

BGS Central Enquiries Desk

Tel 0115 936 3143 Fax 0115 936 3276
email enquiries@bgs.ac.uk

Environmental Science Centre, Keyworth, Nottingham NG12 5GG

Tel 0115 936 3241 Fax 0115 936 3488
email sales@bgs.ac.uk

Murchison House, West Mains Road, Edinburgh EH9 3LA

Tel 0131 667 1000 Fax 0131 668 2683
email scotsales@bgs.ac.uk

Natural History Museum, Cromwell Road, London SW7 5BD

Tel 020 7589 4090 Fax 020 7584 8270
Tel 020 7942 5344/45 email bgslondon@bgs.ac.uk

Columbus House, Greenmeadow Springs, Tongwynlais, Cardiff CF15 7NE

Tel 029 2052 1962 Fax 029 2052 1963

Maclean Building, Crowmarsh Gifford, Wallingford OX10 8BB

Tel 01491 838800 Fax 01491 692345

Geological Survey of Northern Ireland, Colby House, Stranmillis Court, Belfast BT9 5BF

Tel 028 9038 8462 Fax 028 9038 8461

www.bgs.ac.uk/gsni/

Parent Body

Natural Environment Research Council, Polaris House, North Star Avenue, Swindon SN2 1EU

Tel 01793 411500 Fax 01793 411501

www.nerc.ac.uk

Website www.bgs.ac.uk

Shop online at www.geologyshop.com

Foreword

This report presents the collated results from the BGS-led project *Science-based environmental baseline monitoring associated with shale gas development in the Vale of Pickering (including supplementary air quality monitoring in Lancashire)*. The project has been funded by a grant awarded by DECC for the period August 2015 – 31st March 2016. It complements (and extends to air quality) an on-going project, funded by BGS and the other project partners, in which similar activities are being carried out in the Fylde area of Lancashire.

The project has initiated a wide-ranging environmental baseline monitoring programme that includes water quality (groundwater and surface water), seismicity, ground motion, atmospheric composition (greenhouse gases and air quality), soil gas and radon in air (indoors and outdoors). The motivation behind the project(s) was to establish independent monitoring in the area around the proposed shale gas hydraulic fracturing sites in the Vale of Pickering, North Yorkshire (Third Energy) and in Lancashire (Cuadrilla) before any shale gas operations take place.

As part of the project, instrumentation has been deployed to measure, in real-time or near real-time, a range of environmental variables (water quality, seismicity, atmospheric composition). These data are being displayed on the project's web site (www.bgs.ac.uk/Valeofpickering). Additional survey, sampling and monitoring has also been carried out through a co-ordinated programme of fieldwork and laboratory analysis, which has included installation of new monitoring infrastructure, to allow compilation of one of the most comprehensive environmental datasets in the UK.

It is generally recognised that at least 12 months of baseline data are required. The duration of the grant award (7 months) has meant that this has not yet been possible. However there are already some very important findings emerging from the limited datasets which need be taken in to account when developing future monitoring strategy, policy and regulation. The information is not only relevant to the Vale of Pickering and Lancashire but will be more widely applicable in the UK and internationally. Although shale gas operations in other parts of the world are well-established there is a paucity of good baseline data and effective guidance on monitoring.

It is hoped that the monitoring project will continue to allow at least 12 months of data for each of the work packages to be compiled and analysed. It will also allow the experience gained and the scientifically-robust findings to be used to develop and establish effective environmental monitoring strategies for shale gas and similar industrial activities.

Acknowledgements

This project has been made possible following the award of a grant by the Secretary of State for Energy and Climate Change (DECC) and the financial and in-kind contributions from the project partners for the complementary Lancashire project (British Geological Survey (BGS); Universities of Birmingham, Bristol, Liverpool, Manchester, York; National Centre for Atmospheric Science (NCAS); Public Health England (PHE)).

A large number of people have been involved in delivering different aspects of the monitoring project both associated with the individual research organisations and also outside. Without this support the project would not have been as successful as it has been. In particular we would like to thank Chris Luton, Jackie Swift, Sheryl White, Martin Brown, Gemma Nash, Humphrey Wallace and Jan Wraith.

We would also like to thank the local communities in both Lancashire and the Vale of Pickering for their co-operation and the land owners who are allowing access to their boreholes for sampling and/or installation of monitoring equipment. We would also like to thank Third Energy and Cuadrilla for allowing access to their sites for independent sampling and measurement, and also in the provision of information.

Contents

Foreword	i
Acknowledgements	ii
Contents	iii
1 Introduction	1
2 Monitoring results	4
2.1 Water monitoring.....	4
2.2 Seismic monitoring.....	18
2.3 Ground Motion – analysis of satellite (InSAR) data.....	27
2.4 Atmospheric Composition.....	33
2.5 Soil gases.....	67
2.6 Radon monitoring.....	78

FIGURES

Figure 1. Superficial geology of the Vale of Pickering, including cross sections (bedrock constitutes Amphill & Kimmeridge Clay; courtesy J Ford, BGS 2016).....	4
Figure 2. Geological model of the Corallian Group strata in the Vale of Pickering showing location of boreholes used in construction of the model (yellow) and importance of faulting (Newell et al., 2016).....	5
Figure 3. Simplified geological map of the Vale of Pickering showing water points (groundwater, streams) in the monitoring network and locations of drill sites.	7
Figure 4. Box plots showing the inorganic chemistry of groundwater from the a) Quaternary aquifer, b) Corallian aquifer and c) streams.	8
Figure 5. Distributions of NO ₃ , SO ₄ and CH ₄ in groundwater from the Vale of Pickering (fourth sampling round).....	9
Figure 6. Representative distributions of organic compounds in groundwater determined by GC-MS and LC-MS screening.	11
Figure 7. Representative distributions of organic compounds in streams determined by GC-MS and LC-MS screening.	12
Figure 8. Time-series plots for selected parameters measured from groundwater in the Quaternary superficial aquifer (September 2015 to February 2016).....	13
Figure 9. Time-series plots for selected parameters measured from groundwater in the Corallian aquifer (September 2015 to February 2016).....	14
Figure 10. Time-series plots for selected parameters measured in streams (September 2015 to February 2016).....	15
Figure 11. Location of surface and borehole seismometers and geophones across the Vale of Pickering. © Crown Copyright and/or database right 2016. Licence number 100021290 EUL.....	18
Figure 12. PDFs for five of the monitoring stations installed around Kirby Misperton and the permanent BGS station, GDLE, in the North Yorkshire Moors.....	19

Figure 13. Modelled detection capability for the surface network of sensors around the KM8 site (red star), showing the spatial variation in magnitudes that can be detected.	20
Figure 14. Modelled detection capability for seismic monitoring including borehole sensors (triangles). Contours represent event detection magnitude.	21
Figure 16. Seismic events detected by the Vale of Pickering stations and permanent BGS monitoring stations in the north east of England from 1/10/2015 to 31/3/2016. Diagonal crosses show earthquakes. Square crosses show events of a suspected explosive origin, e.g. quarry blasts. © Crown Copyright and/or database right 2016. Licence number 100021290 EUL.	22
Figure 15. Recordings of a magnitude 1.7 ML earthquake near Worksop, Nottinghamshire at stations in the Vale of Pickering, along with the recording at station HPK just north of Leeds.	22
Figure 17. Recorded ground motions from a magnitude 7.5 earthquake in the Hindu Kush at 09:09 on 26/10/2015 measured at stations in the Vale of Pickering and the permanent BGS monitoring station GDLE. The dashed lines mark the arrival times of various seismic waves that have propagated along different paths through the Earth.	23
Figure 18. Historical and instrumentally recorded earthquakes (grey circles) from the BGS earthquake catalogue within a 100 km by 100 km square centred on the Kirby Misperton 8 well from. The symbols are scaled by magnitude. © Crown Copyright and/or database right 2016. Licence number 100021290 EUL.	24
Figure 19. The seismic source zone for mainland Britain Ireland (large polygon) and used to estimate average earthquake activity rate. The red shaded areas show the Vale of Pickering study area.	25
Figure 20. InSAR SBAS (top) and ISBAS (bottom) analysis of ERS-1/2 satellite imagery (1992-2000) for the Vale of Pickering. Radar data supplied to BGS by ESA under grant id.31573. Contains Ordnance Data © Crown Copyright and database rights 2016. Licence number 100021290 EUL.	29
Figure 21. InSAR SBAS (top) and ISBAS (bottom) analysis of ENVISAT satellite imagery (2002-2009) for the Vale of Pickering. Contains Ordnance Data © Crown Copyright and database rights 2016. Licence number 100021290 EUL.	31
Figure 22. Top panels: left: Little Plumpton measurement site, right: location of the measurement site and proposed Cuadrilla site close to Little Plumpton. Bottom panels: left, measurement site within the Kirby Misperton Third Energy Site, right: location of the measurement site. © University of Manchester, 2016.	33
Figure 23. Wind rose for the LP site showing wind speed and direction statistics for the period November 2014 – March 2015. The radius defines the percentage of total time in each of 12 wind direction cones (30 degree span), while the colour scale defines the wind speed (redder colours indicating strong wind speeds > 6 ms ⁻¹ and yellow colours indicating light or stagnant winds. © University of Manchester, 2016.	37
Figure 24. 5-day airmass history surface footprint statistics for the period 13 Jan 2016 to 15 March 2016, as seen from the LP site for an Atlantic scale (left panel - at a spatial resolution of 1 x 1 degree) and the UK National scale (right panel - at a spatial resolution of 0.25x0.25 degree). Frequency refers to the fraction of the total trajectories passing over each grid cell. © University of Manchester, 2016.	39
Figure 25. Time series of carbon dioxide (grey) and methane (red) in units of ppm as measured at LP between 4 Dec 2014 and 15 Feb 2016. © University of Manchester, 2016.	40

Figure 26. Greenhouse gas concentrations (as per colour scale) in air as a function of wind direction for: left panel - methane (units of ppm), and right panel - carbon dioxide (units of ppm) as measured at LP. © University of Manchester, 2016.	41
Figure 27. Carbon dioxide concentration time series, colour-coded for wind direction as per legend as measured at LP. © University of Manchester, 2016.....	41
Figure 28. Correlation between CO ₂ and CH ₄ concentrations measured at LP. Colours indicate the density of sampling (number of coincident measurements). One count refers to a one-hour period of data. © University of Manchester, 2016.....	42
Figure 29. Polar bivariate representation of methane (left) and carbon dioxide (right) as a function of wind direction. The colour scale indicates fraction of total measurement time weighted for concentration. See text for further details. ©University of Manchester, 2016.....	43
Figure 30. Mobile vehicle survey of methane concentrations around the local area of the LP site on March 9th 2016. Local features such as landfill, agriculture and sewage installations are marked on the map as per legend. © Royal Holloway Univ London, 2016.	44
Figure 31. Keeling plot of carbon-13 (in methane) depletion for local sources of methane measured around the LP site as measured by mobile vehicle surveys on 9th and 10th March 2016. © Royal Holloway Univ London, 2016.	45
Figure 32. Time series for air quality trace gas concentration data at the LP site. © Univ York, NCAS, 2016.....	47
Figure 33. Diurnal variations for the air quality measurements at LP. © Univ York, NCAS, 2016.	48
Figure 34. Hebdomadal variations for the air quality measurements at LP. © Univ York, NCAS, 2016.	49
Figure 35. Polar plots for NO, NO ₂ , NO _x , O ₃ , PM _{2.5} , PM ₁₀ at the LP site. © Univ York, NCAS, 2016.....	50
Figure 36. Wind rose for the LP site showing wind speed and direction statistics for the period January 2016 – 10 March 2016. The radius defines the percentage of total time in each of 12 wind direction cones (30 degree span), while the colour scale defines the wind speed (redder colours indicating strong wind speeds > 6 ms ⁻¹ and yellow colours indicating light or stagnant winds. © University of Manchester, 2016.....	52
Figure 37. Temperature and Air Pressure time series for the KM site. © University of Manchester, 2016.....	52
Figure 38. 5-day airmass history surface footprint statistics for the period 13 Jan 2016 to 15 March 2016, as seen from the KM site for an Atlantic scale (left panel - at a spatial resolution of 1 x 1 degree) and the UK National scale (right panel - at a spatial resolution of 0.25x0.25 degree). Frequency refers to the fraction of the total trajectories passing over each latitude-longitude grid cell. © Univ Manchester, 2016	53
Figure 39. Time series of methane (red) and carbon dioxide (grey) concentration in air measured at KM. Units are parts per million (ppm). © Univ Manchester, 2017	54
Figure 40. Greenhouse gas concentrations (as per colour scale) in air as a function of wind direction for: left panel - methane (units of ppm), and right panel - carbon dioxide (units of ppm), as measured at KM. © Univ Manchester, 2017	54
Figure 41. Correlation between CO ₂ and CH ₄ concentrations measured at KM. Colours indicate the density of sampling (number of coincident measurements). One count refers to a one-hour period of data. © Univ Manchester, 2017	55

Figure 42. Time series for the current set of air quality measurements at the KM site. © Univ York, NCAS, 2016.	57
Figure 43. Diurnal cycles for Ozone, NO, NO ₂ , NO _x at the KM site. © Univ York, NCAS, 2016.	58
Figure 44. Hebdomadal cycles for O ₃ and NO _x at KM.....	59
Figure 45. Polar plots for NO, NO ₂ , NO _x , O ₃ , PM _{2.5} , PM ₁₀ at the KM site. © Univ York, NCAS, 2016.....	59
Figure 46. NMHCS for KM weighted by mean to for every WAS collected. © Univ York, NCAS, 2016.....	60
Figure 47. Box and whisker plot showing the variance in the NMHC measurements at KM. © Univ York, NCAS, 2016.	61
Figure 48. Carbon dioxide (top panel) and methane (bottom panel) concentrations at the LP site (red) and KM site (grey) for the period of simultaneous measurement between 10 Jan and 9 Mar 2016. © Univ Manchester, 2016.	62
Figure 49. Methane temporal cycles at KM (blue) and LP (pink) by time of day and day of week (top panel), hour of day (bottom left), month of year (bottom centre), day of week (bottom right). In each case, the thick centre line denotes the mean concentration while the semi-transparent shadowed area represents the one standard deviation range of the mean. © Univ Manchester, 2016.	63
Figure 50. Carbon dioxide temporal cycles at KM (blue) and LP (pink) by time of day and day of week (top panel), hour of day (bottom left), month of year (bottom centre), day of week (bottom right). In each case, the thick centre line denotes the mean concentration while the semi-transparent shadowed area represents the one standard deviation range of the mean. © Univ Manchester, 2016.....	64
Figure 51. Wind rose for the High Muffles AURN site. © Univ Manchester, 2016.	65
Figure 52. Polar plots for O ₃ , NO and NO ₂ for the High Muffles AURN site. © Univ York, NCAS, 2016.....	66
Figure 53 Soil gas measurement.	68
Figure 54 Soil gas study area to the east of Kirby Misperton within the red circle.	69
Figure 55. Normal probability plot of soil gas CO ₂ data from the Vale of Pickering.	70
Figure 56. Plot of the concentration of CO ₂ in soil gas in the Vale of Pickering, November 2015.	70
Figure 57. Plot of the flux of CO ₂ from the soil in the Vale of Pickering, November 2015.	71
Figure 58. Plot of CO ₂ versus O ₂ for November 2015 soil gas data. Lines show the trends for deep leakage of CO ₂ , biogenic CO ₂ (plant and microbial respiration) and CO ₂ produced by methane oxidation. Dissolution of CO ₂ in soil pore water, and reaction with any carbonate present moves points away from the trend lines in the direction of the arrow.	72
Figure 59. Plot of CO ₂ versus Balance (mostly N ₂ and some Ar) for November 2015 soil gas data. Lines show the trends for deep leakage of CO ₂ , biogenic CO ₂ (plant and microbial respiration) and CO ₂ produced by methane oxidation. Dissolution of CO ₂ in soil pore water, and reaction with any carbonate present moves points away from the trend lines in the direction of the arrow.	72
Figure 60. Comparative box and whisker plots for soil gas CO ₂ and CO ₂ flux between the two farms in the study area, November 2015.	73
Figure 61. Comparative box and whisker plots for soil gas CO ₂ and CO ₂ flux with different land use for the two farms in the study area, November 2015.	73

Figure 62. (a). Measurement of CO ₂ and CH ₄ flux and (b). Very wet ground conditions in March 2016.	74
Figure 63. Plot of the flux of CO ₂ from the soil in the Vale of Pickering, March 2016.	74
Figure 64. Comparative box and whisker plots of CO ₂ flux at the same sites visited in November 2015 and March 2016.	75
Figure 65. Preliminary calculated CO ₂ concentrations and fluxes from initial Lancashire eddy covariance data (15 minute averaged processed data from original 10Hz observations).75	
Figure 66. CO ₂ concentrations plotted with temperature. Note that CO ₂ concentrations tend to be inversely proportional to temperature, except during brief periods of rapid heating.76	
Figure 67. CO ₂ concentrations plotted against wind speed. The tailing off of CO ₂ concentration at higher wind speeds is indicative of the baseline mixing ratio of the boundary layer (blue line).	76
Figure 68. Outdoor radon sampling points in the Vale of Pickering. © PHE, 2016.	79
Figure 69. Average radon concentrations at the sampling points around Yedingham, Kirby Misperton and Pickering. © PHE, 2016.	80
Figure 70. Average radon concentrations at the sampling points in the Vale of White Horse, Oxfordshire. © PHE, 2016.	81
Figure 71. Radon potential in the Vale of Pickering. © PHE, 2016.	81
Figure 72. Indoor radon concentrations in the area of Kirby Misperton and Little Barugh. © PHE, 2016.	83

TABLES

Table 1. Work Packages and partner roles.	2
Table 2. Analyses of InSAR processing for the Vale of Pickering.	27
Table 3. Measurements at both sites, dates when measurements became active, and measurement frequency (as streamed via the cloud). Note that NMHC refers to non-methane hydrocarbons and PM refers to particulate matter.	35
Table 4. Detailed descriptions of the QA / QC for data collected at both KM and LP measurement sites.	35
Table 5. Carbon-13 (in methane) depletion measurements and uncertainty statistics (mean and 2 standard deviation uncertainty) for local methane sources around the LP site from mobile surveys on 9 March and 10 March 2016.	45
Table 6. Statistical metrics for greenhouse gases measured at LP. Percentages represent percentile thresholds.	46
Table 7. Statistical metrics for air quality pollutants measured at LP. Percentages represent percentile thresholds. Note that LOD refers to a measurement below the instrumental detection limit.	46
Table 8. Statistical metrics for greenhouse gas concentrations measured at KM. Percentages refer to percentiles (to 2 d.p).	55
Table 9. Statistical metrics for air quality pollutants measured at KM. Percentages refer to percentiles. LOD refers to measurements below the limit of detection of the instrument.	56

Table 10. Statistical air quality metrics for the HM, KM and LP measurement sites. 64

Table 11. Range and distribution of indoor radon measurements. 84

1 Introduction

The Environmental Baseline Monitoring Project - *Science-based environmental baseline monitoring associated with shale gas development in the Vale of Pickering (including supplementary air quality monitoring in Lancashire* – to which this report relates, was initiated in August 2015 following the award of a grant by the Secretary of State for Energy and Climate Change (DECC). The grant has allowed similar on-going monitoring activities in Lancashire (initiated in early 2015) to be extended to a new area of the country, the Vale of Pickering, and add some additional air quality monitoring to the Lancashire programme. The two areas were chosen as they currently have planning applications being considered for hydraulic fracturing associated with shale gas development. At the time of preparation of this report neither planning application had been determined, so without any development there was opportunity to acquire baseline information.

It is widely recognised that there is a need for good environmental baseline data ahead of any shale gas/oil development to enable future changes that may occur as a result of industrial activity to be identified. Continued monitoring would then enable any deviations from the baseline, if they were to occur, to be identified and investigated independently to determine the possible causes and significance to the environment and public health. The absence of baseline data in the US has led to major controversy and inability to identify and effectively deal with impact/contamination where it has occurred. There are a growing number of cases being reported where the absence of a baseline has led to the need for extremely costly investigations and court cases.

Recent scientific and other commissioned studies have also highlighted that credible and transparent monitoring is key to gaining public acceptance and providing the evidence base to demonstrate the industry's impact on the environment and importantly on public health. As a result BGS initiated, in early 2015, a co-ordinated programme of environmental monitoring in the Fylde, Lancashire around two proposed shale gas production sites at Roseacre Wood and Preston New Road (Cuadrilla). Following the successful initiation of this project BGS and its partners were invited by DECC to develop a proposal for extending this work to the Vale of Pickering around Kirby Misperton (Third Energy). This report presents the results of the DECC grant-funded work and the initial interpretation of these data.

The overarching objective of this project is to establish an independent environmental monitoring programme to characterise baseline conditions across the Vale of Pickering (and immediate surrounds) in Yorkshire and to extend the monitoring programme in the Fylde area of Lancashire to include air quality. The programme includes monitoring/measurement of: water quality (groundwater and surface water), seismicity, ground motion, atmospheric composition (greenhouse gases and air quality), soil gas and radon in air (indoors and outdoors). The outcomes of the monitoring will allow:

- Improved public understanding of environmental baselines and their importance in relation to shale gas activities;
- Regulators and industry to better define their monitoring strategies and protocols, establish good practice for the UK onshore hydrocarbon industry and provide independent data for verification purposes;
- Improved scientific understanding of the sub-surface and near-surface environments in the UK context for unconventional hydrocarbons (UK conditions are significantly different from those in the USA and Canada).

The collaborative monitoring programme described in this report is led by BGS in partnership with a number of internationally recognised scientists/researchers. The project comprises six scientific work packages as shown in Table 1. The project executive is Professor Rob Ward, Director of Science, BGS.

Table 1. Work Packages and partner roles.

Work Package (WP)	WP Lead	WP Partners
1. Water	BGS (Dr Pauline Smedley)	University of Birmingham (Prof John Tellam/Dr Mike Rivett)
2. Seismicity	BGS (Dr Brian Baptie)	University of Bristol (Prof Mike Kendall) University of Liverpool (Prof Andreas Rietbrock)
3. Atmospheric Composition	University of Manchester (Dr Grant Allen)	NERC - National Centre for Atmospheric Science (NCAS)/University of York (Prof Alistair Lewis/Dr Ruth Purvis)
4. Ground Motion	BGS (Dr Colm Jordan)	
5. Soil Gas	BGS (Dr David Jones)	
6. Radon	Public Health England (PHE) (Dr Zornitza Daraktchieva)	

The considerable progress made by this extremely ambitious project is reported in the following sections. It represents the analysis and interpretation of the most recent available data (to mid-March 2016). Monitoring has continued to the end of the month and these data will be used to update the report and interpretation, and the project web pages, once available and for completeness.

To achieve the level of monitoring activity and analysis reported here, considerable effort has been required over a short period of time to establish the monitoring programme(s). It has involved procurement and commissioning of monitoring equipment, installation of new monitoring infrastructure (e.g. boreholes), and considerable logistics to establish a co-ordinated sample collection, analysis, reporting framework and operation. As the bulk of the infrastructure installation and monitoring has been carried out during the winter months, a period during which there was severe wet weather and extensive flooding, a number of difficulties were encountered. These mostly related to access to land for sampling and delays to various installation activities. Despite this, all planned infrastructure has been installed and an extensive monitoring dataset, which includes results from all work packages, has been acquired.

The results are already indicating some highly relevant and scientifically interesting findings. For groundwater and surface water, results indicate impact, albeit at generally low

levels, from anthropogenic activities with pesticides, plasticisers, poly aromatic hydrocarbons (PAHs) and pharmaceuticals all detected. Significantly elevated concentrations of methane in groundwater have also been detected at a number of monitoring points across the Vale, including in some of the newly drilled boreholes. Further work is needed to identify the source of the methane but initial indications suggest that it is geogenic in origin but not associated with the presence of current or abandoned hydrocarbon wells in the area.

Installation of a network of seismic monitoring stations including four into some of the newly-drilled boreholes has significantly improved the earthquake detection capability in the area. No events have been detected in the immediate locality of the Vale of Pickering; however, 31 earthquakes and around 45 quarry blasts from elsewhere have been detected during the project period. The largest of these was a magnitude 2.2 ML earthquake south of Worksop, Nottinghamshire. The monitoring array has also picked up significant earthquakes occurring elsewhere in the world.

Analysis of satellite data to calculate ground motion indicates that the majority of the area around the Vale of Pickering is stable but that there are discrete areas of subsidence and uplift. The subsidence appears to be due to both anthropogenic factors (coal mining) and natural factors (compressible peat sediments), while the zone of uplift is related to cessation of water extraction when mining ceased.

The results for the air quality monitoring also include measurements made in Lancashire as well as the Vale of Pickering as the DECC grant award also included funding for these activities. In Lancashire and the Vale of Pickering the greenhouse gas and air quality concentrations are currently within the typical range for a UK semi-rural environment. Some variation is observed in relation to the prevailing wind direction with local (landfill, agriculture and nearby roads) and regional (urban centre) greenhouse-gas-enhanced airmasses observed when winds are from the direction(s) of these various emission sources.

The soil gas monitoring was severely hampered by saturated ground conditions. Despite several attempts, only a limited dataset was acquired. Analysis of the data available appears to indicate no correlation between soil gas concentration/flux and proximity to geological faults and/or locations at which high concentrations of methane in groundwater had been recorded. However the ground conditions over the winter would significantly inhibit upward migration of any gases into the soil zone and so no conclusions should yet be inferred from the data.

A very successful campaign has resulted in 145 households agreeing to participate in the radon study. The first sets of results for both indoor and outdoor radon are presented and indicate that in both cases are consistent with concentrations expected elsewhere in the UK with similar radon potentials. This included a small number of homes in the radon affected areas (Malton and Pickering) that were found to be at or above the Radon Action Level.

2 Monitoring results

2.1 WATER MONITORING

2.1.1 Introduction

The objective of the water monitoring work package has been to characterise the aquifers of the Vale of Pickering and establish the baseline chemistry of water in and around the proposed shale-gas exploration site at KM8. This allows the assessment of any changes in water quality that may occur as a result of subsequent activities related to exploration and/or production, should planning permission be granted. In order to provide a robust baseline for water quality, activities have involved:

- assessment of the geology and hydrogeology of aquifers in the area around KM8, including 3D geological modelling to understand the extent and character of the aquifers;
- establishment of a network of sites for monitoring of water from existing boreholes and streams (also including new water boreholes from the hydrocarbon operator);
- drilling new boreholes at strategic locations to establish new monitoring sites and

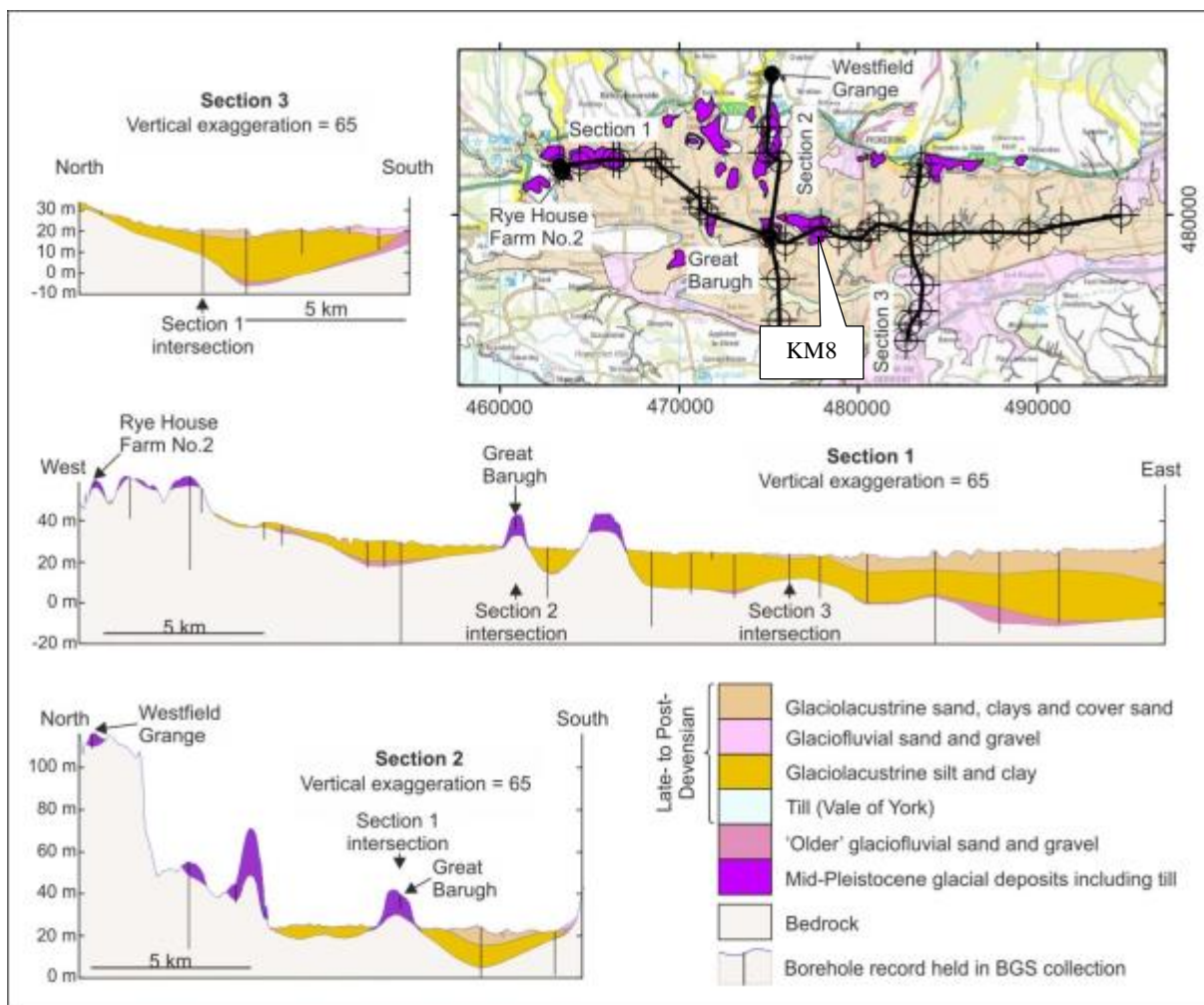


Figure 1. Superficial geology of the Vale of Pickering, including cross sections (bedrock constitutes Ampthill & Kimmeridge Clay; courtesy J Ford, BGS 2016)

instigate real-time monitoring of water level and quality;

- collection, analysis, collation and evaluation of water monitoring data;
- reporting including display of summary results and real-time data on the BGS website.

These activities have been carried out over the seven-month period of the project.

2.1.2 Geological and hydrogeological characterisation

The Vale of Pickering has two main aquifers, the distributions, structure and hydrogeological properties of which have been assessed and described in detail for this project by Ford et al. (2015) and Newell et al. (2016). A covering layer of Quaternary superficial sediments, of mainly glaciolacustrine but also glaciofluvial origin, forms a

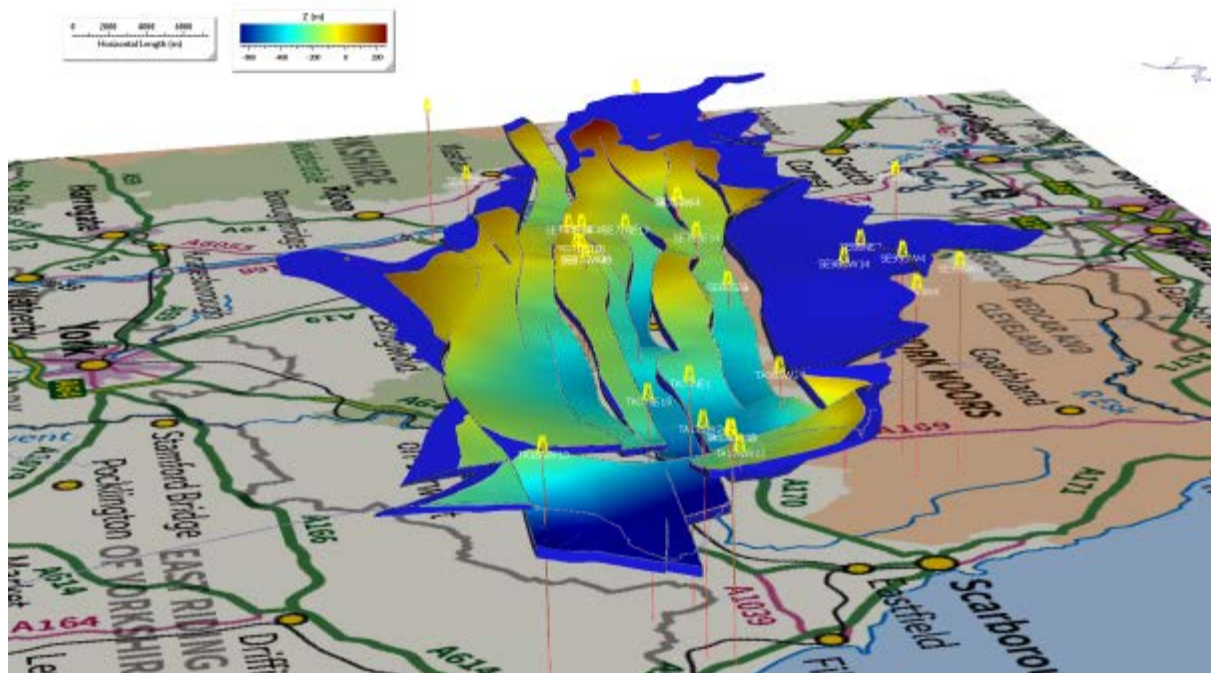


Figure 2. Geological model of the Corallian Group strata in the Vale of Pickering showing location of boreholes used in construction of the model (yellow) and importance of faulting (Newell et al., 2016)

shallow aquifer. Borehole records show that these sediments have variable thickness, typically less than 40 m thick, but are relatively thin or absent in the north and western part of the Vale, and close to KM8 (Figure 1). In the vicinity of KM8 and on the northern flanks of the Vale, discontinuous caps of glacial till occur which form local topographic features and which influence regional shallow groundwater flow in the surrounding more permeable sediments but are unlikely to contain groundwater themselves. Ford et al. (2015) also identified an increased abundance of relatively permeable horizons within the Quaternary superficial deposits along the margins of the Vale. This is consistent with the occurrence of marginal fan deposits. Numerous discontinuous lenses of sand/gravel appear elsewhere throughout the Quaternary profile. The Quaternary superficial aquifer provides small-scale private water supplies to properties within the Vale.

Limestones of the Corallian Group constitute a second important aquifer in the region. This is defined as a Principal aquifer and provides a source of water for public, private supply and industry, though is only exploited along the margins of the Vale (shown in blue on Figure 2). Within the centre of the Vale, the Corallian Limestone is not used as a water resource,

presumably because of its depth (typically 200 m+ in the central area) and likely variable salinity.

A further Principal aquifer, the Chalk, occurs in North Yorkshire, though to the south-east of the Vale of Pickering at some 10 km or more from the KM8 site. The northern escarpment of the Chalk forms an unconfined aquifer which sustains a number of private water supplies.

Our investigations have shown that, despite the dominantly argillaceous (fine-grained) nature of the deposits of the Amphill & Kimmeridge Clay which underlies the Quaternary superficial aquifer, the clays also contain sandy horizons. These can sustain small-scale private water supplies locally. In the vicinity of KM8, groundwater from shallow boreholes derives at least in part from Amphill & Kimmeridge sediments.

Investigations of the deeper geology of the Vale of Pickering have focussed on the post-Permian structure and 3D modelling from available seismic and borehole log data (Newell et al., 2016). The modelling has provided support for a strong structural control on spatial distribution of the Corallian aquifer and adjacent strata and a relative abundance of faults which have dissected the aquifer into numerous blocks. These have a predominant east-west orientation (Figure 2).

2.1.3 Water quality

2.1.3.1 SAMPLE DESIGN AND METHODOLOGY

A network of water monitoring points from existing groundwater sources and strategically located low-order stream sites has been established across the Vale (Smedley et al., 2015) as the basis for establishing a baseline monitoring programme. The design of the monitoring network has been based partially on the hydrogeological and geological data provided by the studies described above. However, paucity of available boreholes in the superficial aquifer in the centre of the Vale has meant that all suitable sites (to the best of our knowledge) have been monitored or at least investigated for suitability. Stream choices reflect a combination of location with respect to KM8 and suitability and safety of site access. Site selection for Corallian boreholes around the periphery of the Vale has been based on geological and hydrogeological data, with a combination of confined and unconfined sites included, and at varying distances from KM8. Most boreholes in the Corallian abstract from the unconfined aquifer, but a few occur at locations where the Corallian is confined by superficial deposits and/or Amphill & Kimmeridge Clay (Figure 3).

The resultant water monitoring network across the Vale of Pickering consists of 24 groundwater sites and 10 stream sites. Additional samples have been collected from the Chalk aquifer on the Wolds to the south-east edge of the Vale, but these are not included in the monitoring network.

The network of water monitoring sites has been sampled monthly since September 2015 and at the time of writing, 6 sets of samples have been collected. Water from each site has been subjected to on-site analysis of unstable parameters (e.g. pH, temperature, dissolved oxygen, redox potential) and samples have been collected for laboratory analysis of major ions, trace elements, dissolved gases (CO₂, methane, ethane), stable isotopes of water and carbon, radon, tracers (CFCs) and a range of organic compounds (hydrocarbons, broad-scan organic screens).

A borehole drilling programme has also been completed for characterisation and real-time monitoring of groundwater at strategic locations within the Vale. Criteria involved in site selection have included proximity to KM8; thickness, distribution and texture of superficial deposits; structure of Mesozoic formations (locations of faults); logistical considerations (flood risk, accessibility, landowner agreements). The drilling programme has produced six pairs of shallow boreholes in the superficial aquifer at depths in the range 10–40 m and two

deep boreholes in the confined Corallian aquifer (depths 190 m+). These sites will be incorporated into the groundwater monitoring network. Seismic monitoring equipment has also been co-located within some of the boreholes (see Section 2.2).

2.1.3.2 INORGANIC COMPOSITIONS

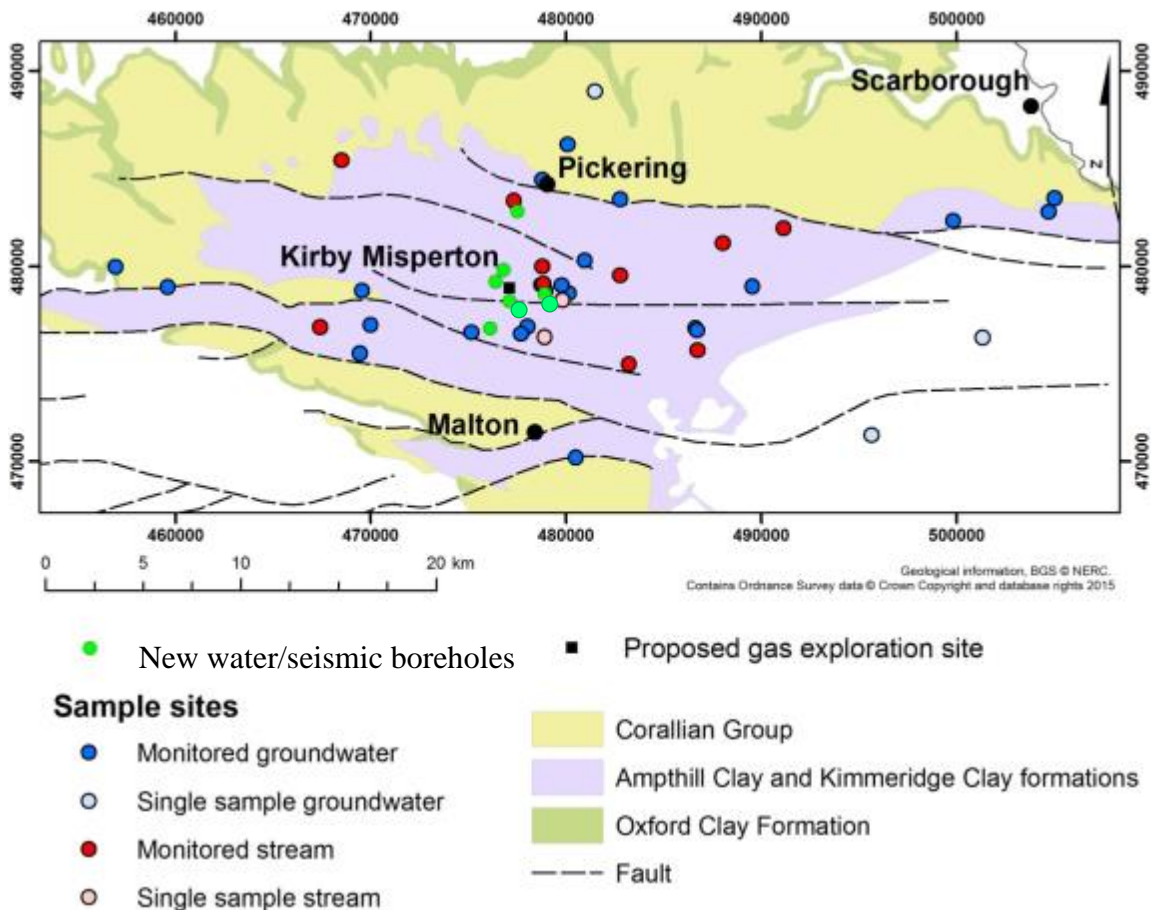


Figure 3. Simplified geological map of the Vale of Pickering showing water points (groundwater, streams) in the monitoring network and locations of drill sites.

Summary results for inorganic constituents are shown as box plots in Figure 4. Major ions and selected minor constituents are given for groundwater samples from the Quaternary superficial aquifer, Corallian aquifer and for stream waters. National standards for inorganic constituents in drinking water, where set, are also shown (red lines).

Results for the Quaternary aquifer (Figure 4a) show the overwhelming anoxic nature of the groundwater with mostly low concentrations of nitrate (NO_3), some low concentrations of sulphate (SO_4) and often relatively high concentrations of iron (Fe) (up to 2.3 mg/L), manganese (Mn) (up to 0.5 mg/L), ammonium (NH_4) (up to 2.2 mg/L as N) and occasionally arsenic (As) (up to 18 $\mu\text{g/L}$). The elevated concentrations arising from the anoxic conditions. High concentrations of dissolved methane (CH_4) are also a natural feature of some groundwaters. These reach up to 26 mg/L though in most boreholes are below 1 mg/L. Some, though not all groundwaters, have relatively high salinity (higher total dissolved solids). Concentrations of Cl reach up to 400 mg/L and Na up to 695 mg/L. Although the groundwater is currently not being used for drinking water supply, some

measurements exceed European drinking-water limits, i.e. for Na, SO₄, Fe, Mn, NH₄ and As, as well as boron (B).

Results for the Corallian aquifer along the margins of the Vale (Figure 4b) show a lower overall salinity (lower concentrations of the dominant ions). Chemistry here is dominated by Ca-HCO₃, as expected for a limestone groundwater. A majority of the groundwaters from the Corallian aquifer is oxic, as indicated by commonly higher concentrations of NO₃, as well as low concentrations of Fe, Mn, As, NH₄ and CH₄. Anoxic groundwater is present

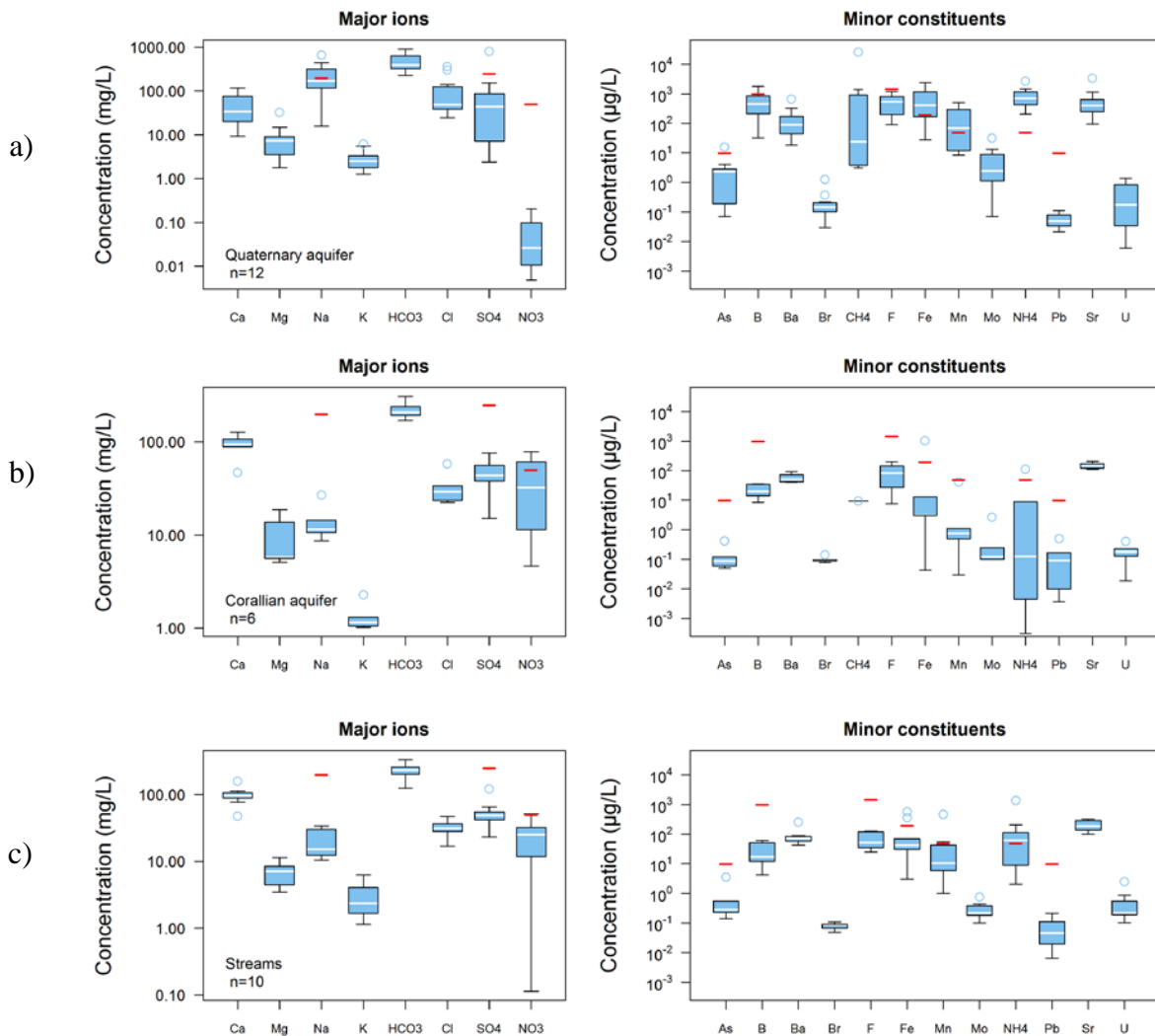


Figure 4. Box plots showing the inorganic chemistry of groundwater from the a) Quaternary aquifer, b) Corallian aquifer and c) streams.

along the edge of the aquifer confined by superficial deposits and/or Amphill & Kimmeridge Clay.

Results for the streamwaters (Figure 4) show the dominance of Ca-HCO₃, the large range in concentrations of NO₃ and relatively large range in NH₄. Most solutes have concentrations below drinking water limits, although the concentrations of NO₃ reach up to 58 mg/L (as NO₃), which is slightly above the limit for NO₃. Dissolved CH₄ was not analysed in streams but is expected to be low.

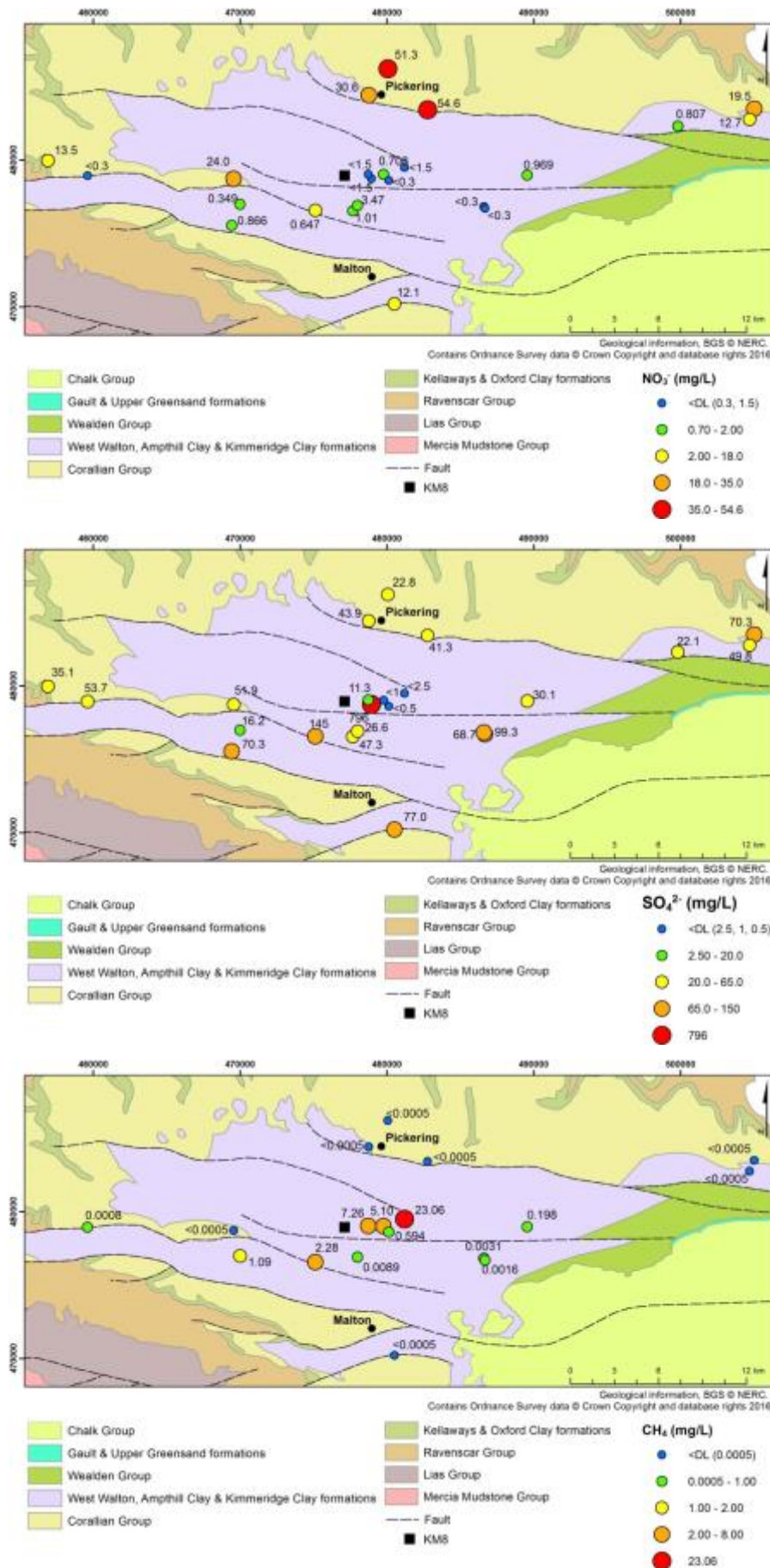


Figure 5. Distributions of NO₃, SO₄ and CH₄ in groundwater from the Vale of Pickering (fourth sampling round).

Groundwater from two samples collected from the unconfined Chalk aquifer to the south-east of the Vale of Pickering (Figure 3) on the first sampling round show compositions typical of water in equilibrium with carbonate rock. Major ions are dominated by Ca-HCO₃ and pH averages around 7. The groundwaters are oxic (DO 10 mg/L) and both contain NO₃ at concentrations above the drinking-water limit (up to 86 mg/L as NO₃). Concentrations of redox-sensitive species (Fe, Mn, SO₄, As) reflect the oxic conditions of the groundwater.

Maps of the distributions of NO₃, SO₄ and CH₄ are shown for the water monitoring network from the fourth monitoring round in Figure 5. These demonstrate that shallow groundwater in the central part of the Vale has low NO₃ concentrations, and usually low concentrations of SO₄. One site in the central part has a recorded high concentration of SO₄ but the analytical method used (ICP-MS) records total sulphur rather than specific sulphate species and so this is concluded to be present as sulphide rather than sulphate. This is supported by the strong smell of hydrogen sulphide degassing from the groundwater.

High concentrations of CH₄ in the groundwaters of the superficial aquifer are also mostly located in the central part of the Vale. Preliminary investigation suggests that no clear correlation exists between the locations of high-CH₄ boreholes and locations of existing or abandoned hydrocarbon boreholes, nor of gas pipelines. This is an important finding and will be investigated in more detail. The association of high CH₄ with low NO₃ and SO₄ in the centrally-located groundwaters indicates the strongly reducing nature of shallow groundwater in this part of the aquifer.

The maps show the distributions of typically higher concentrations of NO₃ in groundwater from the margins of the Vale of Pickering, within the Corallian Limestone aquifer. Concentrations of CH₄ are universally low in these locations, as is consistent with the oxic or mildly reducing nature of the groundwaters from this aquifer.

Analysis and evaluation of data for radon in the groundwaters is ongoing and further validation is needed. However, initial indications are that concentrations of dissolved radon are low, usually <10 Bq/L and often <5 Bq/L. Concentrations at the higher end of the spectrum tend to be from the Corallian aquifer. The range compares with literature values for Rn in groundwater (0.05–11 Bq/L for Inferior and Great Oolite groups; 1–10 Bq/L for Neogene to Quaternary aquifers; DWI, 2015). The activities observed are well below the parametric value of 100 Bq/L proposed by the Drinking Water Inspectorate for radon in drinking water.

The occurrence of radon is pertinent in the context of baseline characterisation as radon and other NORM (natural occurring radioactive materials) may be present at higher concentrations in flowback than in natural shallow groundwater, as it contains a significant proportion of deep formation water. Hence, radon measurements serve not only to identify relative health hazard but also to establish an indicator of any future hydrocarbon-related activities and contamination.

2.1.3.3 ORGANIC COMPOSITIONS

Analyses of dissolved organic carbon (DOC) are of the order of 1–6 mg/L for the Quaternary superficial aquifer (usually at the low end of this range), 0.5–3 mg/L for the Corallian (though usually <1 mg/L) and <3 mg/L for the Chalk aquifer.

Analysis of a range of organic compounds, including hydrocarbons (total aliphatics, total aromatics, BTEX, PAHs, VOCs), carried out on the monthly monitored samples, shows that concentrations were universally at or below detection limits. This applies to samples from

all monitoring rounds. The observations are consistent with baseline conditions in the rural areas sampled.

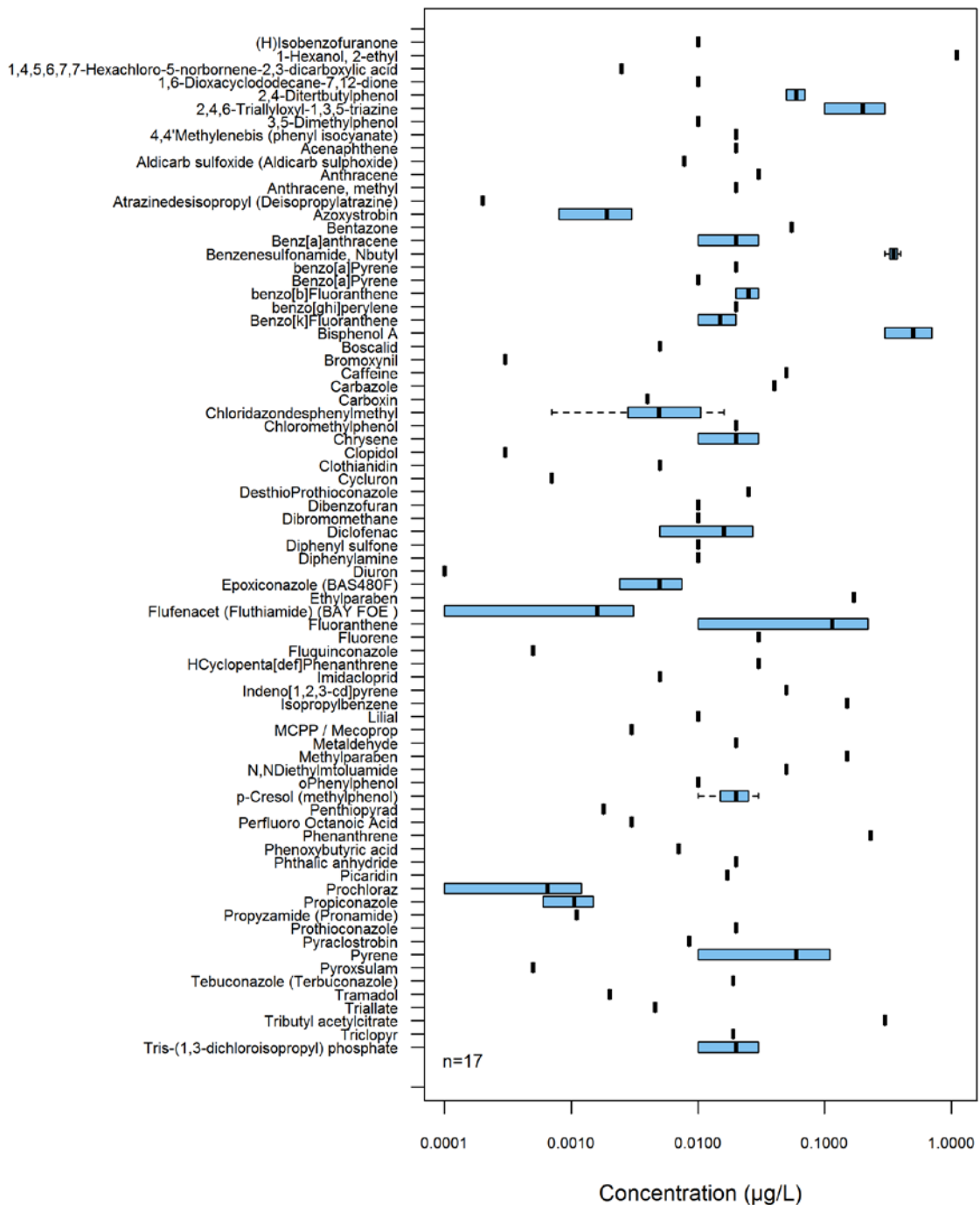


Figure 6. Representative distributions of organic compounds in groundwater determined by GC-MS and LC-MS screening.

Screening of a selection of the water samples has also been carried out for a broad range of organic compounds by gas chromatography-mass spectrometry and/or liquid chromatography-mass spectrometry. The methodology identifies compounds by comparison with a reference library but provides semi-quantitative rather than fully quantitative validated data. Results of the screening for groundwater samples taken in the first sampling round (September 2015) are given in Figure 6. The results for groundwater samples

(Quaternary and Corallian, n=17) show the presence of a number of compounds including plasticisers, pesticides and PAHs, although all were at low concentrations, almost all below 0.1 µg/L.

Results for streams (Figure 7), albeit for only three samples, show the presence of compounds including pesticides (including organophosphates), pharmaceuticals (e.g. ibuprofen) and lifestyle compounds (e.g. caffeine). Concentrations are low however, typically in the 0.001–0.1 µg/L range.

More analyses of broad screens will be carried out in due course to compare with the initial sets of organics data.

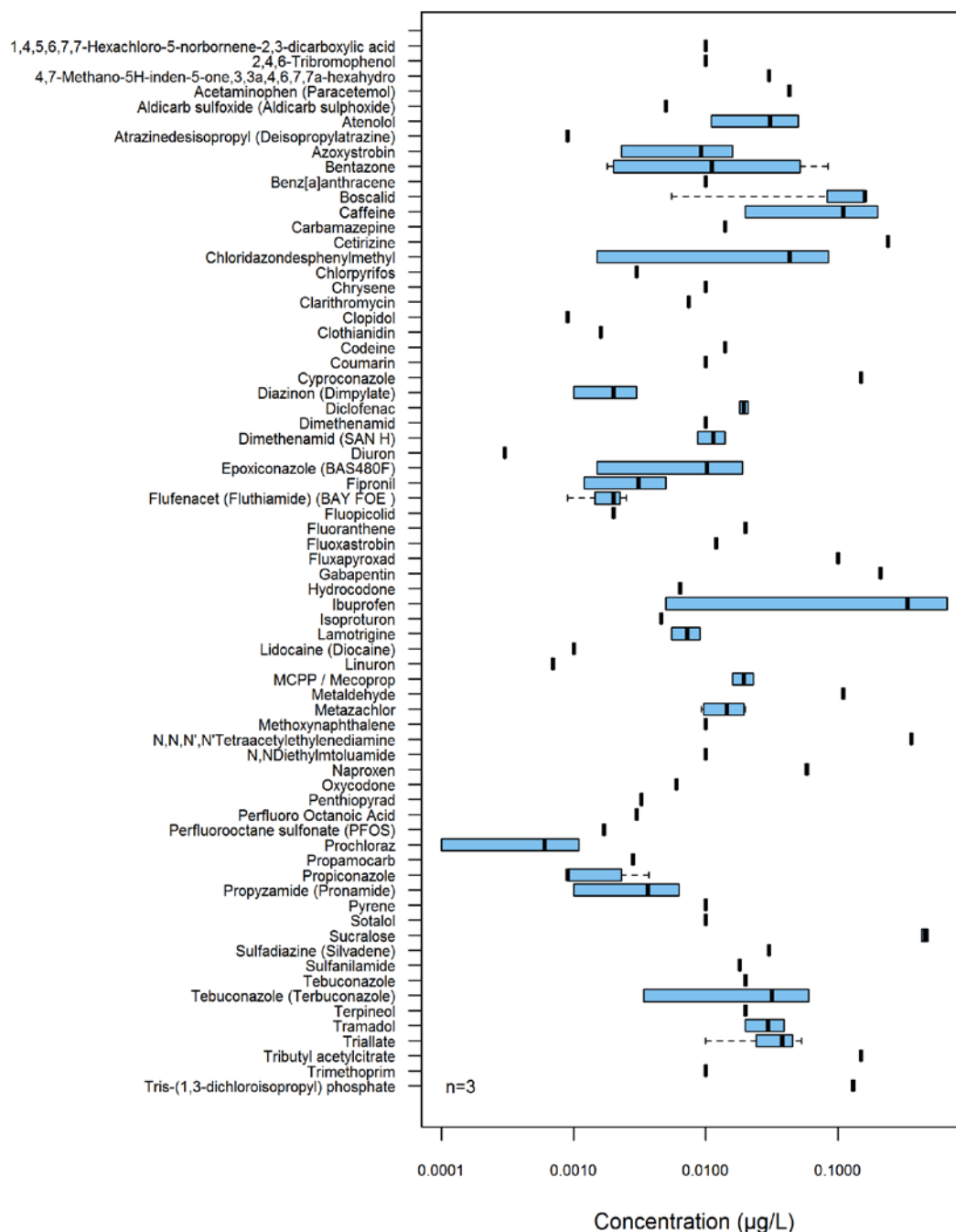


Figure 7. Representative distributions of organic compounds in streams determined by GC-MS and LC-MS screening.

2.1.3.4 WATER MONITORING

Time-series data for the six monthly rounds of water sampling from the Vale are given for the Quaternary aquifer in Figure 8, for the Corallian aquifer in Figure 9 and for the streams

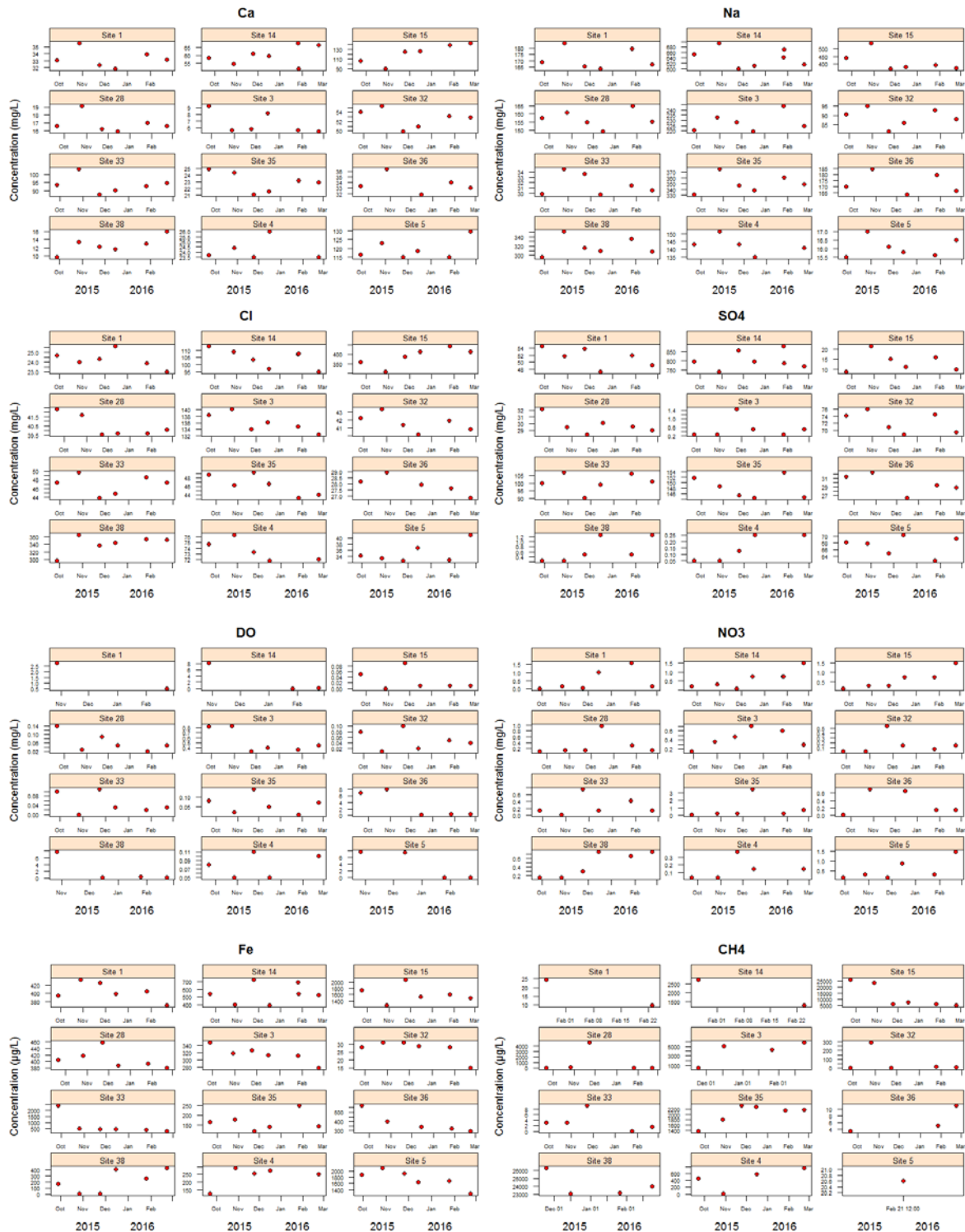


Figure 8. Time-series plots for selected parameters measured from groundwater in the Quaternary superficial aquifer (September 2015 to February 2016).

in Figure 10. Plots are provided for a selection of major ions (Ca, Na, Cl, SO₄) which define the main water-quality characteristics, and for dissolved oxygen (DO), NO₃, Fe and CH₄ which define the redox condition. Not all sites were sampled on all occasions and where missing data exist, this is usually due to site accessibility problems.

The time-series plots show some temporal variability in chemical concentrations. However, for the 12 sites shown from the Quaternary superficial aquifer, 7 sites from the Corallian and 7 sites from the streams, variations are usually small (within about 20%) for all parameters shown. Sampling covers only the autumn and winter months. Further sampling during the

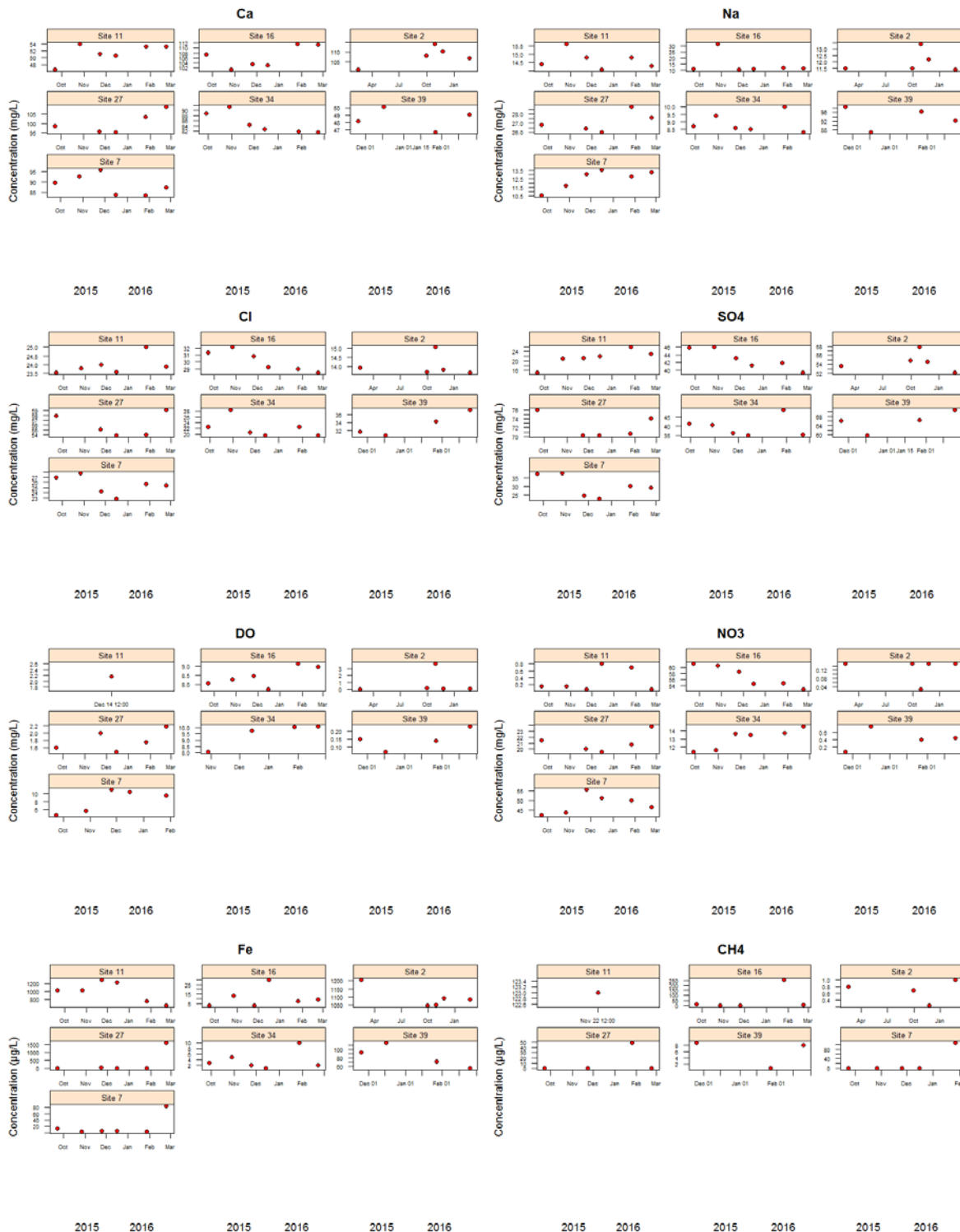


Figure 9. Time-series plots for selected parameters measured from groundwater in the Corallian aquifer (September 2015 to February 2016).

spring and summer months (ongoing) will serve to clarify the variability over an annual cycle. However, data presented so far indicate that the water quality characteristics depicted by the box-plot distributions from one sampling round (Figure 4) is representative of the groundwater in the aquifers and of the streams.

The consistent anoxic conditions in the shallow Quaternary aquifer are seen from the reproducibly high concentrations of methane in the time series. Two sites in the monitoring network (Sites 15, 38; Figure 9) have concentrations of methane above 20 mg/L (up to 26 mg/L) which is below but close to the solubility of CH₄ in water at ambient groundwater temperature (ca. 11°C).

The water quality in the streams shows some variability though with mostly consistent

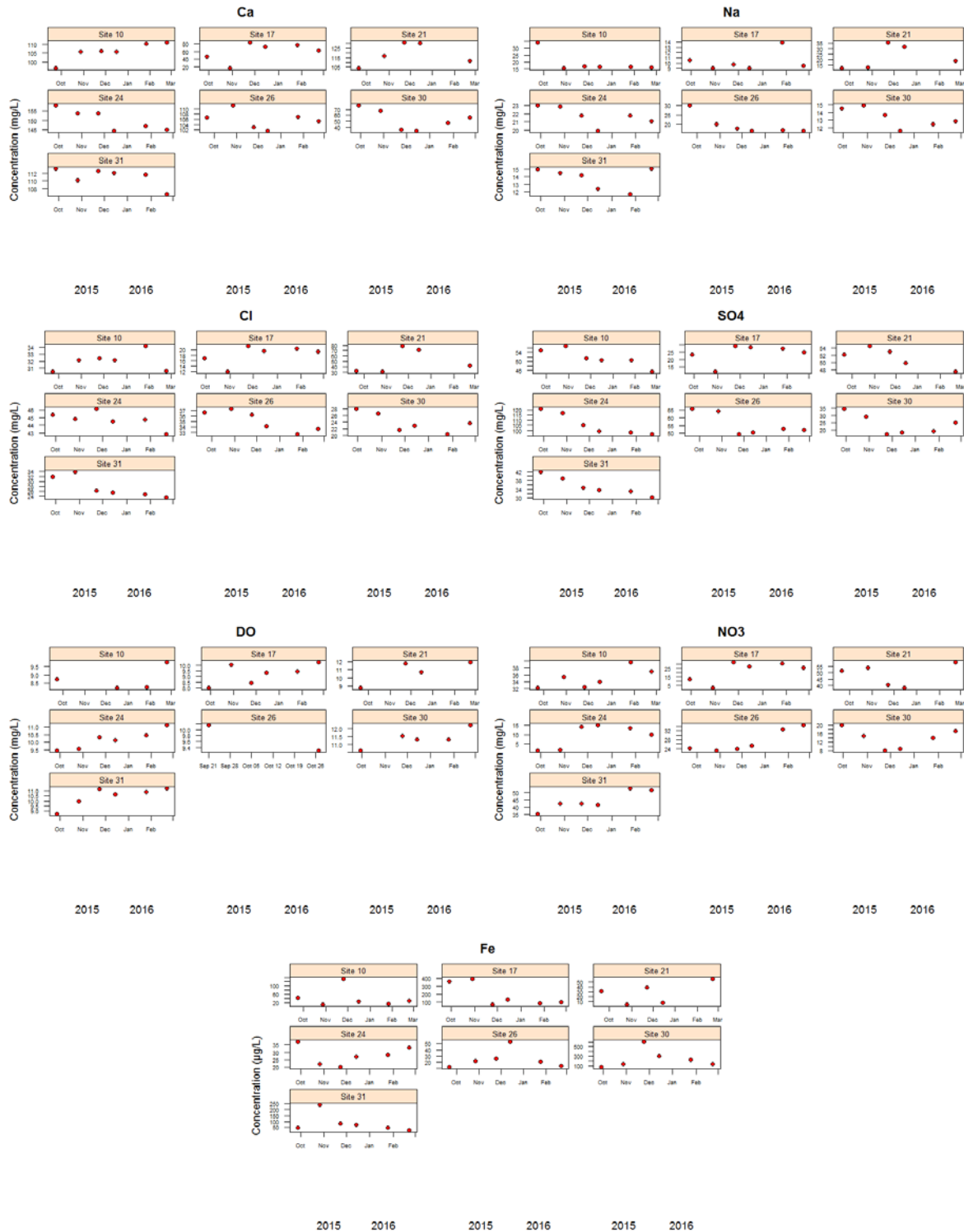


Figure 10. Time-series plots for selected parameters measured in streams (September 2015 to February 2016).

results over the interval of sampling (Figure 10). The waters are pH-neutral and have major-ion characteristics broadly comparable to local groundwater (Ca around 50–130 mg/L, Cl around 20–70 mg/L, alkalinity typically 150–350 mg/L as HCO_3). Completion of an annual cycle of monitoring will help to establish the seasonal variations that might affect the streams, arising from variable inputs of baseflow (groundwater) in comparison with surface runoff. Annual variability in chemical compositions is expected to be greatest in the streams because of the varying influence of rainfall and the immediacy of the effect on surface flows.

2.1.3.5 NEW GROUNDWATER BOREHOLES

The six shallow (10–40 m) pairs of new boreholes, installed at locations around KM8 (Figure 3) to investigate groundwater quality (and seismicity) further capture permeable horizons in the superficial deposits. As noted above, superficial deposits are thin or absent in this area and so boreholes penetrate variably the superficial glaciolacustrine deposits and/or the Ampthill & Kimmeridge Clay. Water levels are shallow (a few metres below ground level in most cases).

The new boreholes serve to augment the groundwater monitoring network and provide additional water-quality data at key locations in the Vale. Equipment for real-time monitoring are currently being installed in a selection of the boreholes and preliminary data acquisition is in progress.

Preliminary data from new boreholes support the observations from samples in the pre-existing water monitoring network, showing an anoxic groundwater. One site has a measured concentration of dissolved CH_4 of 23 mg/L, comparable to some of the higher concentrations observed in groundwater from the monitoring network. The full suite of results from the laboratory analyses is not yet available.

2.1.3.6 ORIGINS OF METHANE

The surveys of shallow groundwaters from the Quaternary aquifer in the Vale of Pickering demonstrate that the baseline groundwater compositions include relatively high concentrations of methane. Highest observed concentrations are an order of magnitude higher than those found elsewhere in England & Wales as part of the BGS national methane baseline survey (bgs.ac.uk/research/groundwater/shaleGas/methaneBaseline/home.html).

The high concentrations are consistent with the strongly reducing nature of the groundwaters in the central portion of the Vale. This appears not to be associated with the presence of current or abandoned hydrocarbon wells, though further work is needed to test this preliminary assessment further.

Hydrocarbons in Kirby Misperton were discovered by Taylor Woodrow in 1985 (DECC, 2013), but evidence exists for the occurrence of dissolved methane in shallow groundwater from the Vale dating back to the 1970s or earlier (Ford et al., 2015). This also suggests against a link with existing hydrocarbon infrastructure.

The source of the CH_4 is currently unknown though the possibilities include:

- i) in-situ generation by microbial activity in the strongly reducing conditions of the Quaternary superficial aquifer, aided by organic carbon in the sediments and dissolved in the water,
- ii) in-situ generation in the Ampthill & Kimmeridge deposits which either underlie the superficial deposits or outcrop at surface, the generation either by biogenic or thermogenic processes, or

- iii) transfer of CH₄ gas of thermogenic origin from deeper formations (Namurian Bowland Shale/sandstone) along faults.

The Amphill & Kimmeridge formations are an important source of hydrocarbons in the North Sea but, though bituminous, have not been considered sufficiently mature to be a source of hydrocarbons in the Cleveland Basin including the Vale of Pickering (Powell, 2010). Nonetheless, petrographic and fission-track evidence suggests that Middle Jurassic strata have been buried to depths of some 2–3 km (Powell, 2010), with potential implications for hydrocarbon generation. Clearly, the Amphill & Kimmeridge formations are an area for further investigation with respect to CH₄ generation in shallow groundwater.

Molar ratios of C1/C2 (methane/ethane) for a selection of high-methane groundwaters from the Quaternary aquifer are <1000 (albeit with few analysed samples). The ratios point potentially to a thermogenic source of CH₄, although ratios of δ¹³C for CH₄ in analysed groundwater samples are mostly of the order of -80 ‰ (one was -40 ‰). This suggests instead a dominantly biogenic origin. The methane may be of mixed biogenic/thermogenic origin and needs further investigation.

2.1.4 References

DWI, 2015. Understanding the Implications of the EC's Proposals Relating to Radon in Drinking Water for the UK: Final Report. Report to the Drinking Water Inspectorate, Ricardo-AEA, BGS and PHE. Ricardo-AEA/R/ED59170.

Ford, J R et al. 2015. The Vale of Pickering: an initial summary of the Quaternary/superficial geology and data holdings. BGS Open Report, OR/15/064.

Newell, A J, Ward, R S, and Fellgett, M W. 2016. A 3D geological model of post-Permian aquifers and aquitards in the Vale of Pickering, North Yorkshire, UK. Open Report OR/15/068 (in press).

Smedley, P L, Ward, R S, Allen, G, Baptie, B, Daraktchieva, Z, Jones, D G, Jordan, C J, Purvis, R M and Cigna, F. 2015. Site selection strategy for environmental monitoring in connection with shale-gas exploration: Vale of Pickering, Yorkshire and Fylde, Lancashire. British Geological Survey Open Report OR/15/067.

2.2 SEISMIC MONITORING

2.2.1 Background

The primary aim of the seismicity work package is to deploy a network of seismic sensors to monitor background seismic activity in the vicinity of proposed shale gas exploration and production near Kirby Misperton. The data collected will allow reliable characterisation of baseline levels of natural seismic activity in the region. This will facilitate discrimination between any natural seismicity and induced seismicity related to future shale gas exploration and production. A further aim is to make recommendations for a suitable traffic-light system to mitigate earthquake risk. The initial design requirement for the seismic monitoring network was reliable detection and location of earthquakes with magnitudes of 0.5 and above within a 20 km by 20 km area around the Kirby Misperton site.

2.2.2 Design and Deployment of the Monitoring Network

A total of eleven stations were installed in the period from September 2015 to March 2016. These are shown by the coloured squares in Figure 11. The instrumentation consists of seven near-surface sensors (red squares) and four sensors installed in boreholes (orange). The latter comprised of three downhole geophones and a downhole broadband seismometer. The sensors are situated at a depth of approximately 30 m below the surface and are all close to the Kirby Misperton drill site. Installing these instruments in boreholes should improve the signal-to-noise ratio of the recorded data and allow smaller events to be detected and located. This will be particularly important for reliable independent detection and location of any small earthquakes that may be induced by hydraulic fracturing if it is permitted, as well as for the baseline monitoring. A surface sensor has also been installed at the site of the downhole broadband seismometer and at one of the downhole geophones in order to assess the improvement in signal-to-noise ratio and characterise the effect of the near-surface geology on the propagation of seismic waves and to help predict possible ground motions from induced earthquakes in the region.

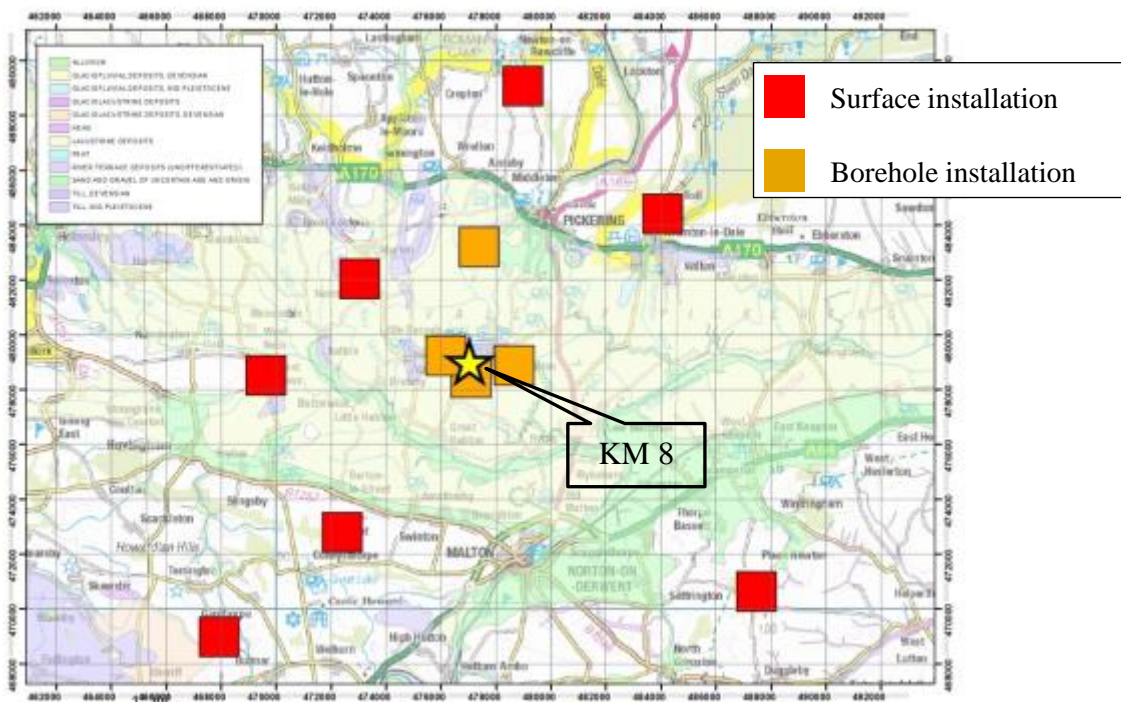


Figure 11. Location of surface and borehole seismometers and geophones across the Vale of Pickering. © Crown Copyright and/or database right 2016. Licence number 100021290 EUL.

In general, the near-surface sensors were deployed on bedrock, since hard, dense rocks that have high seismic velocities are preferable to superficial sediments such as clays or poorly consolidated soils, which have a low seismic velocity and can act as efficient waveguides for ambient noise from cultural sources. The sites were also chosen to minimise the effect of cultural noise sources such as roads, towns and villages.

2.2.3 Station Performance

Seismograms always contain noise from ambient Earth vibrations as well as transient recordings from earthquakes. Seismic noise from human activity is often referred to as “cultural noise” and originates primarily from the coupling of traffic and machinery energy into the Earth. This cultural noise propagates mainly as high-frequency surface waves (>1-10 Hz, 1-0.1 sec) that attenuate within a few kilometres of the noise source and often shows very strong diurnal variations. High noise levels can limit the ability to detect and reliably locate small transient signals from earthquakes or other disturbances.

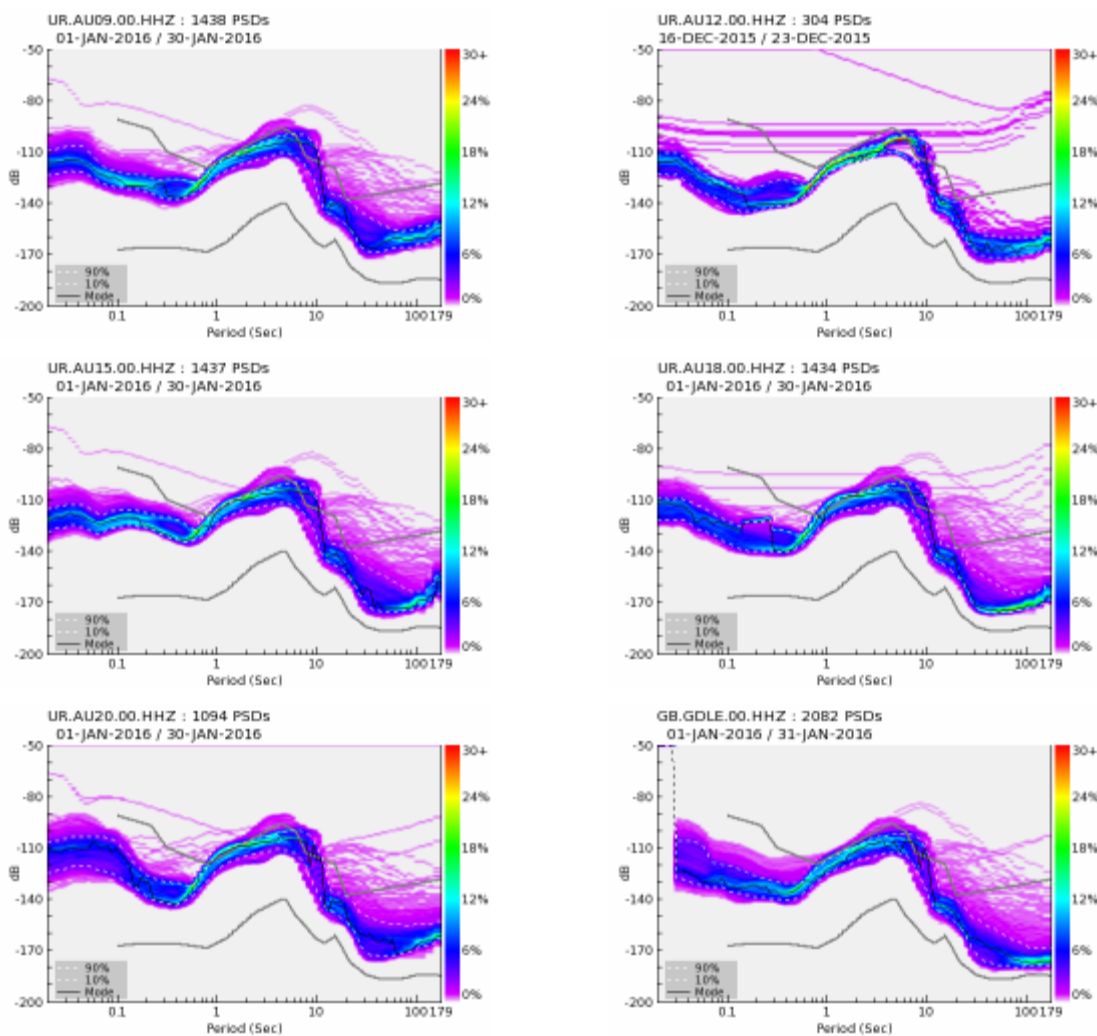


Figure 12. PDFs for five of the monitoring stations installed around Kirby Misperton and the permanent BGS station, GDLE, in the North Yorkshire Moors.

We use power spectral density (PSD), calculated from one hour segments of continuous data, to characterize noise levels in a range of frequencies or periods at each of the installed stations. A statistical analysis of the PSDs yields probability density functions (PDFs) of the

noise power for each of the frequency bands at each station and component. PDFs calculated from PSDs of the vertical component of ground motion for each of the five installed stations are shown in Figure 12. A colour scale gives the probability of a given noise power (magenta to red). The solid grey lines show the low and high noise models for seismic stations obtained by Peterson (1993). The mode of the PDF and the tenth and ninetieth percentiles are shown by the black and white dashed lines respectively.

The noise power probability for each station varies smoothly as a function of period (1/frequency), with a central peak between 1-10 s, which generally falls to lower powers at longer and shorter periods. This mirrors the shape of the high and low noise models. In the cultural noise band (periods less than 1 s), there is evidence of diurnal variations in noise at all five stations. In addition, the noise power varies from station to station, with AU12, AU18 and AU20 generally showing lower levels of noise than stations AU09 and AU15.

2.2.4 Detection Capability

The detection capability of any seismic network is a complex function of many factors including the distribution, density and characteristics of individual stations, their local site and noise conditions, as well as processing software and processing strategies. The amplitude of the ground motions caused by any earthquake is a function of both the magnitude of the earthquake and the distance of the earthquake from the recording position. An event may be undetected because it is too small or too distant, so its signal is indistinguishable from the background noise on the seismograph. Also, many detection algorithms require the signal from an event to exceed the background noise level by a certain ratio on a number of stations for an event to be detected. If the station density is low, this will only happen for larger events. The detection of small earthquakes thus requires relatively high station densities.

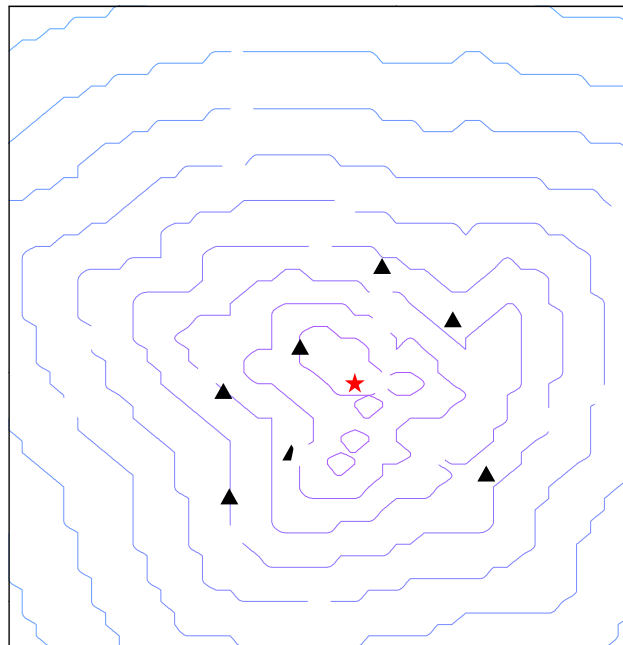
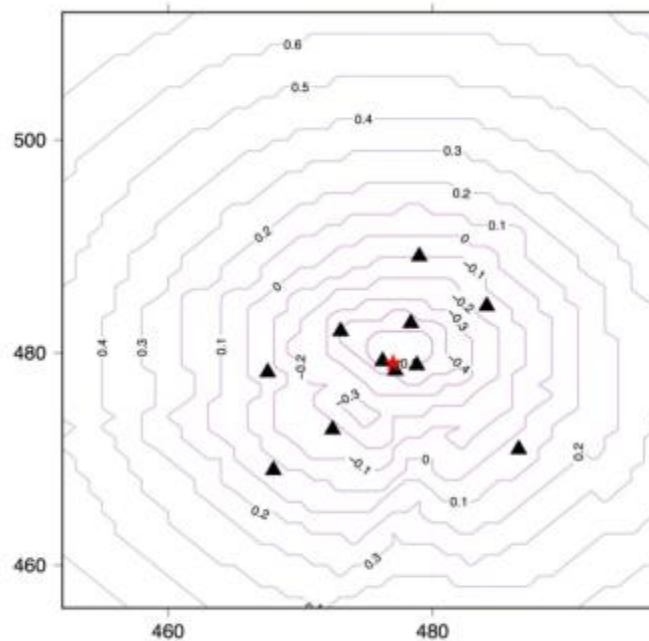


Figure 13. Modelled detection capability for the surface network of sensors around the KM8 site (red star), showing the spatial variation in magnitudes that can be detected.

We used theoretical models of the expected amplitude of seismic waves as a function of magnitude and distance, together with estimates of seismic noise at each monitoring station to model the current detection capability of the network for earthquakes of different magnitudes. The results are shown in Figure 13 and suggest that the existing stations should

allow any earthquakes with a magnitude of 0.5 or above across most of the study area to be detected. In the centre of the network, earthquakes with a magnitude of 0.3 or greater are likely to be detected. The installation of the borehole sensors will further increase the detection capability of the network. Using the same theoretical models incorporating these additional monitoring stations (Figure 14) suggests that at the centre of the network, earthquake magnitudes of 0.0 or greater are likely to be detected, and earthquakes with



negative magnitudes should be detected around the KM8 drill site.

Figure 14. Modelled detection capability for seismic monitoring including borehole sensors (triangles). Contours represent event detection magnitude.

2.2.5 Data Processing and Analysis

Continuous data from all installed stations are transmitted in real-time to the BGS offices in Edinburgh and have been incorporated in the data acquisition and processing work flows used for the permanent UK network of real-time seismic stations operated by BGS. A simple detection algorithm is applied to the data from the Vale of Pickering stations as well as data from permanent BGS monitoring stations in the region to detect possible events.

All detections have been reviewed by an experienced analyst. Detected events in the northeast of England in the time period from 1/10/2015 to 31/3/2016 are shown in Figure 16. Diagonal crosses show earthquakes. Square crosses show events of a suspected explosive origin, e.g. quarry blasts. No events have been detected in the immediate locality of the Vale of Pickering, however, a number of other earthquakes and quarry blasts from elsewhere have been detected. These included thirty-one earthquakes, the largest of which was a magnitude 2.2 ML earthquake south of Worksop, Nottinghamshire. This earthquake was part of a sequence of 22 detected earthquakes in this area between 19 and 27 November 2015. Only one other earthquake with a magnitude of 2 or above was detected in northeast England in the monitored period. Forty-five events of a suspected explosive nature were detected, these are almost all quarry blasts, most of which originated from quarries in the Peak District. Six quarry blasts had magnitudes of 2.0 ML or above, the largest of which had a magnitude of 2.2 ML.

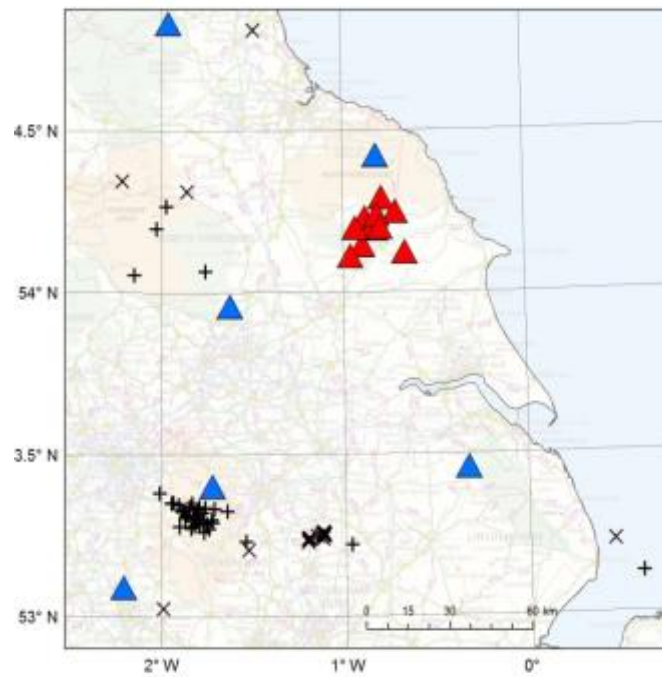


Figure 15. Seismic events detected by the Vale of Pickering stations and permanent BGS monitoring stations in the north east of England from 1/10/2015 to 31/3/2016. Diagonal crosses show earthquakes. Square crosses show events of a suspected explosive origin, e.g. quarry blasts. © Crown Copyright and/or database right 2016. Licence number 100021290 EUL.

Figure 15 shows the ground motions for a magnitude 1.7 ML earthquake near Worksop, Nottinghamshire on 20/11/2015, recorded at five stations in the Vale of Pickering network

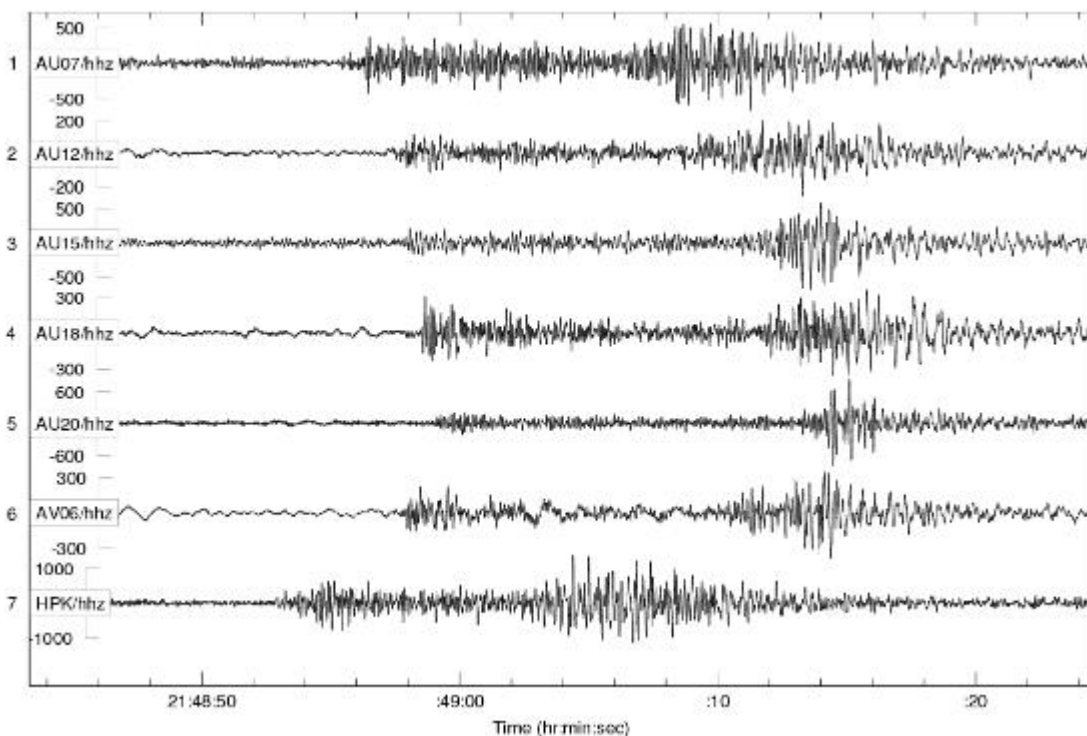


Figure 16. Recordings of a magnitude 1.7 ML earthquake near Worksop, Nottinghamshire at stations in the Vale of Pickering, along with the recording at station HPK just north of Leeds.

along with the recording at station HPK just north of Leeds. The signal to noise ratio is good and the event is well recorded, with clear P- and S-wave arrivals on most stations.

In addition, a number of large earthquakes from elsewhere around the world have also been detected. For example, Figure 17 shows the recorded ground motions from a magnitude 7.5 earthquake in the Hindu Kush at 09:09 on 26/10/2015 at each of the five stations in the Vale of Pickering as well as the permanent BGS monitoring station GDLE. Numerous signals from various seismic waves that have propagated along different paths through the Earth are clearly visible, as marked by the dashed lines, suggesting that the data quality is good. Comparison with the permanent station GDLE suggests that the stations in the Vale of Pickering give a similar data quality to the permanent station.

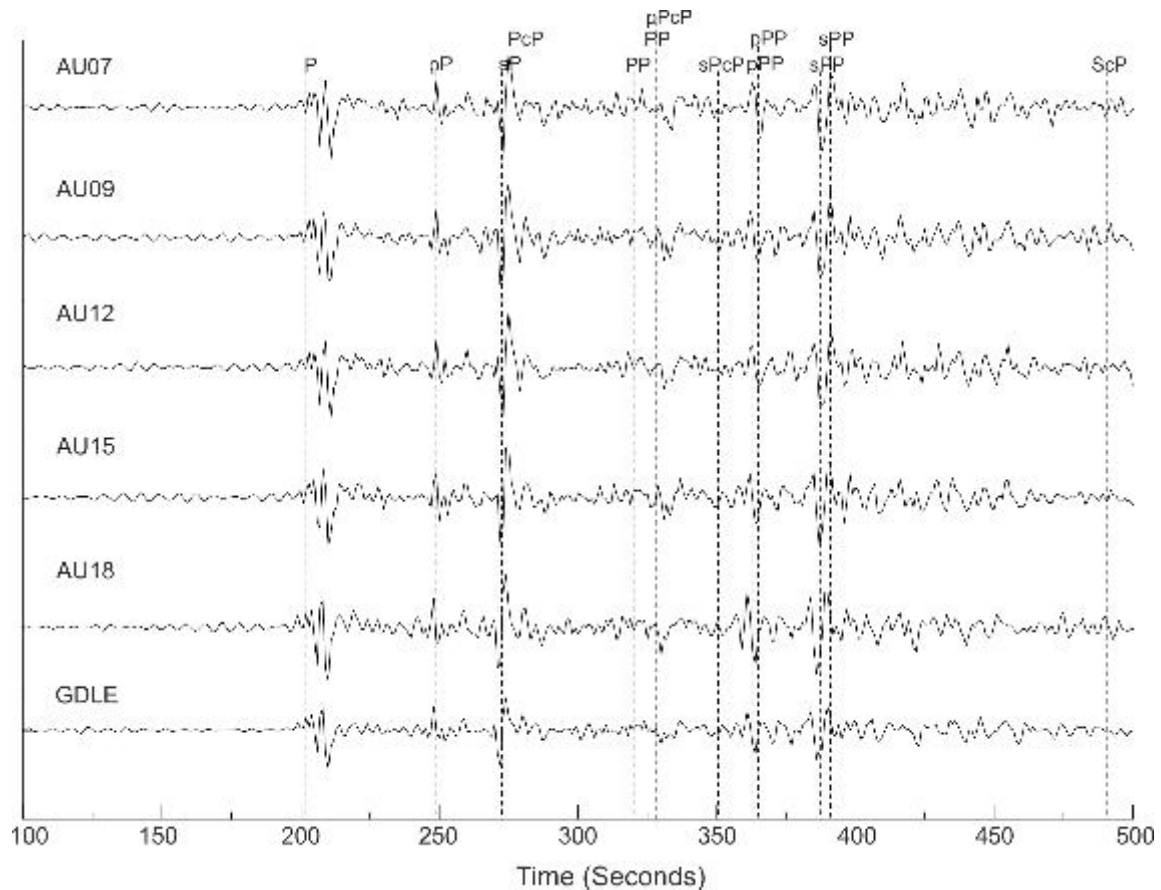


Figure 17. Recorded ground motions from a magnitude 7.5 earthquake in the Hindu Kush at 09:09 on 26/10/2015 measured at stations in the Vale of Pickering and the permanent BGS monitoring station GDLE. The dashed lines mark the arrival times of various seismic waves that have propagated along different paths through the Earth.

2.2.6 Regional Seismicity and Activity Rates

Figure 18 shows both historical and instrumentally recorded earthquake activity within a 100 km by 100 km square centred on the Kirby Misperton 8 well from the BGS earthquake catalogue. This catalogue is a combination of the historical catalogue of Musson (1994) and later revisions for the period up to 1969, and earthquake parameters determined from instrumental data recorded by the UK National Seismic Monitoring Network thereafter (Musson, 1996; Baptie, 2012). It contains almost 10,000 instrumentally recorded local earthquakes from 1970 to present.

The Vale of Pickering region appears to be an area of low seismicity even for the UK with little significant recorded earthquake activity. Historically, the largest earthquake in the region was a magnitude 3.7 earthquake near Market Weighton in 1885. This had a

maximum intensity of 5 EMS in the epicentral area, equivalent to shaking strong enough to cause buildings to tremble and top-heavy objects to topple. There have been a number of instrumentally recorded earthquakes in the region in the last 40 years with magnitudes in the

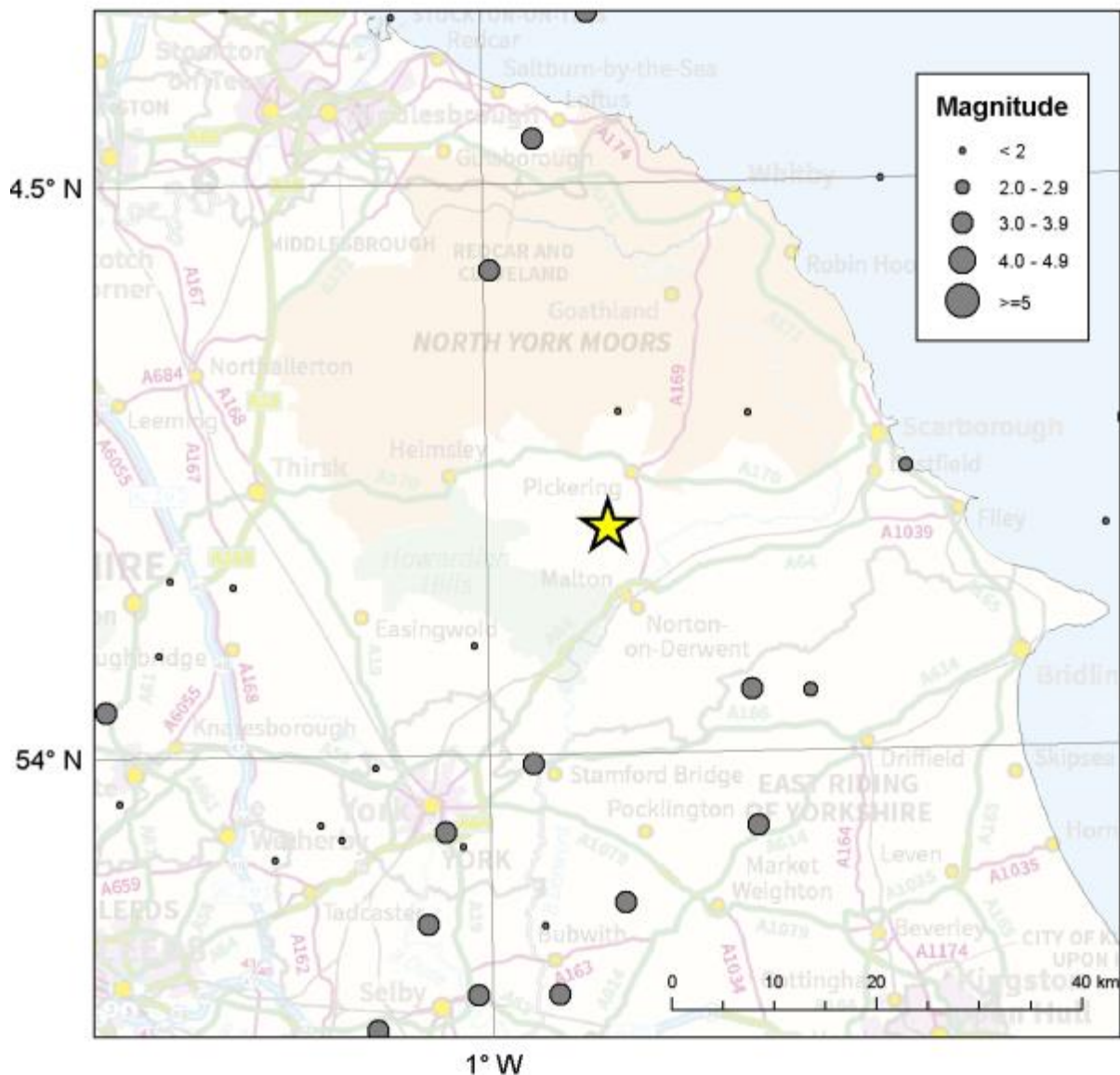


Figure 18. Historical and instrumentally recorded earthquakes (grey circles) from the BGS earthquake catalogue within a 100 km by 100 km square centred on the Kirby Misperton 8 well from. The symbols are scaled by magnitude. © Crown Copyright and/or database right 2016. Licence number 100021290 EUL.

range of 2-3 ML. These include: magnitude 2.9 and 3.0 ML earthquakes near Selby, North Yorkshire in 1978 and 1984 respectively; a magnitude 2.4 ML earthquake near Westerdale North Yorkshire in 1984; a magnitude 2.1 ML earthquake near Sledmere, Humberside in 1992; two earthquakes near York in 2003 and 2005 with magnitudes of 2.3 and 2.5 and, more recently, a magnitude 2.9 ML earthquake near Loftus, Cleveland in 2012. None of these earthquakes was within 20 km of Kirby Misperton.

The relationship between the magnitude and number of earthquakes in a given region and time period generally takes an exponential form that is referred to as the Gutenberg-Richter law (Gutenberg and Richter, 1954), and is commonly expressed as

$$\log_{10} N = a - bM \quad (1)$$

Where, N is the number of earthquakes above a given magnitude M . The constant a , is a function of the total number of earthquakes in the sample and is known as the earthquake rate. This is commonly normalised over period of time, such as a year. The constant b gives the proportion of large events to small ones, and is commonly referred to as the b -value. In general, b -values are close to unity. This means that for each unit increase in magnitude, the number of earthquakes reduces tenfold. Plotting earthquake magnitudes against the logarithm of frequency gives a straight line

The rate parameter typically varies from place to place, such that an active region will have a higher value of than a less active region. Also, in a region of homogeneous seismicity, the value of the rate parameter in any sub-region scales with relative size of the two regions. For example, a region where seismicity is homogeneous and $a = 3$, will have 1000 earthquakes above a magnitude of zero each year. A sub-region, whose area is ten times smaller will have $a = 2$, i.e. 100 earthquakes above a magnitude of zero each year. This has important implications for baseline monitoring in small regions, particularly where activity rates are low, since the number of earthquakes in a given period of time may be very low, so longer



Figure 19. The seismic source zone for mainland Britain Ireland (large polygon) and used to estimate average earthquake activity rate. The red shaded areas show the Vale of Pickering study area.

durations of baseline monitoring are required to reliably determine seismicity rates.

The UK average values for a and b are 3.23 and ~ 1 respectively. This means that within the polygon enclosing mainland Britain shown in Figure 19 we might expect around 17 earthquakes with a magnitude of 2.0 M_w or above each year. Assuming that seismicity is homogeneous and scaling this number to a smaller area of 400 km² the size of the Vale of

Pickering study region, suggests that there will be an earthquake with a magnitude of 2.0 M_W or above only every 65 years, and three earthquakes with a magnitude of 0.0 M_W or above every two years. This highlights the challenge of reliable estimation of background activity rates in low seismicity regions, since it may require many decades of baseline monitoring to reliably determine rates in small areas if the levels of natural seismicity are low.

Applying the UK average seismicity rate parameter to the 100 km² square centred on Kirby Misperton shown in Figure 18, suggests we might expect approximately two earthquakes with a magnitude of 2.0 M_W or above every five years. This is largely consistent with the observed number of earthquakes, as 17 events with this magnitude or greater have been recorded in the last 40 years.

2.2.7 Data Availability

Helicorder plots showing 24 hours of data from each station are available online and can be found on the BGS Earthquake Seismology Team web site at www.earthquakes.bgs.ac.uk/research/BaselineMonitoring.html and at www.earthquakes.bgs.ac.uk/helicorder/heli.html. The web pages also contain background information on the baseline monitoring project as well as educational material to explain the scientific context. Recordings of ground motions from all stations are stored in a publicly open-data archive and can also be downloaded from the web-site. These data are available in the standard data formats developed in the international seismological community for data exchange. In the future, processed event data (automatically determined and manually revised event parameters) will also be made available through this website.

2.2.8 References

- Baptie, B. 2012. UK earthquake monitoring 2011/2012: Twenty-third Annual Report. British Geological Survey Commissioned report, OR/12/092 (Edinburgh).
- Gutenberg, B. and Richter, C.F., 1954. Seismicity of the Earth and Associated Phenomena, 2nd ed. Princeton, N.J.: Princeton University Press.
- Musson, R. M. W. 1994. A catalogue of British earthquakes. British Geological Survey Global Seismology Report, WL/94/04.
- Musson, R. M. W. 1996. The seismicity of the British Isles. *Annali di Geofisica* 39, 463–469.
- Peterson, J., Observation and modelling of seismic background noise, U.S. Geol. Surv. Tech. Rept., 93-322, 1-95, 1993.

2.3 GROUND MOTION – ANALYSIS OF SATELLITE (INSAR) DATA

2.3.1 Background

The investigation in this work package is designed to monitor the surface ground motion (subsidence, uplift or stability) of the target area using line of sight (LOS) satellite radar interferometry (InSAR) prior to any permitted unconventional gas production in the Vale of Pickering. InSAR is an ideal technique for ground motion monitoring because

- a) archive radar data (acquired by satellites since 1992) are available and can be utilised to ascertain a baseline of motion (or lack of motion) prior to any permitted gas operations, and
- b) data from currently-orbiting satellites such as Sentinel-1A can be analysed to acquire information about the ongoing surface ground motion conditions in a region
- c) the analysis produces data over a region rather than at a point location, which other techniques such as GNSS provide.

To date, the InSAR process has not been applied to monitoring energy operations in the UK because of the challenge of gaining coherence over non-urban areas. To resolve this challenge, we processed the data using the conventional SBAS (small baseline subset) process to gain precise results over urban areas and subsequently utilised the ISBAS (intermittent small baseline subset) process to acquire results over the non-urban areas.

BGS has experience of applying InSAR to several ground surface monitoring applications in the UK e.g. utilising 55 ERS-1/2 images between 1992 and 1999 to investigate ground motion linked to ceased mining operations in south Wales (Bateson et al 2015). The InSAR technique was subsequently applied as part of the BGS-funded project to monitor environmental baseline conditions in Lancashire where planning applications were submitted by Cuadrilla in 2014 for the development of shale gas, see www.bgs.ac.uk/research/groundwater/shaleGas/monitoring/lancashire.html. This has been followed by its application across the Vale of Pickering.

The deliverable in this ground motion work package is to provide “an analysis of satellite (InSAR) data”. In order to achieve this, the following steps were followed:

- Obtain stacks of satellite SAR data
- Process the data using the SBAS InSAR techniques (thereby deriving results primarily for urban areas)
- Process the data to ISBAS level, thereby extending the results to non-urban areas)
- Provide an analysis of the InSAR results.

Table 2. Analyses of InSAR processing for the Vale of Pickering.

Satellite	Time period	No. of scenes in the stack	Processing mode	Max velocity (mm/yr)	Min velocity (mm/yr)
ERS-1/2	1992-2000	72	SBAS	+3.3	-3.1
ERS-1/2	1992-2000	72	ISBAS	+6.2	-4.4
ENVISAT	2002-2009	25	SBAS	+5.8	-4.4
ENVISAT	2002-2009	25	ISBAS	+9.3	-7.3

The work package utilised the ISBAS technique of InSAR analysis as it has been found to provide results in non-urban areas where other InSAR techniques fail. The conventional SBAS technique requires that the target shows coherence in every image of the stack, while the ISBAS technique utilises coherence that is intermittent throughout the stack. Both SBAS and ISBAS processing and analysis was undertaken on each stack of radar images to provide results in urban and non-urban areas.

All of the available archive satellite radar data covering the time periods 1992-2000 and 2002-2009 over the Vale of Pickering were processed and analysed (Table 2).

2.3.2 Results of InSAR analysis in the Vale of Pickering.

Two sets of archive satellite radar data were acquired for the Vale of Pickering.

The archive radar data were acquired by the ERS-1/2 and ENVISAT satellites for the periods 1992-2000 and 2002-2009 respectively. These data were provided by the European Space Agency (ESA) to BGS under grant id.31573. Both stacks of data were analysed using SBAS and ISBAS InSAR techniques, i.e. four sets of analysis were undertaken and completed within this ground motion work package (Figure 20 and Figure 21).

There is no satellite coverage in the region between 2009 and 2014 due to the orbital decay of ENVISAT. No alternative commercial data are available to this study due to lack of acquisition in this time period. Nonetheless, we consider the period 1992–2009 is sufficient to provide a meaningful baseline assessment of ground motion prior to unconventional gas operations.

2.3.2.1 ARCHIVE RADAR SATELLITE DATA FROM 1992-2000

75 ERS-1/2 SAR scenes for 1992-2000 are available along satellite track 366 in descending mode. Of the 75 ERS-1/2 scenes in the archive, three were not used due to missing lines within the data. The results of the ERS-1/2 InSAR analysis are shown in Figure 20. Green areas are considered stable, red are subsiding on average over the time period, and blue are undergoing uplift.

The SBAS results are primarily constrained to urban areas (including roads) as these provided coherence in all of the radar images in the stack. It is apparent that the analysis shows that the area was predominantly stable between 1992 and 2000. There does appear to be a discrete zone of subsidence north of Whitby (in the Loftus area) but this is outside the Vale of Pickering monitoring area.

The ISBAS analysis of the ERS-1/2 radar data indicates that the majority of the area was stable. There are three zones of ‘dispersed’ uplift in this analysis, to the west, southwest and south of Scarborough. We believe that these zones in the ISBAS analysis are not related to geological motion (in our experience geological motions are more discrete), but are most likely due to vegetation changes and agricultural practices.

2.3.2.2 ARCHIVE RADAR SATELLITE DATA FROM 2002-2009

25 ENVISAT scenes for 2002-2009 along satellite track 366 in descending mode were ordered from ESA. 24 of the available 25 radar images were utilised; the scene acquired on 8th January 2005 was excluded due to failure to meet the baseline criteria. The relatively low number of scenes in the ENVISAT stack is a data limitation, and may have resulted in reduced compensation for some atmospheric effects. The results indicate a maximum velocity of 9.3 mm/year. The SBAS InSAR analysis comprises 72,697 points while the ISBAS analysis comprises 234,793 points (Figure 21).

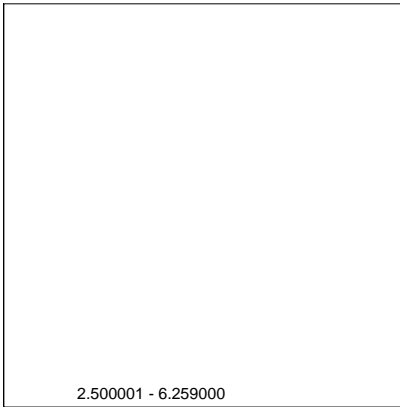
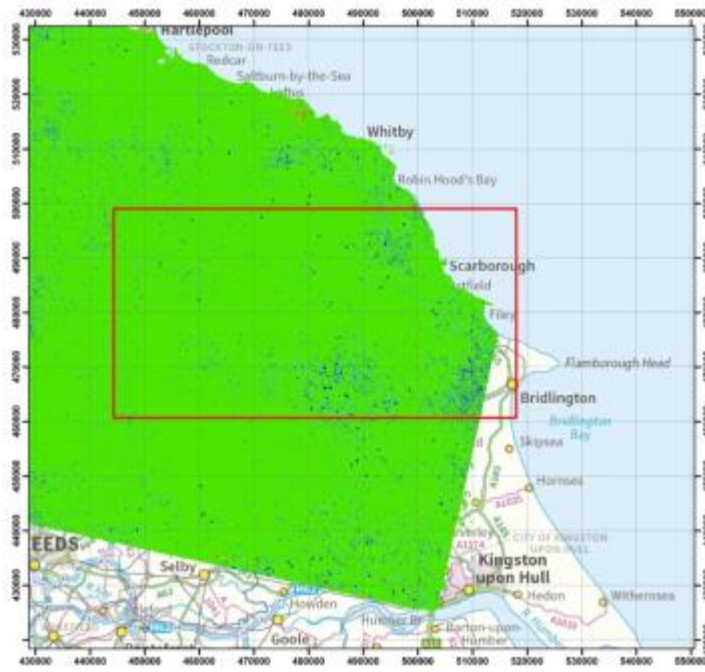
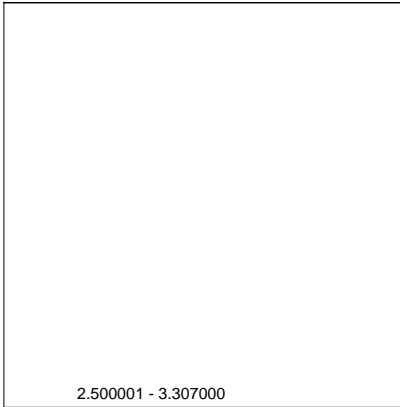


Figure 20. InSAR SBAS (top) and ISBAS (bottom) analysis of ERS-1/2 satellite imagery (1992-2000) for the Vale of Pickering. Radar data supplied to BGS by ESA under grant id.31573. Contains Ordnance Data © Crown Copyright and database rights 2016. Licence number 100021290 EUL.

As with the 1992-2000 InSAR analysis, the SBAS results suggest that the urban areas are not affected by widespread subsidence or uplift, i.e. they are predominantly stable. There are some zones of dispersed uplift, notably along the coast southwards from Scarborough, and in the central and western extremes of the Vale of Pickering. The dispersed nature of the uplift suggests that they are not due to geological motion, and may not be genuine. They could be due to atmospheric effects.

The ISBAS analysis corroborates the SBAS analysis and provides additional results across the region. The ISBAS analysis identifies a discrete zone of subsidence to the south of the Vale of Pickering monitoring area and adjoining its southern boundary. This correlates with

an area of compressible ground in the BGS GeoSure product, and we believe that this is genuine surface ground motion.

Within the Vale of Pickering ISBAS analysis there are significant zones of dispersed uplift. These do not seem to show any correlation with the zones of dispersed uplift in the ERS-1/2 ISBAS analysis, nor do they correlate with bedrock, superficial geology or compressible ground databases. Their dispersed nature suggests that they are not the result of geological motion. Due to the relatively small number of scenes in the stack they could be the result of atmospheric effects.

Further work will be undertaken up to end March 2016 to assess the analysis, particularly in relation to the zones of dispersed uplift and subsidence. The additional work will use the RMS point errors and the time series data for each point.

2.3.2.3 CURRENT SATELLITE RADAR DATA AND INSAR PROCESSING

It should also be noted that ESA launched a new radar satellite, Sentinel-1A, in April 2014. It was hoped that a sufficient stack of Sentinel-1A may have been available by the end of 2015 and it was proposed that BGS could have incorporate the data (when available) to establish current ground conditions in the study area. However to date the satellite has acquired less than 20 images in Interferometric Wide Swath Mode per stack, which is too low to guarantee high precision InSAR analyses. It is expected that a sufficient stack of imagery will be available by ~May 2016 and they could be processed to provide precise current ground motion information within a follow-on project.

2.3.2.4 PROBLEMS / ISSUES ENCOUNTERED AND EXPLANATION OF CAUSE(S)

There were no significant issues encountered. The ENVISAT and ERS-1/2 satellite radar data for the Vale of Pickering has been analysed using both SBAS and ISBAS InSAR techniques.

The number of scenes in the ENVISAT data stack for the Vale of Pickering is relatively low therefore the dispersed zones of uplift and subsidence may be due to some atmospheric effects that the processing could not filter out. This increased the uncertainty in the data (i.e. increased standard deviations). Further analyses of the dispersed zones will be completed by end March 2016 utilising a combination of i) the root mean square error within the data, ii) the time series and iii) expert elicitation.

A sufficient stack of Sentinel-1A data to undertake InSAR analyses will not be acquired by the satellite until ~May 2016.

2.3.3 Risks and mitigation measures

No additional risks have been identified.

2.3.4 Conclusions

The precursor monitoring project in the Lancashire area utilised SBAS and ISBAS InSAR analysis. The project identified that the majority of the area was stable while also identifying discrete areas of subsidence and uplift. It is proposed that the subsidence was due to both anthropogenic factors (coal mining) and natural factors (compressible peat sediments) while the zone of uplift was related to cessation of water extraction when mining ceased.

The Vale of Pickering ground motion analysis entailed processing two stacks of ERS-1/2 and ENVISAT radar satellite data using SBAS and ISBAS techniques (i.e. four levels of analysis in total). The ENVISAT data (2002-2009) consisted of 24 scenes. The SBAS analysis indicated that the urban areas were predominantly stable in the time period. The areas of dispersed motion in the SBAS and ISBAS analyses may be due to atmospheric

effects rather than genuine ground surface motion. Nevertheless, the zone of subsidence in the south of the monitoring area is thought to relate to compressible ground.

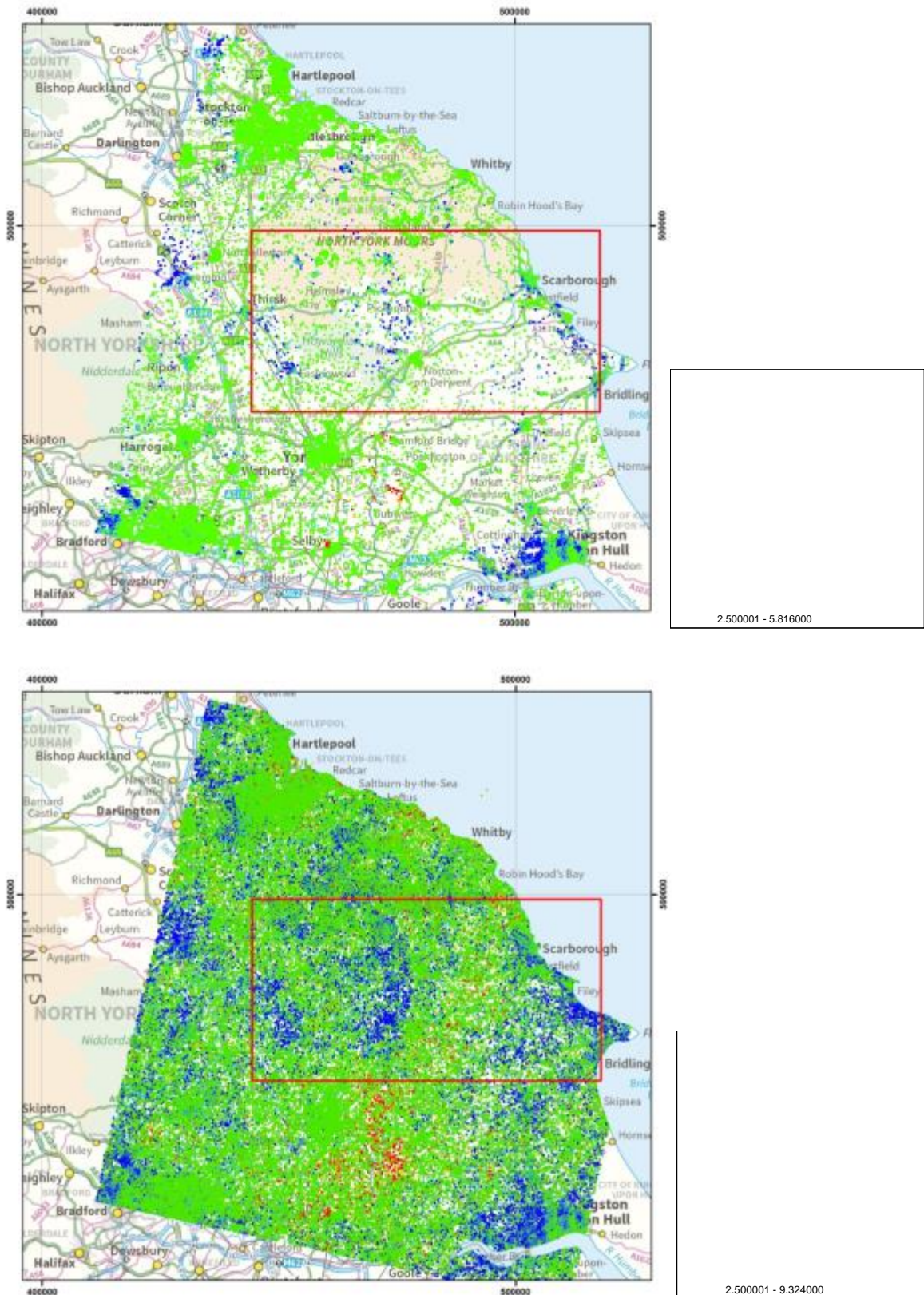


Figure 21. InSAR SBAS (top) and ISBAS (bottom) analysis of ENVISAT satellite imagery (2002-2009) for the Vale of Pickering. Contains Ordnance Data © Crown Copyright and database rights 2016. Licence number 100021290 EUL.

The ERS-1/2 Vale of Pickering dataset comprised 72 satellite radar scenes and it has therefore not been affected by atmospheric conditions. The SBAS analysis revealed that the urban areas and connecting roads are stable i.e. they are not affected by regional subsidence or uplift between 1992 and 2000. The ISBAS analysis also indicated that the area is predominantly stable apart from three zones that appear to display dispersed uplift. Our experience of this type of dispersed result is that it is not due to geological motion (which is more discrete) but it is most likely due to vegetation changes and agricultural practices.

Finally, ESA launched the Sentinel-1A in April 2014 but it did not acquire a sufficient stack of images to allow a precise InSAR analysis within the timescale of this monitoring project. It is expected that a stack will be available by ~May 2016, which will allow the current surface ground motion conditions to be monitored precisely.

2.3.5 References

Bateson, Luke; Cigna, Francesca; Boon, David; Sowter, Andrew. 2015 The application of the Intermittent SBAS (ISBAS) InSAR method to the South Wales Coalfield, UK. *International Journal of Applied Earth Observation and Geoinformation*, 34. 249-257. [10.1016/j.jag.2014.08.018](https://doi.org/10.1016/j.jag.2014.08.018)

2.4 ATMOSPHERIC COMPOSITION

2.4.1 Introduction:

The objectives of this work package were to establish a fixed atmospheric monitoring station in the Vale of Pickering and to augment an analogous site in Lancashire at Little Plumpton, close to areas with planning applications for hydraulic fracturing by Third Energy and Cuadrilla, respectively. Dataset deliverables were to begin the measurement of 12-month statistical baselines for air pollutants, which are of key concern to human health, and greenhouse gases, which have implications for climate change.

This report discusses the data collected until mid-March 2016 and point to the future development and of a full 12-month baseline dataset in terms of local and regional pollution sources and atmospheric backgrounds. The data so far are interpreted at both sites, focussing on the longer term greenhouse gas dataset at Little Plumpton (recorded since December 2014, as a complimentary component of the partner-funded monitoring) and air quality data from both sites since early January 2016.

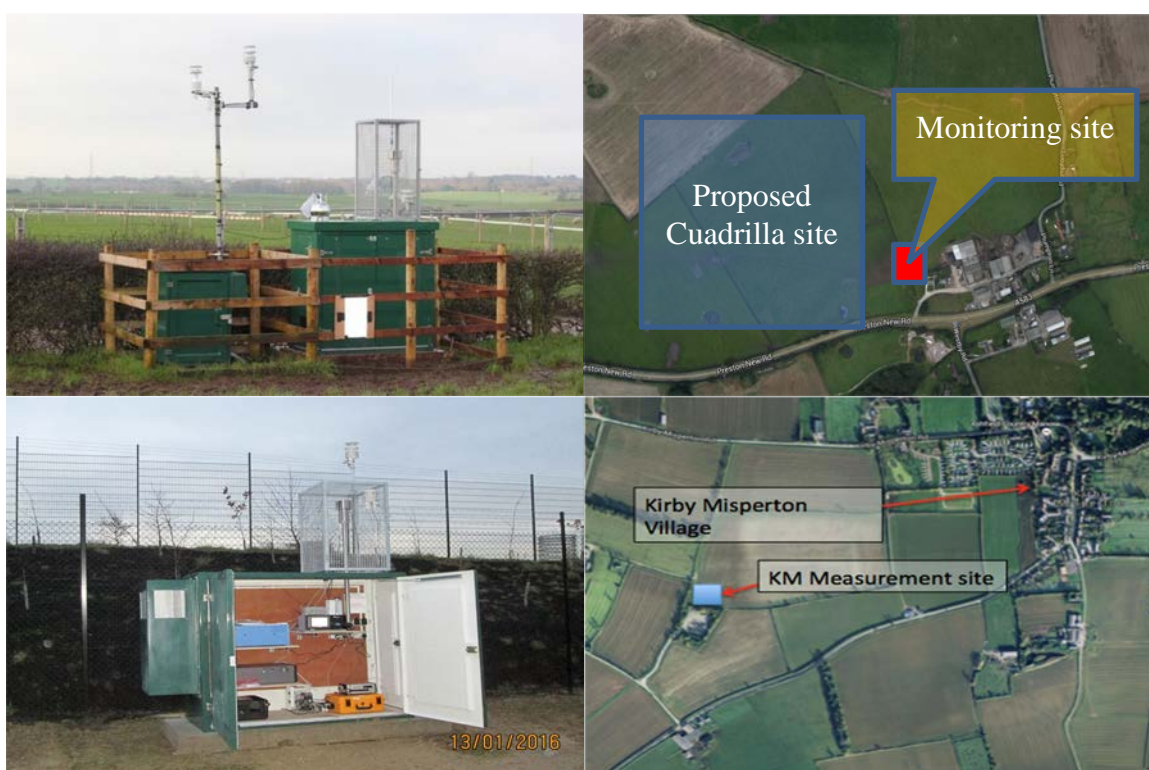


Figure 22. Top panels: left: Little Plumpton measurement site, right: location of the measurement site and proposed Cuadrilla site close to Little Plumpton. Bottom panels: left, measurement site within the Kirby Misperton Third Energy Site, right: location of the measurement site. © University of Manchester, 2016.

The method of baseline interpretation used here allows us to explore the statistical climatology of the atmospheric environment at each site and to explore the mix of pollutant source-types that influences the local area by comparing meteorology and trace gas concentrations as a function of time (such as time of day, day of week, seasonal and annual). A further objective of this package of work is to advise on the spatial transferability of the climatology (i.e. what wider area the baseline can be extended to represent) and the temporal lifetime of the baseline (i.e. how far into the future the statistics can be reasonably assumed to be valid). This is because different locations will typically have very different existing local pollution sources and future development plans, such that baselines have finite extrapolation potential. As this baseline is intended to provide a contextual source of

information from which to compare any future measured increment in local pollution attributable to shale gas activity, it is therefore important to establish the utility of the baseline for this future purpose.

It is important to note that the interpretation of extant sources of pollution impacting each site is greatly empowered when analysed for the full suite of trace gas and meteorological measurements available. This is because different point sources of air pollution and greenhouse gases have different co-emission signatures. For example, sources of NO_x (such as diesel vehicles) typically emit CO₂ (but not CH₄) and modulate ozone downwind (by secondary oxidative chemistry); whereas sources of CH₄ (such as landfill) typically co-emit CO₂ but not NO_x with significantly smaller influence on the chemistry of O₃. Using knowledge of these relationships when discussing the data allows better conclusions to be drawn on the likely mix of pollutant source-types and their relative proximity to the sites.

Therefore, while the analysis of the greenhouse gas dataset for Little Plumpton in this report is relatively extensively - as this is available for a longer timescale - it should be noted that future measurements of air quality (and other) trace gases will enhance the understanding going forward as we complete the 12-month baseline for all gases simultaneously.

2.4.2 Sites and instrumentation

2.4.2.1 SITE DETAILS

At the start of the project in September 2015, new instrumentation was procured and site locations were selected for installation. By early January 2016, both sites were fully operational and collecting the full suite of data detailed in Table 3 below. In the remainder of this discussion, the Little Plumpton site will be referred to as *LP* and the Kirby Misperton site as *KM*. The University of Manchester (Dr Grant Allen, WP lead) is responsible for the maintenance of the LP site and the University of York for the LP site. Greenhouse gas data analysis is the responsibility of Dr Allen, Dr Iq Mead and Mr Joseph Pitt (University of Manchester) and air quality data analysis is provided by Prof Ally Lewis, Dr Ruth Purvis and Dr Rachel Dunmore (University of York).

The position of the measurement sites (see Figure 22) was selected so as to be downwind of future potential exploratory shale gas extraction infrastructure (to optimise potential future operational monitoring) but also to be free of nearby obstruction in order to obtain a representative local baseline ahead of any exploratory activity. Sites consist of a mains-powered outdoor weather proof enclosure containing all scientific instrumentation and a meteorological station to record local thermodynamics (winds and meteorological variables) to aid qualitative source apportionment based on air mass history.

The KM site is situated on a Third Energy site near to the village of Kirby Misperton where there is currently an application to carry out hydraulic fracturing exploration and is subject to 24 hour security. The LP site is situated on privately-owned farmland near to the village of Little Plumpton, where there is an application by Cuadrilla for the same. Both sites have been established with the land-owner's permission and a full risk assessment was carried out for each site prior to installation.

2.4.2.2 INSTRUMENTATION

All instrumentation at the KM site and all air quality instruments at LP were purchased using grant funding from the Department of Energy and Climate Change (DECC) and administered through the British Geological Survey (BGS), including the Whole Air Sampling (WAS) system used here to derive concentrations of hydrocarbons in free air. Air inlets positioned on 2 m high pylons draw air into the instruments to record instantaneous concentrations of trace gases and particulate matter in the air moving over the measurement sites with the prevailing wind. Data are recorded locally and also transmitted wirelessly to a

data storage facility, from where the science team can monitor performance and good operation.

Table 3. Measurements at both sites, dates when measurements became active, and measurement frequency (as streamed via the cloud). Note that NMHC refers to non-methane hydrocarbons and PM refers to particulate matter.

Species	Little Plumpton	Kirby Misperton	Frequency
Meteorological Data (T, q, p, 3D wind vector)	Nov 2014	Jan 2015	1 minute
NO, NO ₂ , NO _x	Dec 2015	Jan 2016	1 minute
O ₃	Dec 2015	Jan 2016	1 minute
PM ₁ , PM _{2.5} , PM ₄ , PM ₁₀	Nov 2015	Jan 2016	1 minute
NMHCs	Jan 2016	Jan 2016	weekly
H ₂ S	March 2016	Feb 2016	weekly
CH ₄	Nov 2014	Jan 2016	1 minute
CO ₂	Nov 2014	Jan 2016	1 minute

Both sites employ quality assurance (QA) and quality control (QC) for air quality data covering all aspects of network operation, including equipment evaluation, site operation, site maintenance and calibration, data review and ratification. All instrumental calibrations are traceable through an unbroken chain to international standards to ensure high accuracy and known uncertainty in the gathered dataset. Metadata concerning the precision and guidance on use of the data is prepared for each measurement reported and will be available to view publicly on the British Atmospheric Data Centre (BADC) after final QC approval. Data is checked online initially before being uploaded to the BADC repository will be quality checked.

Site visits occur at least monthly to check the instruments physically and to perform checks on analyser accuracy, precision and response times as well as calibration. A detailed list of calibrations and checks is listed in the Table 4.

Table 4. Detailed descriptions of the QA / QC for data collected at both KM and LP measurement sites.

Parameter	Calibration and maintenance procedure
NO and NO ₂	Traceable calibration cylinders from the National Physical Laboratory. Monthly checks of analyser accuracy, precision convertor efficiency.
Ozone	Six monthly calibration in the field by a calibration unit links to a primary UV photometric standard that is itself calibrated against a certified national source annually at the National Physical Laboratory.
Particulate matter	Six monthly calibration in the field by a monodust (CalDust), monthly maintenance checks
CO ₂ and CH ₄	Calibration of greenhouse gas concentration data is performed by routine reference to certified gas standards, traceable to the World Meteorological Organisation scale. Instrumentation has also been calibrated by transferrable comparison to other calibrated instrumentation in the laboratory prior to installation at the site.

NMHCS	<p>Calibration of NMHCs is performed by reference to an NPL ozone precursor mix. This calibration scale has been adopted by the GAW-VOC network and hence the measurements of NMHCs made by this instrument are directly comparable to those made by all of the WMO-GAW global observatories.</p> <p>Calibrations are performed each month or more frequently if field deployment allows. A long-term data set of the response of the instrument is held and regularly updated to ensure that the instrument responses do not change and to highlight any issues with stability of components within the gas standards used.</p>
-------	--

2.4.3 Data and discussion

This section presents the data collected, to the date of this report (March 2016), at each site in turn and discusses the data in terms of the baseline understanding. Data are interpreted in the context of the local background, and extant local and regional pollution sources that appear to impact the site over the measurement period.

Much of the analysis here relates to what is described as the airmass history. In atmospheric science, the term *airmass history* refers to the character of a volume of air in terms of any impacts on the air's composition as air moves over and through its upwind environment. Airmass composition (e.g. trace gas concentrations) is continually perturbed as air moves through Earth's atmosphere, experiencing chemical and dynamical changes associated with inputs (e.g. pollution sources), chemical modulation (due to atmospheric chemistry), physical modulation (due to dry and wet deposition) and diffusion/ dispersion processes as airmasses mix as a function of the meteorology. The sum of all of these processes results in the measurements that might be seen at a fixed location. Put simply, these impacts - in the context of air pollution - can be additive, representing a mix of pollution added to the airmass as it advects over various sources upwind, subtractive due to chemical and physical removal, and dispersive as airmasses mix with each other.

Detailed airmass characterisation in atmospheric science research requires the use of cutting edge chemical transport models and highly detailed and comprehensive (global) measurement datasets and remains the subject of much academic research well beyond the scope of this report and this project. Therefore, in this project, which is concerned with impacts on the local environment, interpretation is limited to local and regional pollutant sources and a relatively recent airmass history to understand how these factors impact the measurement sites in a statistical framework to obtain a baseline climatology.

2.4.4 Lancashire (Little Plumpton)

2.4.4.1 METEOROLOGY

The principal meteorological variable of interest to baseline characterisation and pollution source interpretation is the local wind speed and direction, as an indicator of the local airmass history. The instantaneous wind speed and direction can point to relatively nearby sources of pollution (within ~ 10 km). When discussing more long-range sources of pollution (such as may be added over cities many 100s of km upwind), the timescales of interest to airmass history typically extend to no more than around 5 days. Beyond this time, the uncertainty in the path of air upwind (and the chemical changes in such air) increases rapidly and interpretation becomes less meaningful. Therefore, our analysis is limited to the utility implicit in these timescales only.

2.4.4.2 CLIMATOLOGY

The wind statistics observed at LP over the full measurement period (4 December 2014 to 14 March 2016) are shown in Figure 23 as a conventional wind rose. This type of illustration simply shows the frequency of instances when wind blows from various directions (seen as the vector and radius). The colour scale then illustrates the corresponding proportion of winds in each direction for a range of surface wind speeds (see colour legend in Figure 23).

As expected at this site (as for any exposed site in the UK) the dominant wind direction is from the western quadrant (~50% of the time), consistent with the UK's location as an island in the Atlantic mid-latitude storm track. This is also the direction from which the strongest winds are observed (red colours in Figure 23), typically coinciding with the passage of mid-latitude cyclones over the UK mainland.

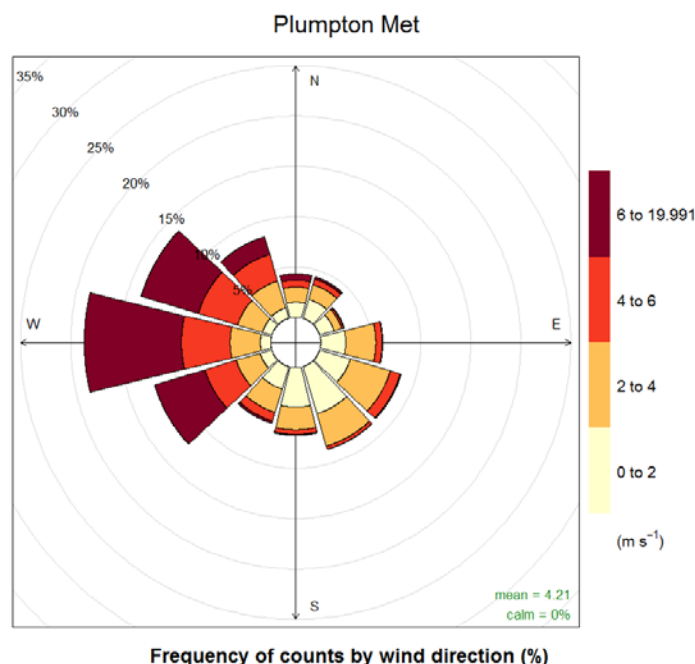


Figure 23. Wind rose for the LP site showing wind speed and direction statistics for the period November 2014 – March 2015. The radius defines the percentage of total time in each of 12 wind direction cones (30 degree span), while the colour scale defines the wind speed (redder colours indicating strong wind speeds $> 6 \text{ ms}^{-1}$ and yellow colours indicating light or stagnant winds. © University of Manchester, 2016.

This has important implications for the local baseline. The position of the LP site near to the Blackpool shoreline means that winds bringing air from the Atlantic will typically carry relatively well-mixed and background airmasses to the measurement site. In this context, a *background* can be conceived to be an airmass relatively unaffected by local or regional pollution sources, broadly representative of the average composition of Northern Hemispheric air at the time. These airmasses often represent the Northern Hemispheric seasonal average concentrations of greenhouse gases especially, as these gases are relatively inert on the time and spatial scales of advection across the Atlantic in mid-latitude cyclones. As these airmasses dominate the statistical climatology at the LP site, the baseline for this wind direction provides a very useful background from which to assess future local changes in pollution sources in the immediate upwind vicinity. The position of the LP site just a few 10s of metres to the east of the proposed Cuadrilla site makes the dominant westerly wind direction highly favourable for any future operational assessment.

Northerly, easterly and southerly winds are less frequent, representing around 15% in each quadrant over the course of the 12 months considered to date. Wind speeds in these quadrants are also typically much lighter (dominated by light breeze winds in the range 2-4

ms^{-1}). This is due to a number of factors: 1) that winds from these directions are moderated by passage over the mainland UK land surface, and 2) that winds from these directions usually represent flow in less frequent high pressure regimes to the north and east or from low pressure systems to the south and west. Light winds from these directions will typically carry airmasses that have spent a significant time in dynamic contact with the surface of the UK mainland and may also represent air that has passed over Western Europe. These airmasses typically contain pollution added to the surface air as they pass over a range of anthropogenic (manmade) and biogenic (natural) sources upwind of the measurement site such as cities, landfill, industry, transport, agriculture etc. This air may be a mix of both local (<10 km distant), regional (UK mainland) and more distant (Western Europe) pollution sources, making it difficult to de-convolve the relative inputs of each. However, the frequency and duration of transient enhancements seen in trace gas concentration data offers important clues on the proximity (and type) of pollution source, as regionally impacted airmasses will typically display broad (longer timescale) and more invariant enhancements relative to background westerly airmasses, while local inputs are often seen as sharper and shorter-lived enhancements (see following section).

Regional and more distant (long range inter-continental) pollution sources are typically interpreted using Lagrangian back trajectories. Back trajectories are a useful indicator of the path that air has taken in the atmosphere up to and over the previous 5 days. Beyond this time, the accuracy of hindcasted trajectories degrades rapidly due to numerical and meteorological uncertainty associated with Lagrangian transport models and the accuracy of reanalysis meteorological data. Put simply, back trajectories attempt to trace back the path of neutrally buoyant single particles in the atmosphere as they are carried on the wind (this is known as Lagrangian advection). Back trajectory models use wind fields from meteorological reanalyses (hindcasted winds calculated by forecast models that use assimilated measured data).

In this analysis, the Hybrid Single Particle Lagrangian Integrated Trajectory Model (HYSPLIT) has been used along with hourly United States National Center for Environmental Prediction Global Forecast System reanalysis meteorological data at a spatial resolution of $0.5^\circ \times 0.5^\circ$. 5-day back trajectories have been calculated with endpoints at the location of the KM site at 6-hourly intervals across the measurement period (1200 trajectories in total between December 2014 and March 2016).

Figure 24 shows the air mass history of air sampled at LP as a function of time throughout the period. This statistical representation of the history of air can be interpreted as a surface “footprint”, illustrating a surface area over which air measured at LP has been influenced by potential surface sources. The left panel of Figure 24 shows the frequency (as a fraction of total time) that air has passed near to the surface in a latitude-longitude grid with a 1-degree latitude/longitude grid spacing. The red colours indicate that air received at LP is most characterised by air that has previously passed over Ireland and the Atlantic Ocean. It also shows less frequent contact with the surface to the north and south west and rare contact with the surface to the east and south east. This pattern is consistent with the analysis and conclusions drawn about the local meteorology earlier and suggests that land-based sources of pollution from the east (over the UK and mainland Europe) are experienced relatively infrequently compared to maritime air received from the west. A more focussed (0.25° degree grid spacing) and local view of this footprint is seen in the right panel of Figure 24, which shows the same general pattern.

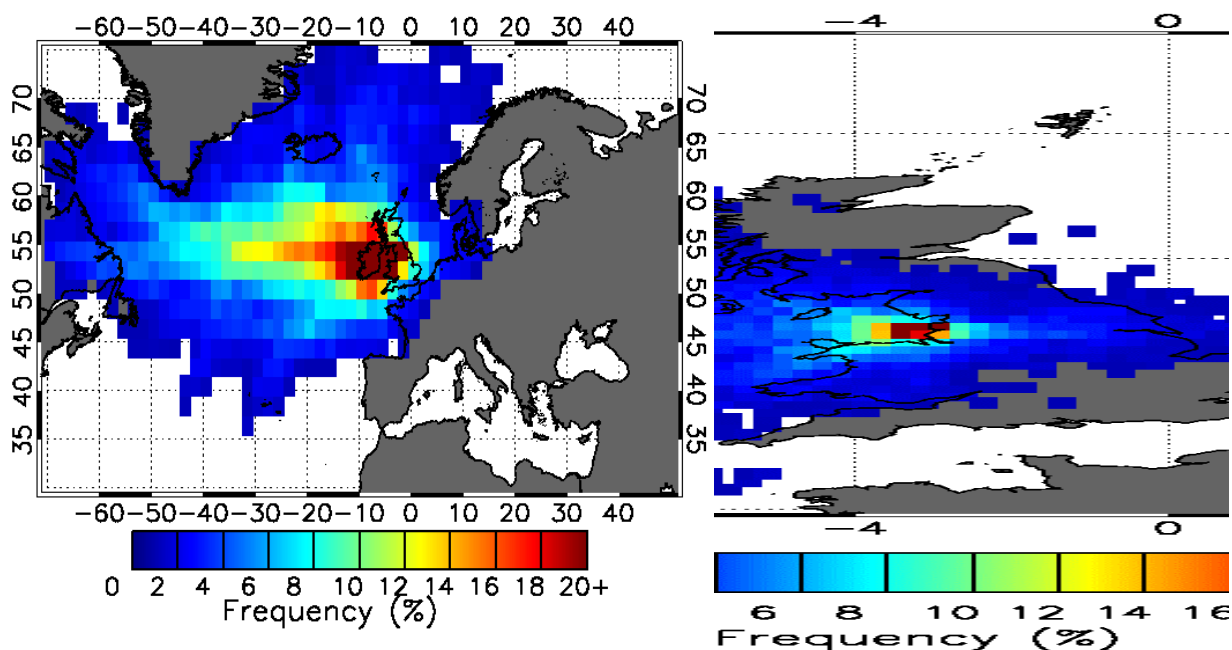


Figure 24. 5-day air mass history surface footprint statistics for the period 13 Jan 2016 to 15 March 2016, as seen from the LP site for an Atlantic scale (left panel - at a spatial resolution of 1 x 1 degree) and the UK National scale (right panel - at a spatial resolution of 0.25x0.25 degree). Frequency refers to the fraction of the total trajectories passing over each grid cell. © University of Manchester, 2016.

2.4.4.3 GREENHOUSE GASES

Figure 25 illustrates the measured ambient CO₂ and CH₄ concentrations at LP as a function of time for the full measurement period. The gap in the data series in January 2015 was due to a power interrupt in the Christmas 2014 period and cannot be reconstructed. Data gaps in May and June 2015, and Aug/Sep 2015, represent periods where data has not yet been quality assured due to technical problems with the UGGA instrument; data for these periods are in the process of being corrected for instrumental drift and may be reconstructable after recalibration of the instrument, which is planned for 2016. Data shortages such as these may be minimised in the remainder of the baseline period after the installation of remote (cloud-based) real-time monitoring of the data stream, which now allows the science team to identify and tackle problems quickly (within days, as opposed to monthly maintenance visits conducted prior to December 2015).

Figure 26 and Figure 27 illustrate how the measured concentrations relate to wind direction. Several important summary features can be seen in this time series when comparing salient concentration features with wind direction:

1. There are clear periods of background - where CO₂ and CH₄ concentrations appear relatively flat at around 400 parts per million (ppm) and 2 ppm (Figure 25), respectively. These periods coincide with westerly winds seen in Figure 26 and represent the seasonal Northern Hemispheric average.
2. There are prolonged periods of marginally enhanced CO₂ and CH₄ (between 400-450 ppm and 2-4 ppm, respectively). These periods coincide most often with moderate easterly and southerly winds.

- There are short-lived (less than a few hours) but large enhancements or “spikes” in the data (greater than 4 ppm CH₄ and 500 ppm CO₂). These coincide most often with light south easterly and northerly wind directions seen in Figure 26.

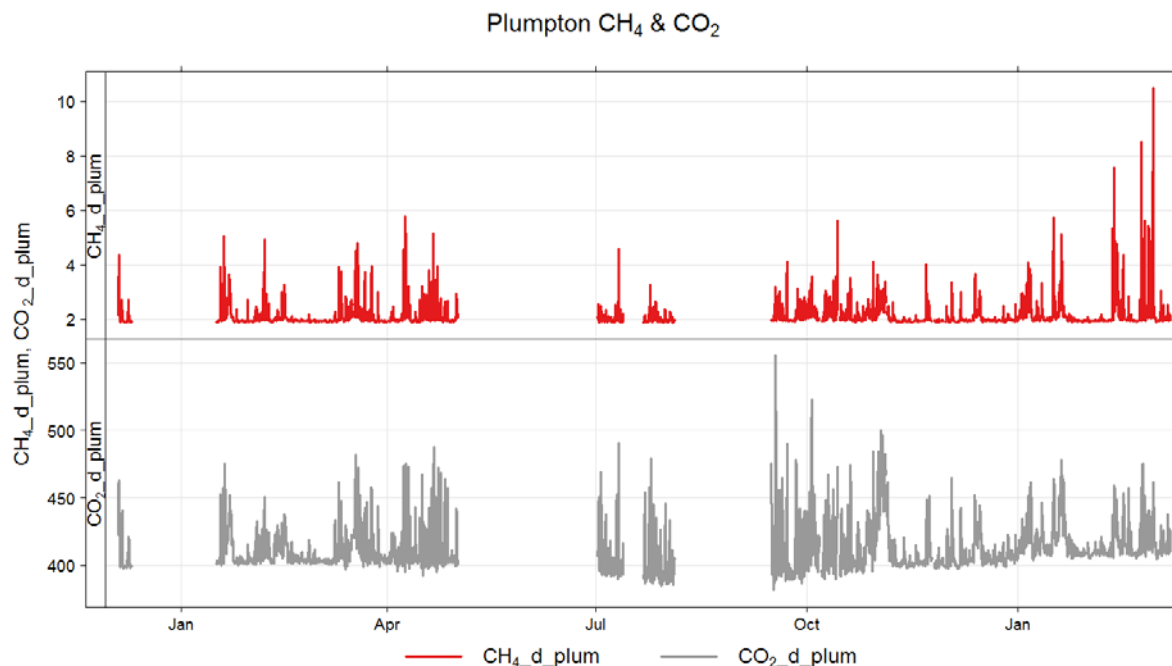


Figure 25. Time series of carbon dioxide (grey) and methane (red) in units of ppm as measured at LP between 4 Dec 2014 and 15 Feb 2016. © University of Manchester, 2016.

Interpreting this further, it can be seen that westerly wind directions invariably bring relatively unpolluted air to the LP site. Other wind directions deliver more complex airmasses likely comprising a wide mix of pollutant sources upwind, both local and regional, requiring additional interpretation (see below).

Figure 28 illustrates the correlation between measured CO₂ and CH₄ concentration in air, colour-coded for sampling density (averaged to one-hourly data intervals from 1 Hz raw data). Warmer colours indicate more frequent sampling. Each count represents 1 hour of measurement. Clear correlations between different trace gases delineate so-called mixing lines. Such correlations (or mixing lines) often correspond to specific airmass types where co-emission or common airmass chemistry may be active. There are two broad correlations and one dominant feature, as follows:

- A dominant mixing line with a relationship of $[CO_2] = 9.8[CH_4] + 386$ – representing co-emission or bulk mixing of CO₂ and CH₄ sources upwind to the east and north east.
- A weaker but clear mixing line with a relationship of $[CO_2] = 4.9[CH_4] + 386$ – representing co-emission or bulk mixing of CO₂ and CH₄ sources upwind to the east and south east as seen in Figure 26 and Figure 27.
- A dominant red cluster centred at ~400 ppm CO₂ and 2 ppm CH₄ – this represents the dominant and frequent background signal seen in westerly Atlantic airmasses (Figure 28). Note that the darkest red colours in this cluster correspond to >25 total days of measurement each.

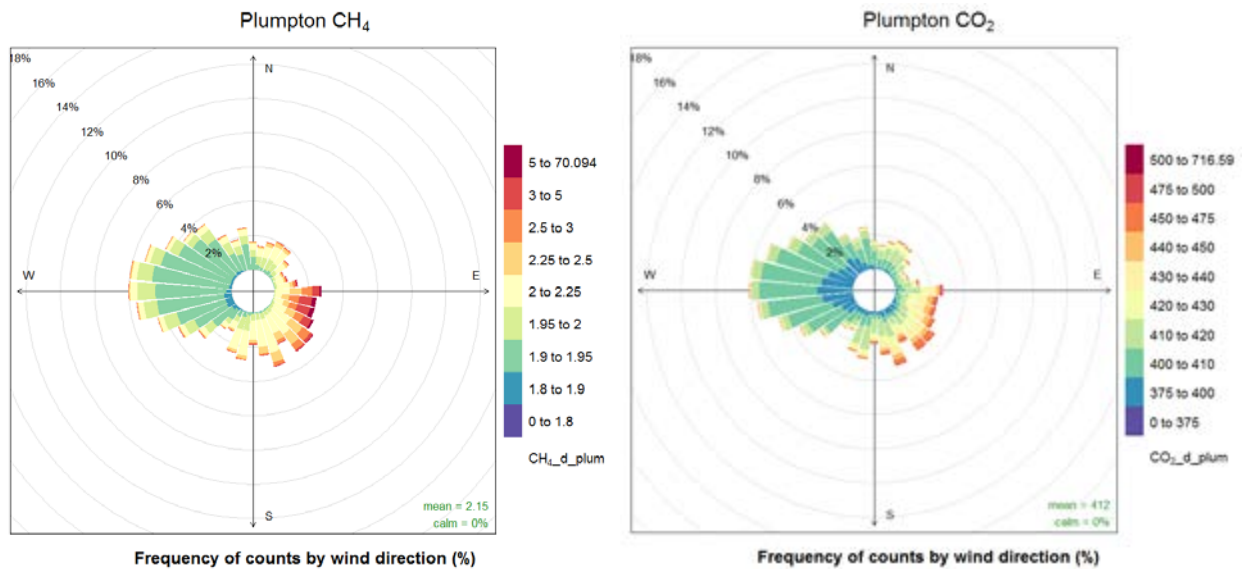


Figure 26. Greenhouse gas concentrations (as per colour scale) in air as a function of wind direction for: left panel - methane (units of ppm), and right panel - carbon dioxide (units of ppm) as measured at LP. © University of Manchester, 2016.

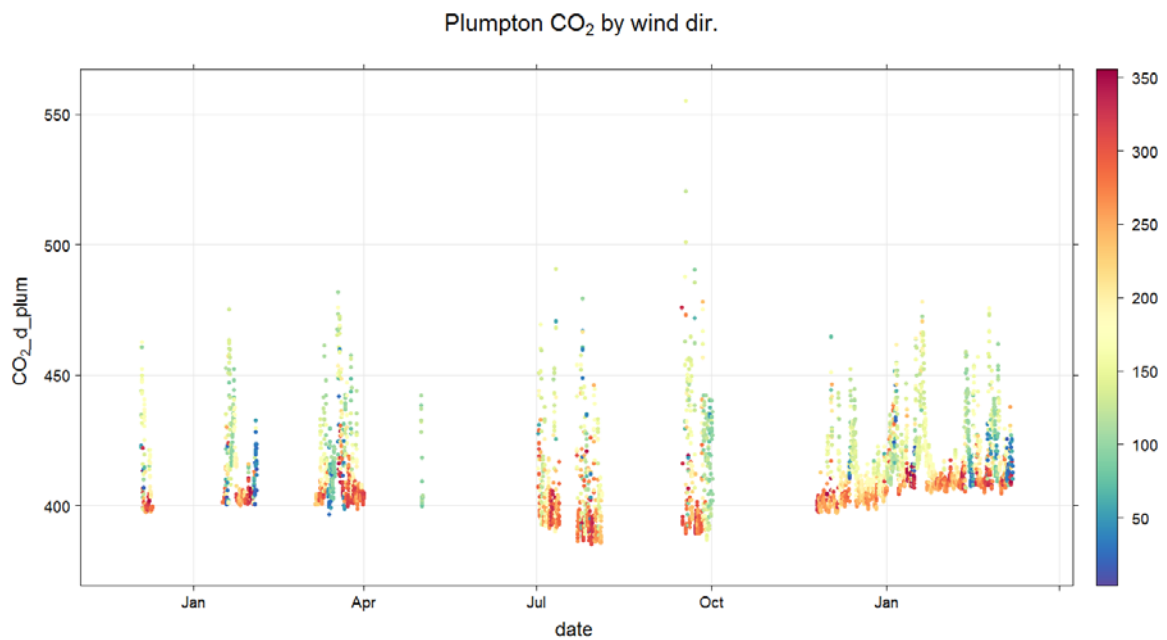


Figure 27. Carbon dioxide concentration time series, colour-coded for wind direction as per legend as measured at LP. © University of Manchester, 2016.

Mixing lines such as these are a powerful differentiator of bulk source types, especially at the regional and national spatial scale. When temporally averaged (as data in Figure 28 have been), they characterise airmasses that have passed over a large fetch of similar pollution source types and where the airmass has had time to mix internally. The two dominant mixing line modes seen in Figure 28 are seen to correspond to the less frequent easterly and south-easterly wind directions. Considering the location of LP, these wind directions represent air that has passed over the Pennines and the cities of Manchester, Leeds and Sheffield in the case of easterlies, and the cities of Birmingham and London in the case of south-easterlies. While cities and infrastructure are a principal source of UK pollution

(including greenhouse gases), biogenic sources such as the biosphere, landfill and agriculture would also be expected to feature in the fetch of such airmasses when upwind of the LP site. The summative mix of all of these longer range pollution types upwind for easterly and south-easterly wind directions gives rise to the dominant (but infrequent) mixing lines observed.

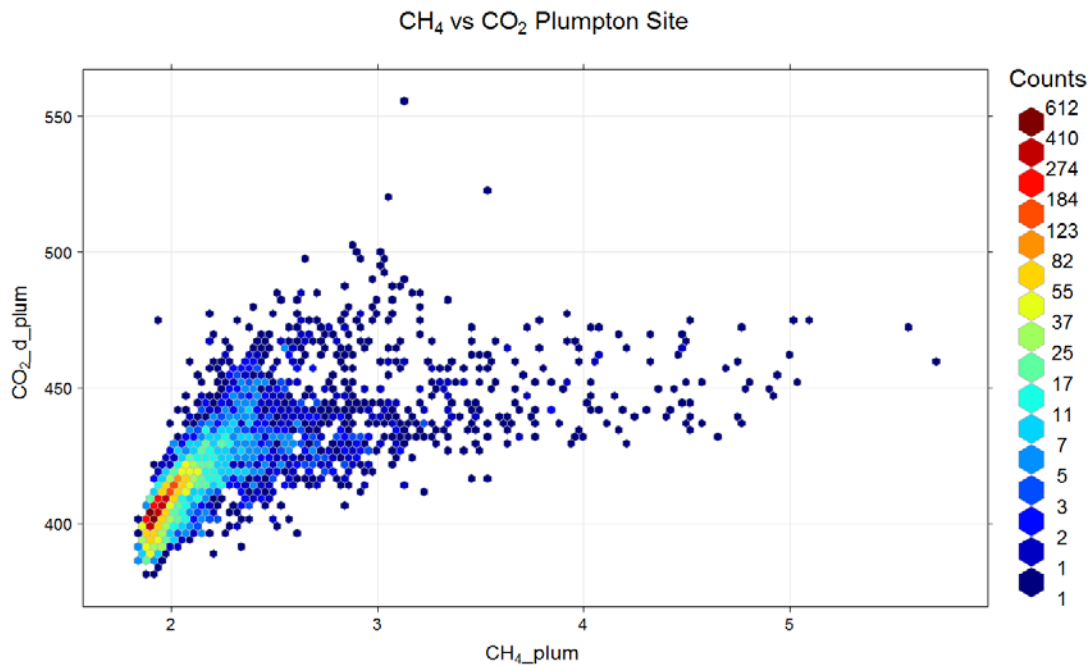


Figure 28. Correlation between CO₂ and CH₄ concentrations measured at LP. Colours indicate the density of sampling (number of coincident measurements). One count refers to a one-hour period of data. © University of Manchester, 2016.

To interpret more local sources of pollution (within ~10 km), the focus needs to be on the more transient features in the high temporal resolution dataset. To do this on an event-by-event basis for a year of data would be meaningless in the context of the baseline analysis here, though event-led (case study) analysis may well be advisable during any operational monitoring. However, it is possible to interpret the relative role of proximal pollutant sources to the overall baseline by considering short-lived but significant excursions from the average baseline and comparing these with wind speed and direction. Figure 29 illustrates a polar bivariate representation of the relationship between both wind speed and direction and greenhouse gas concentration. The colour scale highlights the wind speed and wind direction conditions that dominate the overall concentration average seen at the measurement site (as a weighted mean of concentration \times frequency of occurrence). The red areas seen in both panels (CO₂ and CH₄) correspond to light winds from the south east indicating a well-constrained local source for both gases. Given the site's location, these local sources to the south east are likely to be the nearby farm (on which the site is located) and the nearby A583 road and M55 motorway. The fact that the red area does not extend to higher wind speeds in the south east is consistent with an interpretation that longer range sources of pollution may not contribute significantly to the overall average baseline at the site. However, given that high wind speeds from a south-easterly direction are relatively rare in this dataset, it should be noted that this interpretation may suffer from a lack of robust statistical evidence; and therefore that the role of longer range sources cannot be reliably deconvolved from more local sources at this stage of the analysis. The lighter blue areas seen in Figure 29 to the west indicate a long range and diffuse source consistent with longer range transport of moderately enhanced airmasses, although this sources relative contribution to the baseline is much weaker than those sources to the south east

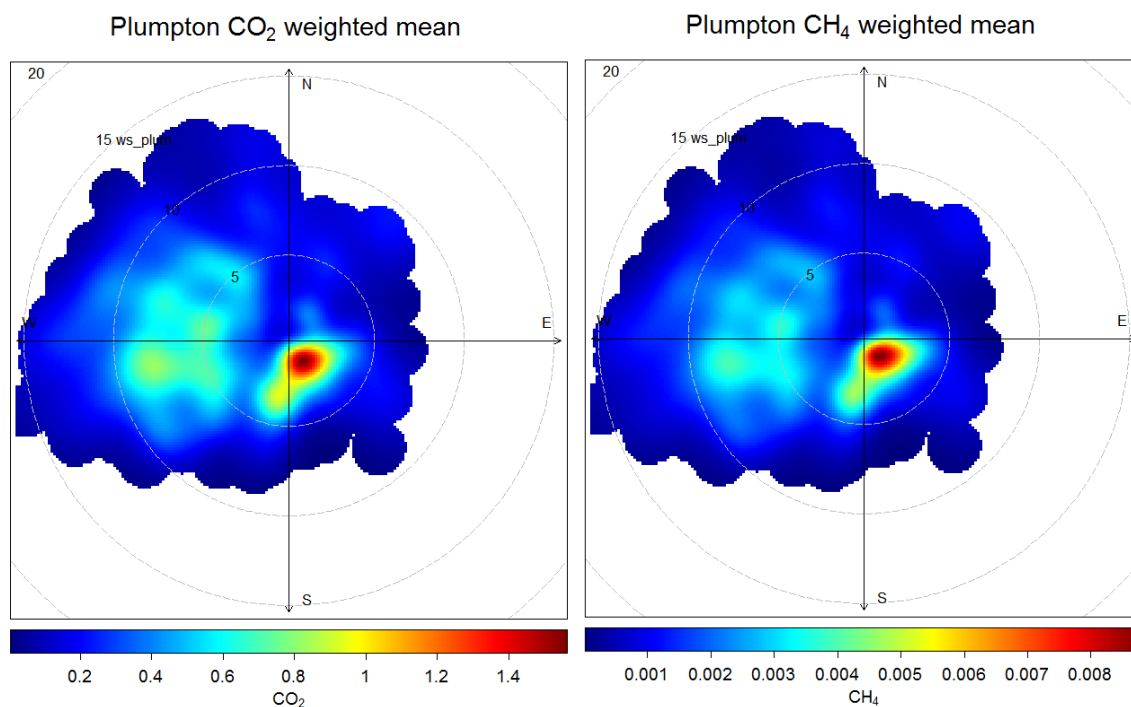


Figure 29. Polar bivariate representation of methane (left) and carbon dioxide (right) as a function of wind direction. The colour scale indicates fraction of total measurement time weighted for concentration. See text for further details. ©University of Manchester, 2016.

2.4.4.4 LITTLE PLUMPTON MOBILE VEHICLE SURVEYS

In addition to the continuous monitoring at the LP site, a mobile vehicle survey was performed by colleagues at Royal Holloway University London (RHUL). This survey was carried out on March 9 and March 10 2016 and consisted of precision methane and methane-carbon-isotopic composition measurements as measured during travel on local roads around the LP site as seen in Figure 30. The purpose of this survey was to establish the influences of local methane sources to the wider LP area and to characterise their carbon isotopic composition. Carbon isotopic composition is a powerful discriminator of methane source type (particularly between thermogenic fugitive emissions and biogenic emission) as each methane source typically has a unique range of carbon isotope composition (particularly carbon-13). The analysis here represents a rapid assessment of this survey given its timing close to the preparation of this report. Further mobile measurements will be carried out in the remainder of the baseline.

The wind was from the north on the 9th March, which should be noted when interpreting the measurements. Measurements to the south of the LP site show near-background methane concentrations (~ 2 ppm), while measurements to the north east of site show elevated concentrations in the range 3-5 ppm due to emission from a landfill site (near Fleetwood) to the north on this day. This local source of methane appears to dominate the extant local methane emissions in the area and may be expected to strongly influence methane measurements during periods of north westerly winds as seen at the permanent LP monitoring site downwind. This further reinforces our recommendation that westerly winds represent optimal operational monitoring conditions in order to isolate shale-specific sources should they proceed.

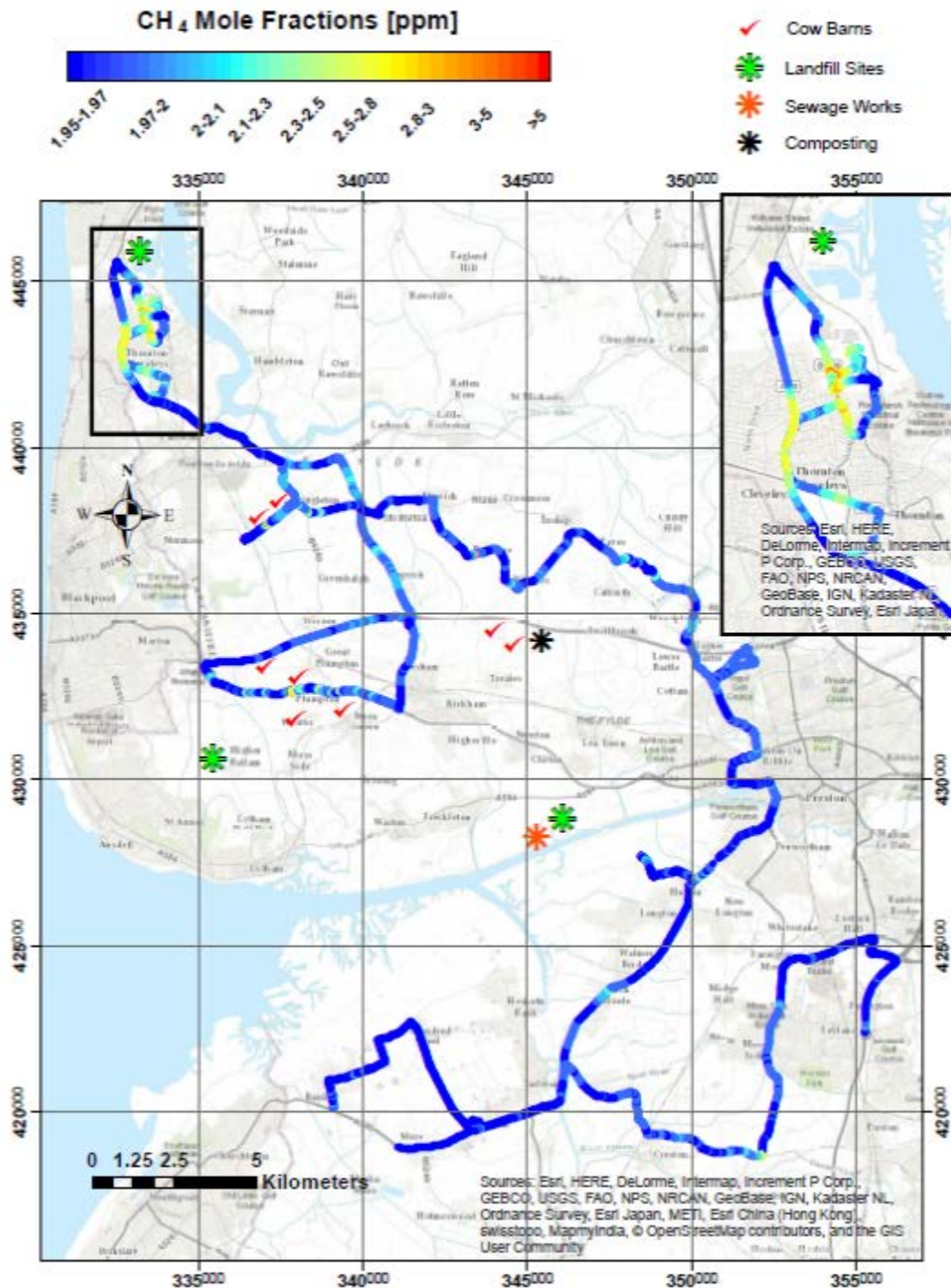


Figure 30. Mobile vehicle survey of methane concentrations around the local area of the LP site on March 9th 2016. Local features such as landfill, agriculture and sewage installations are marked on the map as per legend. © Royal Holloway Univ London, 2016.

Carbon-isotopic signatures for these local sources are displayed in Table 5 and in Figure 31 below. The landfill carbon-13 depletion measured near to LP (at the Fleetwood landfill site) is typical for other UK landfills measured by the RHUL team. Other point C-13 measurements indicate small fugitive emission from existing natural gas infrastructure in the area and represent typical depletion ranges for the northern UK natural gas supply chain. The compost and sewage infrastructure gave a similarly typical signal. Local cow barns

display an isotope signature that suggests that these emissions contain a larger waste (excrement) than breath component compared to previous experiments by the RHUL team; however the magnitude of such emissions remains small compared with the dominance of the Fleetwood landfill site.

Table 5. Carbon-13 (in methane) depletion measurements and uncertainty statistics (mean and 2 standard deviation uncertainty) for local methane sources around the LP site from mobile surveys on 9 March and 10 March 2016.

CH ₄ Source	$\delta^{13}\text{C}$ Signature (2sd)
Landfill	-57.3 ± 1.0
Cow Barns	-58.0 ± 1.6
Compost	-51.6 ± 0.3
Gas Leaks	-41.2 ± 0.7

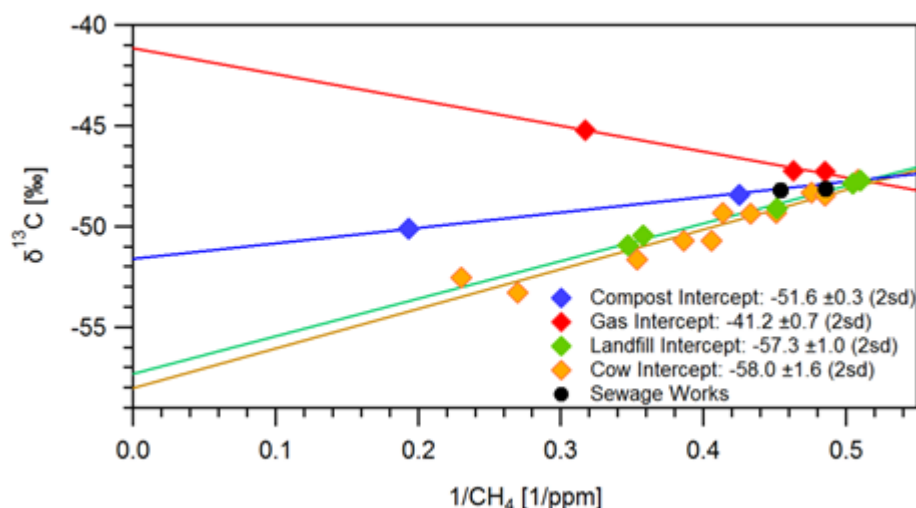


Figure 31. Keeling plot of carbon-13 (in methane) depletion for local sources of methane measured around the LP site as measured by mobile vehicle surveys on 9th and 10th March 2016. © Royal Holloway Univ London, 2016.

2.4.4.5 GREENHOUSE GAS ANNUAL STATISTICS

Greenhouse gas background concentrations are also linked to a range of natural and human-related cycles corresponding to net sinks and emissions of each gas. These can vary from diurnal (daily) cycles in emissions of CO₂ associated with traffic for example, to seasonal cycles associated with the respiration of the biosphere. These temporal cycles for LP will be discussed in Section 2.4.5.10 when comparing measurements for both measurement sites. However, the annualised statistical concentrations of CO₂ and CH₄ at LP are shown in Table 6, which encapsulate the range of this natural variability.

Table 6. Statistical metrics for greenhouse gases measured at LP. Percentages represent percentile thresholds.

Compound	10%	25%	33%	Mean	75%	90%	95%
CH ₄ (ppm)	1.93	1.94	1.95	2.22	2.12	2.68	3.66
CO ₂ (ppb)	399.13	402.52	403.74	412.83	418.16	435.12	447.34

2.4.4.6 GREENHOUSE GAS SUMMARY

In all cases, it must be stressed that the levels of greenhouse gas concentrations seen at this site do not represent any known hazard to human health and are well within the typical range seen for any land-based measurement site. Even the largest transient enhancements seen in the collected dataset are in what would be considered to be a normal modern range and the conclusions drawn in this report on the existing sources of local pollution do not indicate any cause for local alarm.

To summarise, the purpose of this analysis is to establish the baseline climatology for the area to allow future comparative interpretation. In the context of greenhouse gases, this concerns the future quantification of greenhouse gas mass flux to atmosphere (fugitive emissions) from shale gas operations.

2.4.4.7 AIR QUALITY

Air quality data have only been available for the LP site since November 2015. The data collected between 25th November 2015 and 11th March 2016 are described in the following sections. Future interpretation will match (and add to) that of the greenhouse gas dataset in the previous section, as collected so far. As a detailed analysis is not yet possible, metrics and cycles (in the period of available data) are shown, along with some highlights from the current (and ongoing) data set.

2.4.4.8 METRICS

Metrics for the parameters measured at LP are displayed in Table 7.

Table 7. Statistical metrics for air quality pollutants measured at LP. Percentages represent percentile thresholds. Note that LOD refers to a measurement below the instrumental detection limit.

Compound	10%	25%	33%	Mean	75%	90%	95%
O ₃ (ppb)	11.37	23.77	27.43	33.32	38.85	41.21	42.73
NO (ppb)	0.08	0.19	0.26	0.54	1.26	3.17	7.68
NO ₂ (ppb)	LOD	LOD	0.13	0.96	4.65	12.99	18.93
NO _x (ppb)	LOD	0.20	0.59	1.60	5.72	17.36	26.15
PM ₁ (µg / m ³)	1.06	1.82	2.23	3.01	5.93	12.38	18.12
PM _{2.5} (µg / m ³)	1.92	3.31	4.04	5.57	9.40	14.49	19.59
PM ₄ (µg / m ³)	2.54	4.47	5.49	7.66	11.97	17.64	21.26

PM₁₀ (µg / m³)	3.14	5.61	6.73	9.12	13.90	19.91	23.79
PM_{total} (µg / m³)	3.69	6.55	7.80	10.55	15.87	22.34	26.43
Particle Count (particles / cm³)	15.52	22.70	27.29	41.86	143.30	369.60	490.53

2.4.4.9 TIME SERIES AT LP

Figure 32 shows the time series for O₃, NO, NO₂, NO_x, PM₁, PM_{2.5}, PM₄, PM₁₀ and particle count for LP. The data gap in the NO_x time series is due to an instrument problem, other than that a full dataset is available from December 2015 - present.

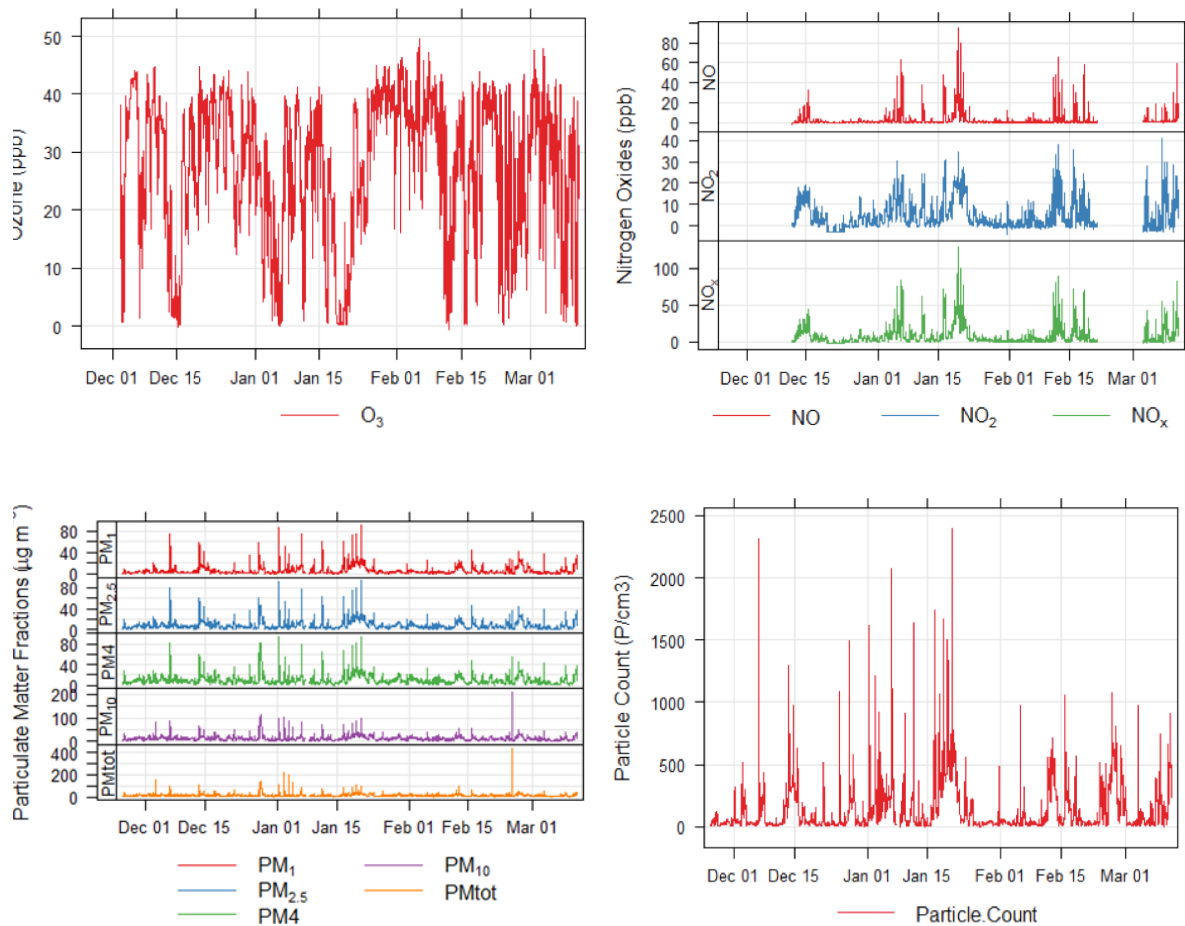


Figure 32. Time series for air quality trace gas concentration data at the LP site. © Univ York, NCAS, 2016.

2.4.4.10 DIURNAL VARIATION AT LP

The diurnal variation for the air quality data is shown in Figure 33. The O₃ concentration reduces at night and peaks just after midday, as expected in the general context of UK oxidative air chemistry. The NO_x data displays a peak in the morning and a smaller peak in the afternoon, showing that the site has a “rush hour” effect as a consequence of having a major road nearby. The A585 Preston New Road runs alongside the site to the south, which is the likely reason for this; and in further analysis of existing baseline conditions, this will have to be taken into account. Particulate Matter (PM) are also seen to increase in tandem with other trace gas variables, with PM₁₀ the most affected; with a longer dataset further analysis will be possible, for example separation of source types based on PM size characteristics and temporal trends.

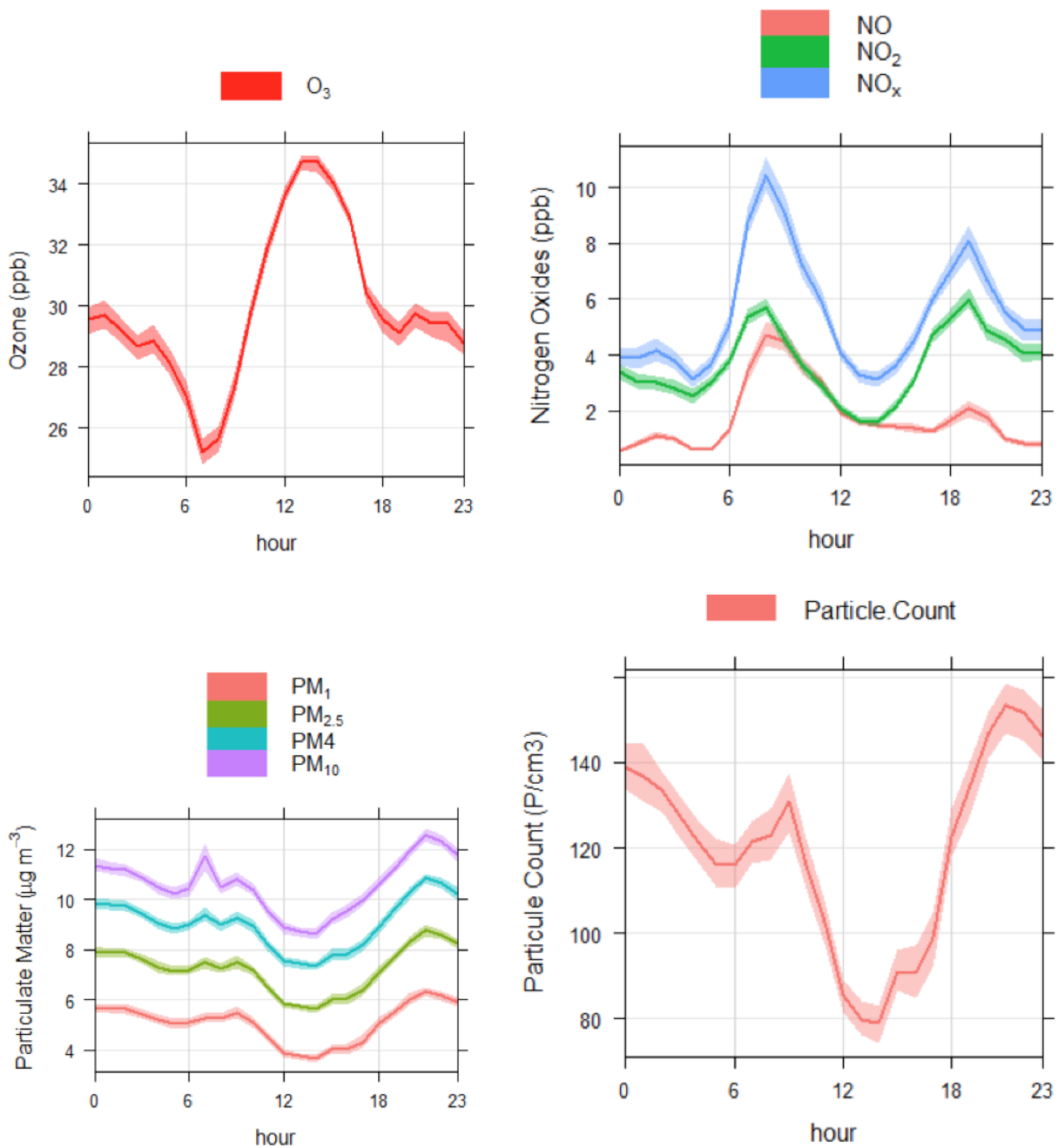


Figure 33. Diurnal variations for the air quality measurements at LP. © Univ York, NCAS, 2016.

2.4.4.11 HEBDOMADAL VARIATION AT LP

The hebdomadal variation is shown in Figure 34. Caution should be taken when interpreting the plots at this stage due to the small dataset. The NO_x concentrations do however appear to reduce at the weekend and O₃ is lowest on a Friday. This may be traffic related but more data are needed to confirm this along with more analysis of PM concentration data.

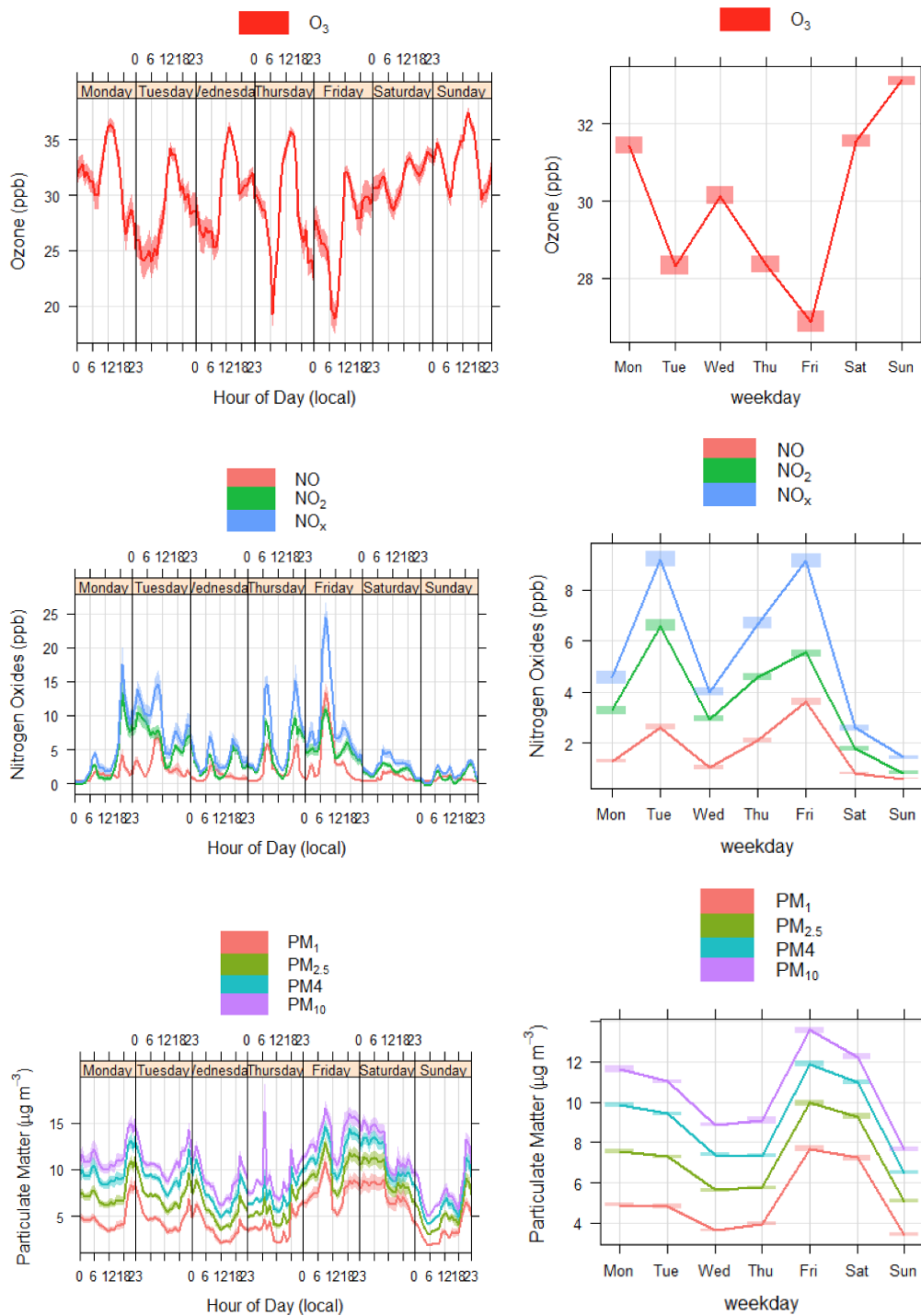


Figure 34. Hebdomadal variations for the air quality measurements at LP. © Univ York, NCAS, 2016.

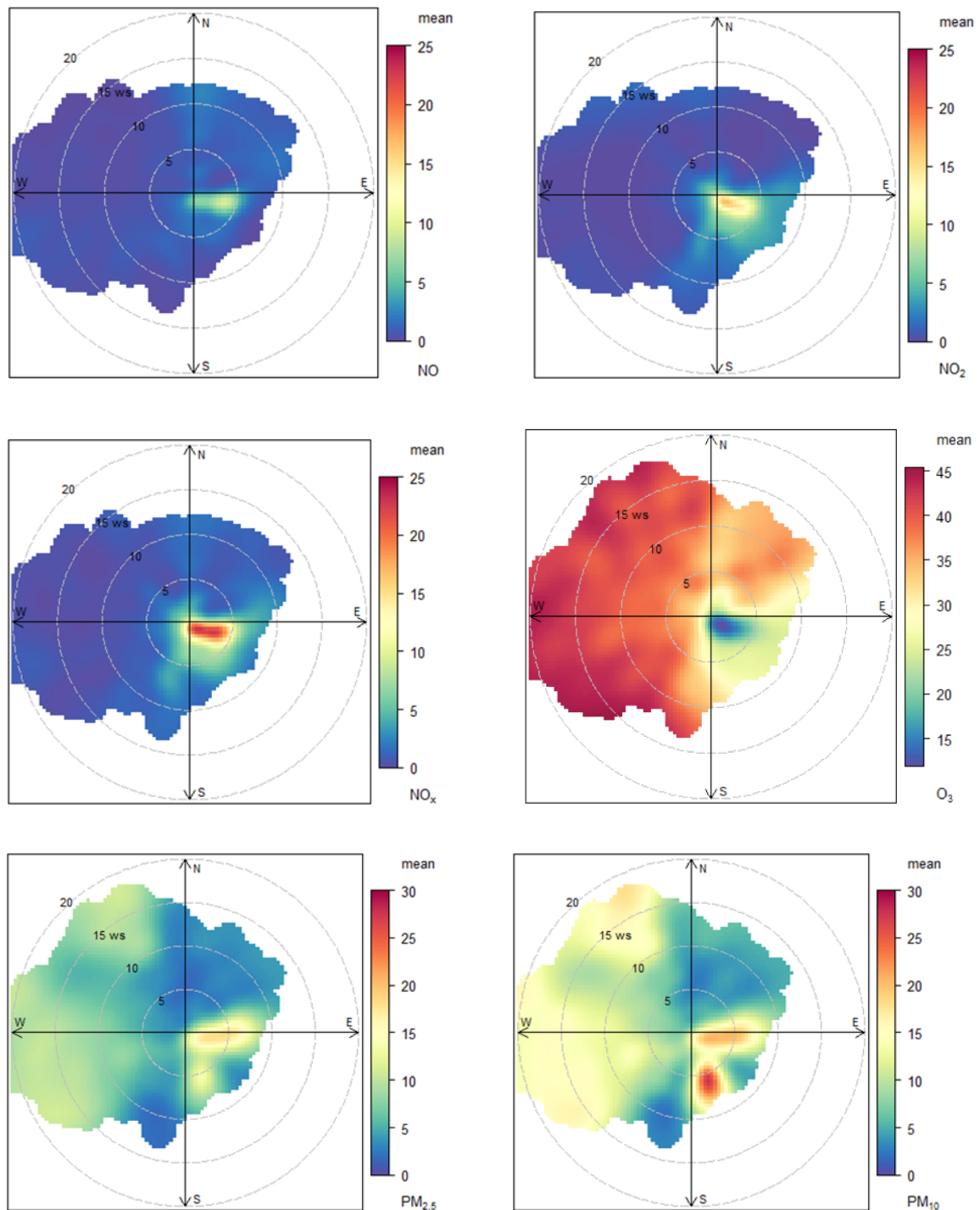


Figure 35. Polar plots for NO, NO₂, NO_x, O₃, PM_{2.5}, PM₁₀ at the LP site. © Univ York, NCAS, 2016.

2.4.4.12 SOURCE APPORTIONMENT

Weighting the concentration by the frequency of occasions that wind has been observed from various directions and wind speeds can give a clearer idea of the conditions that dominate the overall mean concentrations and can reveal useful features about different sources. As discussed previously in the meteorology analysis, LP is close to the west coast of the UK and the dominant wind direction of westerlies brings Atlantic air which is well mixed and can be classed as a “background” air mass. This is highlighted in the air quality measurements shown in Figure 35. The ozone shows elevated typical maritime

concentrations when the wind is at its highest speed (20 ms^{-1}) and from the west. This elevated ozone is indicative of an aged air mass and is broadly reflective of prevailing Atlantic ozone at this time. The influence of the Atlantic air is also shown in the PM measurements, which are all enhanced in the higher wind-speed westerly air masses, particularly in the coarser fraction arising from maritime aerosols.

Local influence is also shown in Figure 35. The less frequent winds from the south and east bring a mix of locally and regionally polluted air masses to site. This is in agreement with the greenhouse gas measurements. The influence of the road running alongside the site has been mentioned previously and will be one of the sources of the local NO_x .

2.4.4.13 NONMETHANE HYDROCARBONS

There is not a sufficient NMHC sample size for the LP site to permit further useful analysis at this stage.

2.4.4.14 CONCLUSIONS (LITTLE PLUMPTON SITE, LANCASHIRE)

To summarise the findings to date at the LP site:

- Meteorology appears dominated by a westerly flow bringing Atlantic background air to the measurement station.
- Less frequent winds from the east and south east bring a mix of local and regionally greenhouse-gas-enhanced airmasses to the site, with current analysis suggesting that local sources such as nearby agricultural infrastructure and a landfill site near to Fleetwood to the north west (~10 km distant) dominate the contribution to the current baseline statistical variability. Sources of natural gas infrastructure fugitive emission are evident in a singular mobile survey but do not represent significant emission compared to other local methane sources.
- The position of the site (to the east of proposed shale gas activity) makes this site ideally placed for any future operational monitoring by taking advantage of the relatively unpolluted maritime air arriving from the west (also the dominant wind direction). Operational assessment could use these westerly wind directions for optimal case study conditions to minimize the need to account for extraneous pollution sources known to exist when sampling air from other wind directions. This would allow more accurate interpretation of shale-specific emissions if such activity goes ahead.
- Current concentrations of greenhouse gases and air quality trace gases are within a typical range for a UK semi-rural environment in our academic and research experience, and at higher wind-speeds in westerlies are reflective of typical North Atlantic conditions.

2.4.5 Kirby Misperton

Data from Kirby Misperton (KM) hasve only been collected since January 2016 so detailed seasonal and trend analysis is not currently possible. The available data are shown below and highlights so far have been identified. Future interpretation will match (and add to) that for LP.

2.4.5.1 METEOROLOGY

Wind direction was previously analysed as part of the work conducted for rationale of site location. This indicated over the full year that the dominant wind direction was NE. Data for the first few months of measurement at KM are shown in Figure 36. This shows that over

the winter 2015/16 period the dominant wind direction was from the south west quadrant (~40%), which is also the direction from which the strongest winds were observed. This is consistent with expectations given the vigorous Atlantic storm track during the winter.

Northerly and easterly winds have been less frequent in the first few months of operation and generally display lower wind speeds.

A time series showing air pressure and temperature is shown in Figure 37. Temperature ranges from below 0 °C to 14 °C.

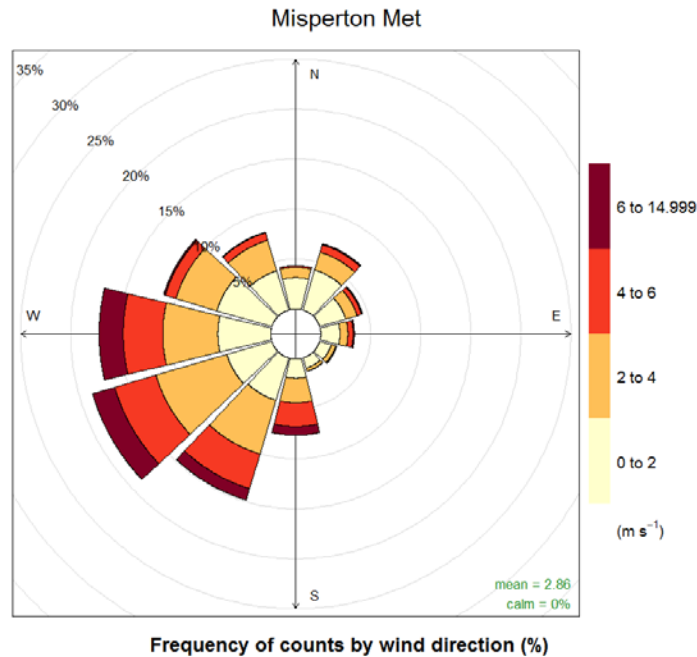


Figure 36. Wind rose for the LP site showing wind speed and direction statistics for the period January 2016 – 10 March 2016. The radius defines the percentage of total time in each of 12 wind direction cones (30 degree span), while the colour scale defines the wind speed (redder colours indicating strong wind speeds > 6 ms⁻¹ and yellow colours indicating light or stagnant winds. © University of Manchester, 2016.

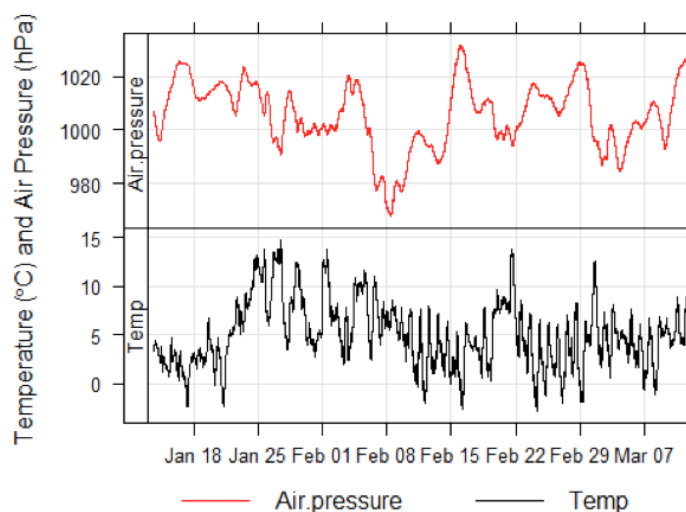


Figure 37. Temperature and Air Pressure time series for the KM site. © University of Manchester, 2016.

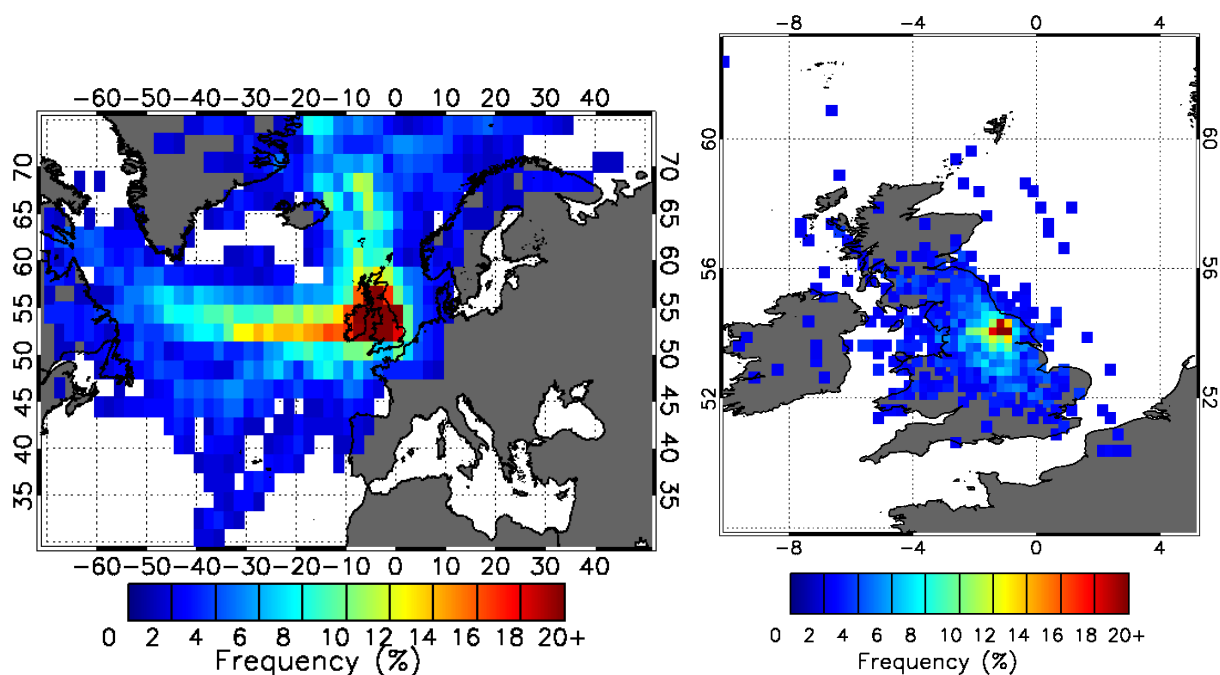


Figure 38. 5-day airmass history surface footprint statistics for the period 13 Jan 2016 to 15 March 2016, as seen from the KM site for an Atlantic scale (left panel - at a spatial resolution of 1 x 1 degree) and the UK National scale (right panel - at a spatial resolution of 0.25x0.25 degree). Frequency refers to the fraction of the total trajectories passing over each latitude-longitude grid cell. © Univ Manchester, 2016

Airmass history and surface footprints for KM are shown in Figure 38. These are analogous to those shown for the LP site in Figure 24. Despite the shorter time period, the patterns in footprint are broadly comparable at the Atlantic scale (left panel of Figure 38), with dominant influence from the west and south west; but with a stronger influence from the north Atlantic and Arctic regions. At the national scale (right panel of Figure 38), we observe a broad footprint covering much of central and eastern England. The stronger influence of the UK mainland in the footprint of the KM site suggests that this location may be subject to a wider range of regional (UK mainland) sources of pollution and emission when compared with the LP site, even for westerly wind directions where the cities of northern and north west England may feature in the fetch upwind. This may mean that the baseline for KM will be significantly different to that for LP and that the two baselines are not spatially transferable. However, the full 12-month baseline will allow further insight into this possibility.

2.4.5.2 GREENHOUSE GASES

Greenhouse gas concentrations have been measured at LP from 13 January 2016. A time series of the data collected to the date of writing are shown in Figure 39. A general correlation between variability in CO₂ and CH₄ can be seen, consistent with that seen for the LP site. Figure 40 illustrates how the measured concentrations relate to wind direction. Unlike the LP site, this figure illustrates that wind directions, from which enhanced greenhouse gas concentrations are observed, display a much more variable character consistent with the different footprint seen discussed above in relation to Figure 38. Excursions from background are seen for every wind direction but with a more dominant mode for south westerly winds (albeit for the very limited dataset).

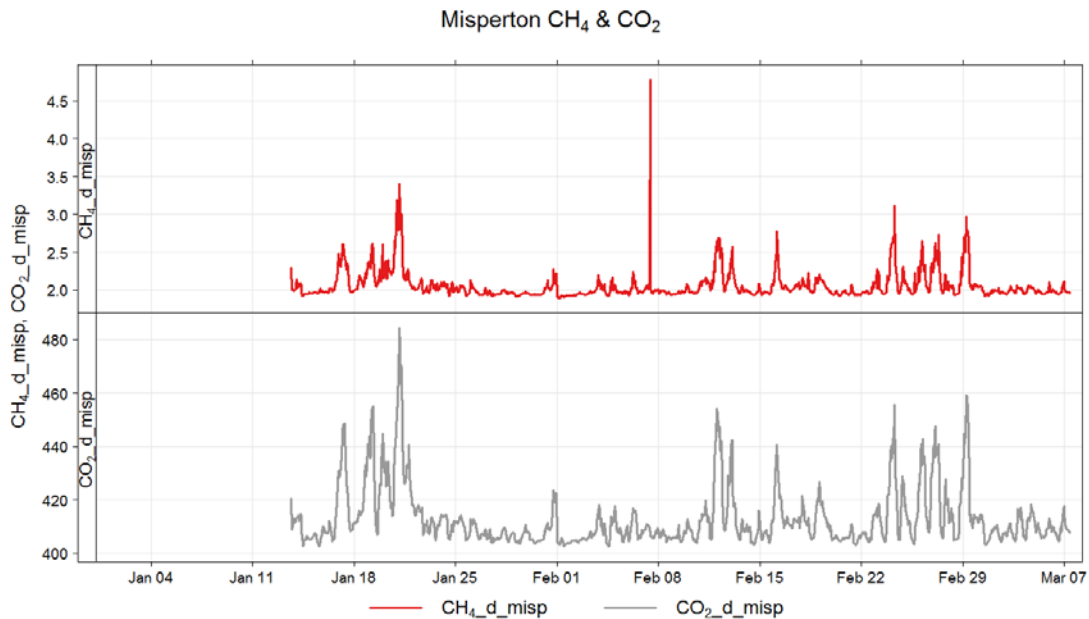


Figure 39. Time series of methane (red) and carbon dioxide (grey) concentration in air measured at KM. Units are parts per million (ppm). © Univ Manchester, 2017

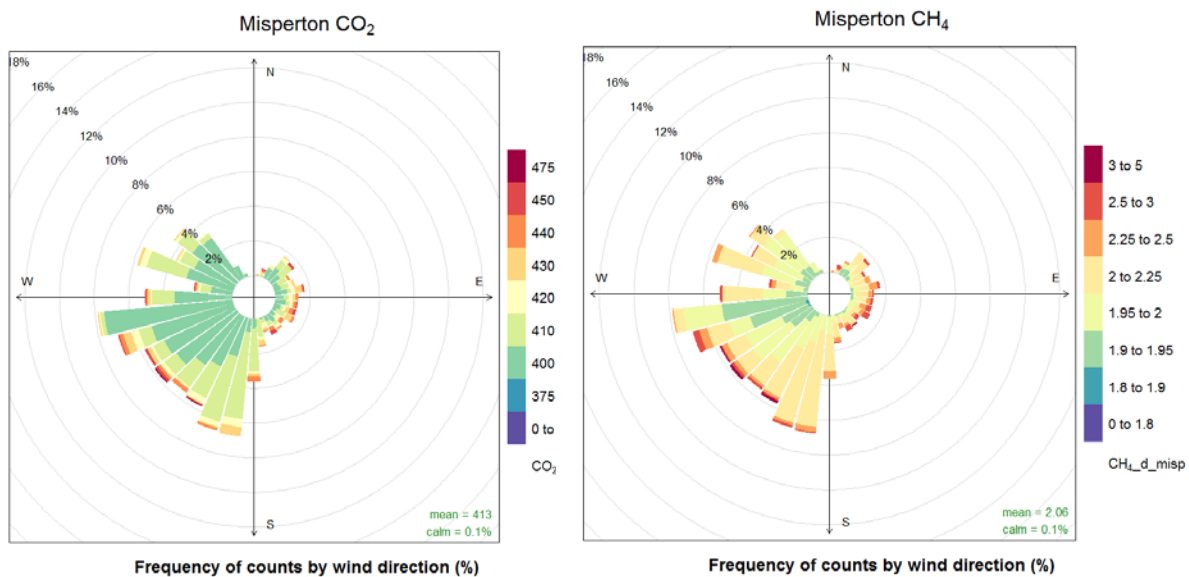


Figure 40. Greenhouse gas concentrations (as per colour scale) in air as a function of wind direction for: left panel - methane (units of ppm), and right panel - carbon dioxide (units of ppm), as measured at KM. © Univ Manchester, 2017

Figure 41 illustrates the correlation between CO₂ and CH₄, colour-scaled for sampling density, analogous to that presented for LP in Figure 28. A dominant mixing line can be seen, with a relationship of $[CO_2] = 20.1x [CH_4] + 403$ ppm. This is more than twice the gradient of that observed in the dominant mixing line seen in Figure 28 for LP, suggesting that sources of CO₂ in mixed (greenhouse-gas-enhanced) airmasses sampled at KM contribute more strongly to air sampled at KM compared with LP. This may be expected due to the long range input of UK cities to the south and south west of the site, compared with LP. However, the dominant red and yellow cluster at background concentrations around 2 ppm [CH₄] and 405 ppm [CO₂] represents ~55 days of total measurement time in

this 60 day dataset. This implies that despite the enhanced role of UK land-based pollution sources on this receptor site compared with LP, the dominant climatology is still represented by a Northern Hemispheric seasonal average for dominant westerly wind directions.

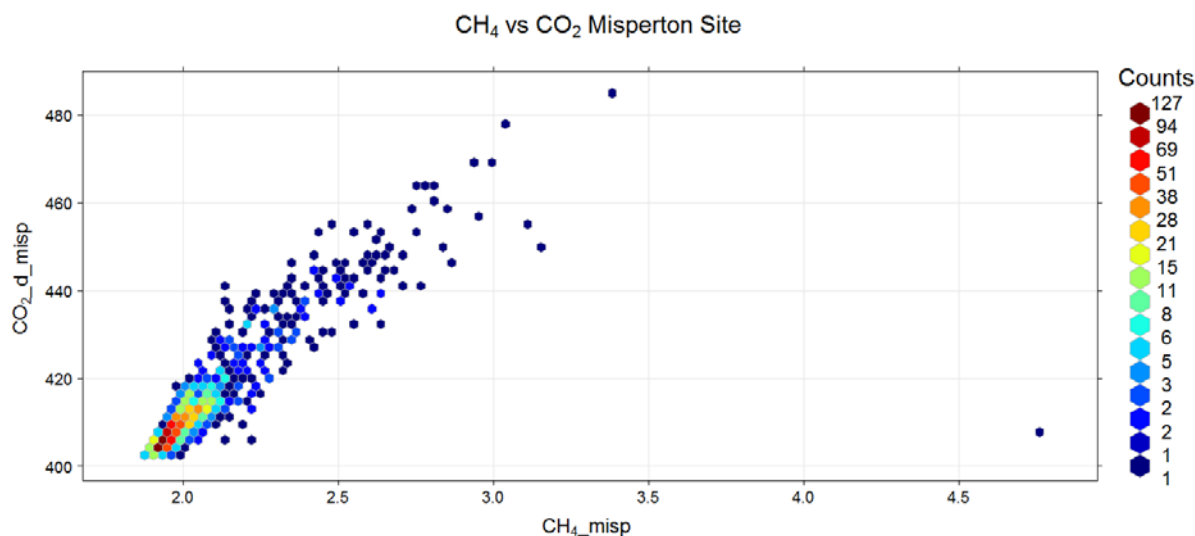


Figure 41. Correlation between CO₂ and CH₄ concentrations measured at KM. Colours indicate the density of sampling (number of coincident measurements). One count refers to a one-hour period of data. © Univ Manchester, 2017

Concentration statistics for the KM greenhouse gas dataset thus far in the baseline study are presented in Table 8. Statistical metrics for greenhouse gas concentrations measured at KM. Percentages refer to percentiles (to 2 d.p) below. The mean concentration of methane is similar to the Northern Hemispheric seasonal average of ~1.9 ppm, while the carbon dioxide site average is marginally enhanced relative to this wintertime hemispheric average (~402 ppm). Extremes in the dataset represent modest enhancements on this background and reflect upwind inputs, which appear to be dominated by the cities of the UK mainland. Unlike the LP site, larger local sources of methane such as nearby agriculture do not appear to contribute significantly to the dataset.

Table 8. Statistical metrics for greenhouse gas concentrations measured at KM. Percentages refer to percentiles (to 2 d.p)

Compound	10%	25%	33%	Mean	75%	90%	95%
CH ₄ (ppm)	1.94	1.96	1.97	2.06	2.08	2.26	2.45
CO ₂ (ppb)	404.73	405.93	406.92	412.97	414.30	428.40	439.25

2.4.5.3 AIR QUALITY

The data at KM has been collected for 3 months (two and a half months available for analysis at the time of this report). Full detailed analysis is not possible at the time of writing. Instead potential areas of interest are highlighted.

2.4.5.4 METRICS

Metrics for the parameters measured from January to mid-March at KM are displayed in Table 2.

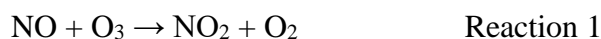
2.4.5.5 TIME SERIES

Figure 42 shows the time series for O₃, NO, NO₂, NO_x, PM₁, PM_{2.5}, PM₄, PM₁₀ and particle count for KM. The data gap in the PM and particle count is due to an instrument problem - the FIDAS instrument had to be removed from site and sent back to the manufacturer in Germany due to a fault.

Table 9. Statistical metrics for air quality pollutants measured at KM. Percentages refer to percentiles. LOD refers to measurements below the limit of detection of the instrument.

Compound	10%	25%	33%	Mean	75%	90%	95%
O ₃ (ppb)	13.36	21.35	23.93	28.92	34.01	38.44	40.53
NO (ppb)	LOD	0.03	0.05	0.10	0.27	0.83	1.66
NO ₂ (ppb)	LOD	0.37	0.63	1.27	2.61	4.97	6.54
NO _x (ppb)	LOD	0.41	0.68	1.41	2.92	5.51	7.86
PM ₁ (µg / m ³)	1.17	2.17	2.92	5.19	13.10	23.53	29.71
PM _{2.5} (µg / m ³)	1.78	3.08	3.87	6.57	14.49	24.94	31.76
PM ₄ (µg / m ³)	2.28	3.86	4.84	7.79	15.66	26.00	33.15
PM ₁₀ (µg / m ³)	2.79	4.55	5.80	8.98	17.68	27.85	34.83
PM _{total} (µg / m ³)	3.17	5.34	6.75	10.29	19.75	30.78	38.26
Particle Count (particles / cm ³)	28.83	57.92	78.73	154.20	407.60	573.96	682.93

From the time series it can be observed that there are times when the site is affected by higher levels of pollution in the form of NO, NO₂ and particles, visible in the spikes in Figure 42. The majority of the high NO_x spikes seen in the data are due to local influence and were found to coincide with vehicle movements on site. These NO_x spikes are also correlated with lower ozone, which is related to atmospheric chemistry; in the immediate vicinity of high NO emission, O₃ is lost in the reaction 1:



All plant activity on site at KM is logged by Third Energy which is provided to the University of York team when requested. This site data will be used in future analysis to pick out periods of site activity that are affecting measurements (e.g. vehicles moving around on site).

2.4.5.6 DIURNAL CYCLES

Diurnal cycles for the air quality parameters are shown in Figure 43. No data are shown for the PM or particle count due to the limited dataset available. The ozone diurnal cycle at KM

is very similar to LP with a peak just after midday and the O₃ decreasing at night. The NO_x data does show an evening peak, but it is a later than a traditional city / town rush hour so may be reflective of commuting patterns over longer distances with later arrival times. More measurements of both NO_x and PM are required to make further conclusions.

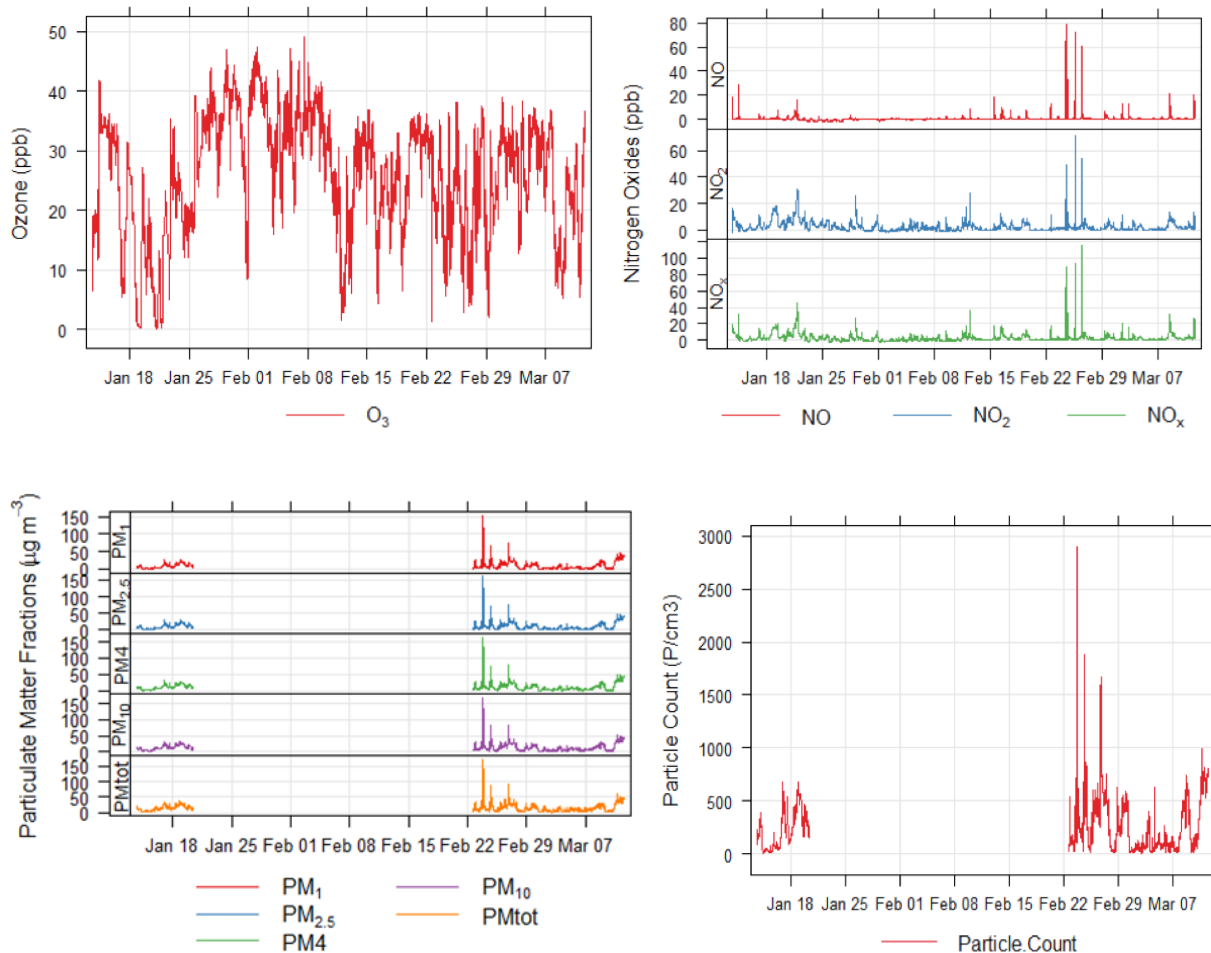


Figure 42. Time series for the current set of air quality measurements at the KM site. © Univ York, NCAS, 2016.

2.4.5.7 HEBDOMADAL CYCLES

As with the diurnal cycles, hebdomadal cycles are only shown for O₃ and NO_x (Figure 23). Similar to LP the ozone decreases through the working week but the NO_x displays a different pattern. The NO_x concentrations appear thus far to be lower at KM than LP. There are simultaneous peaks in NO and NO₂ Monday to Friday, potentially related to local traffic and works on site; this will be explored further

2.4.5.8 SOURCE APPORTIONMENT

Although a more detailed analysis cannot be completed due to the limited amount of data available, plots to show possible sources are shown below. These polar plots show how concentrations vary by wind speed and direction (Figure 45). As with the LP site, when the wind comes from the west at higher wind speeds (15 m/s) the O₃ is at its maximum concentration.

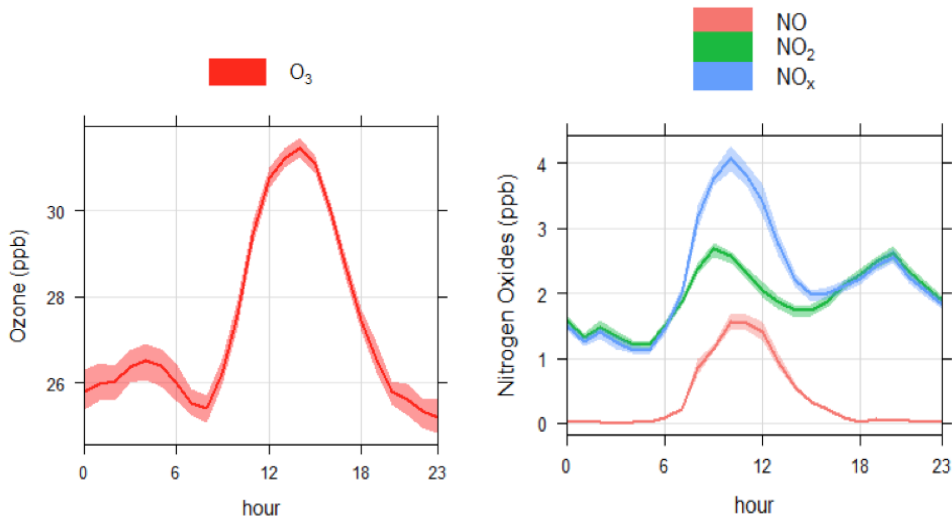
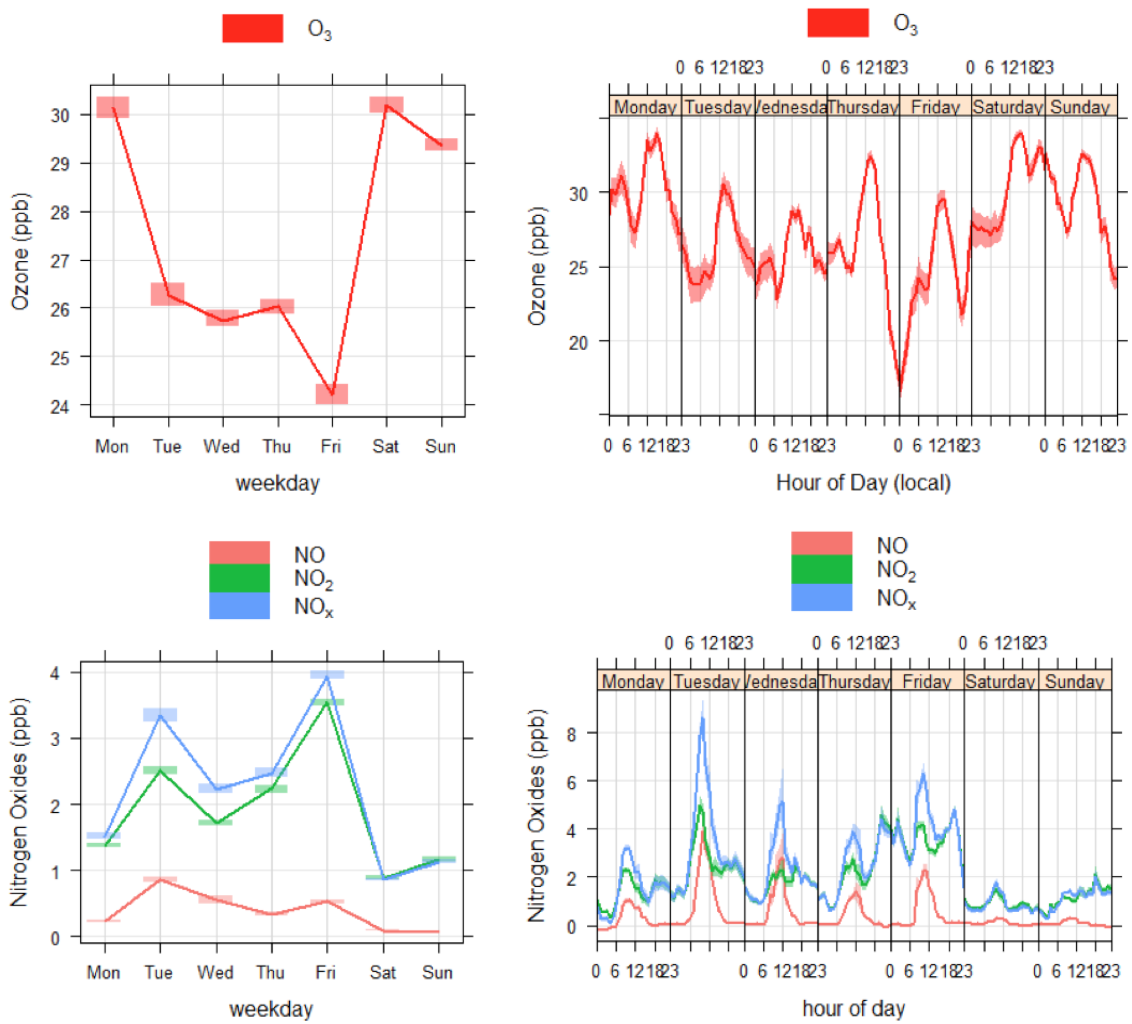


Figure 43. Diurnal cycles for Ozone, NO, NO₂, NO_x at the KM site. © Univ York, NCAS, 2016.



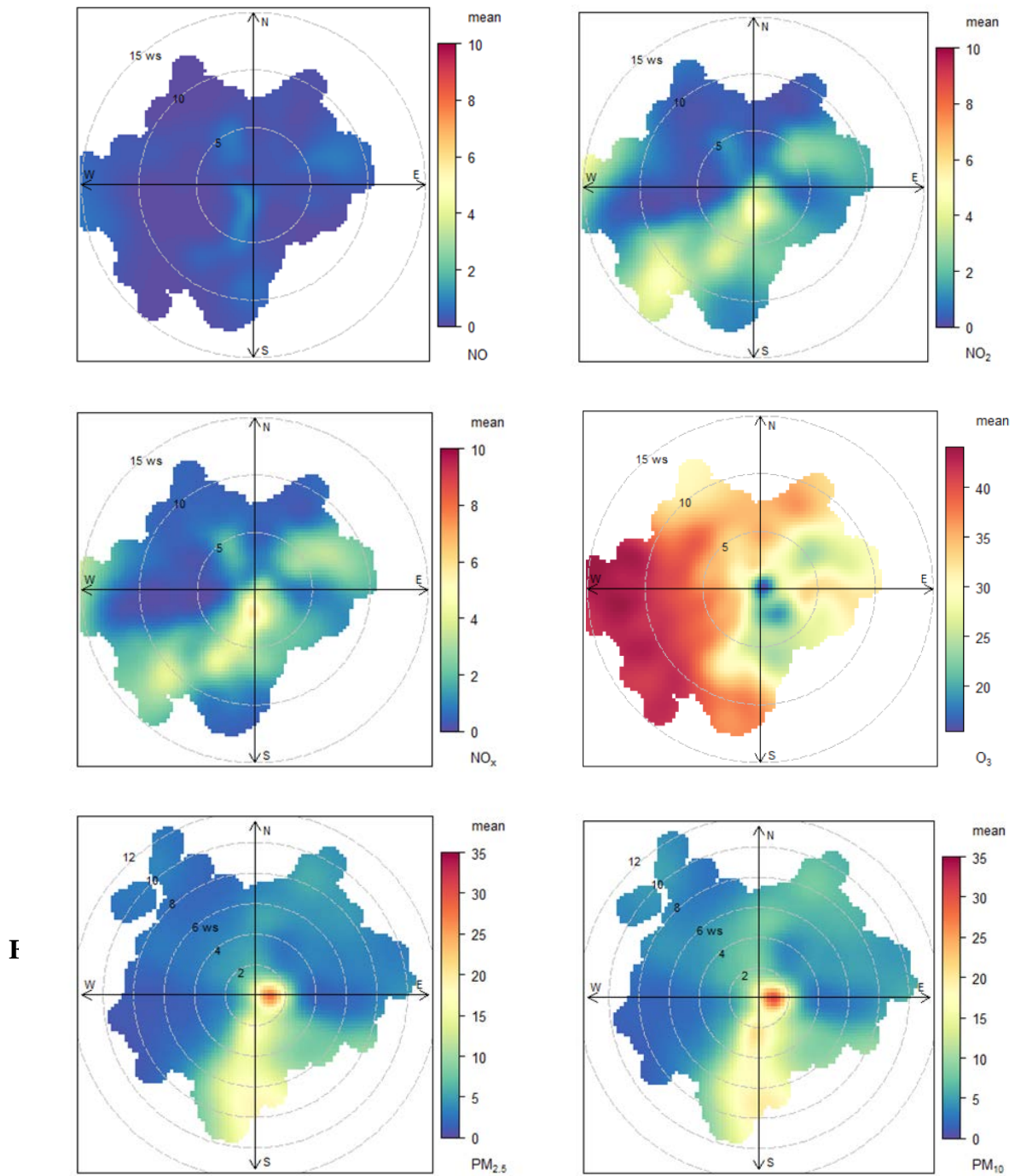


Figure 45. Polar plots for NO, NO₂, NO_x, O₃, PM_{2.5}, PM₁₀ at the KM site. © Univ York, NCAS, 2016.

2.4.5.9 NON-METHANE HYDROCARBONS (NMHC)

NHMCs have been collected weekly, as grab samples in stainless steel containers, apart from two weeks over Christmas and two weeks at the start of the measurement period since October 2015 at KM. Due to the limited data set available to date, it is difficult to complete

a full analysis of sources and their variability. Figure 46 shows the contribution of each hydrocarbon weighted by concentration in every sampled collected so far. The light weight short-chain alkanes are the most prominent as expected in this location, due to its rural environment the most reactive hydrocarbons are not expected to be observed.

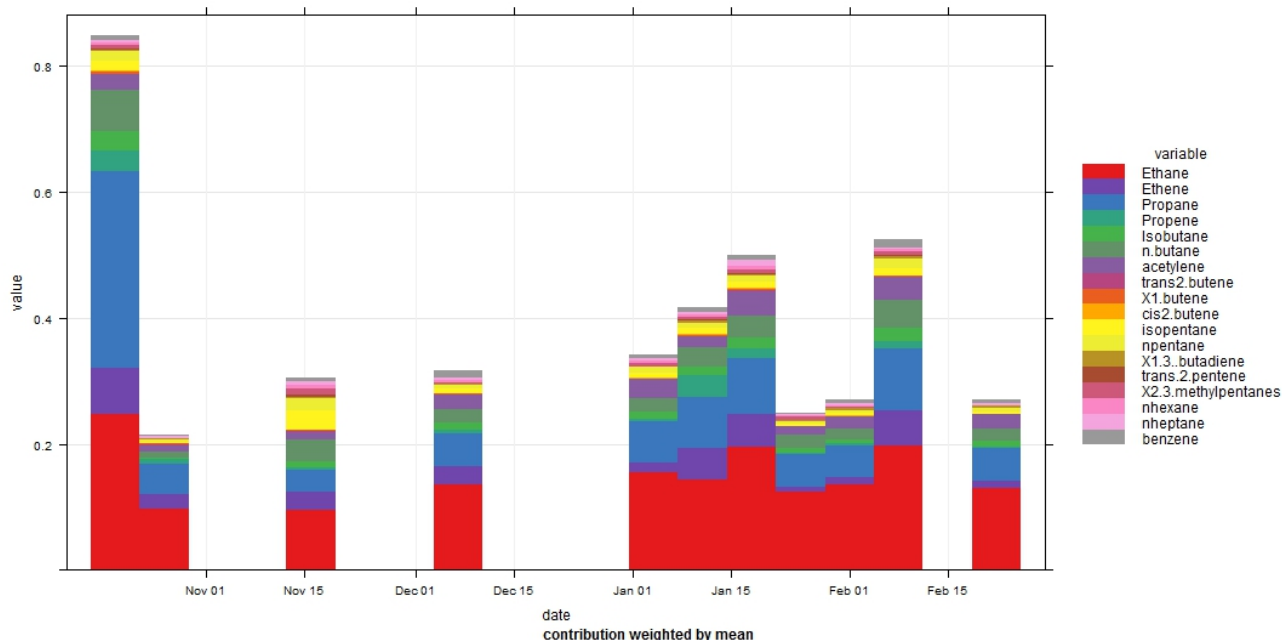


Figure 46. NMHCs for KM weighted by mean to for every WAS collected. © Univ York, NCAS, 2016.

Figure 47 is a box and whisker statistical plot for all NMHCs to show the spread of the data collected so far. Concentrations are in general slightly lower than those currently observed at the Wolfson Atmospheric Chemistry Laboratory in York, reflecting the more rural environment of the KM site, with many species close to detection limit. Benzene and 1,3 butadiene, which have EU Directive limit values, are very low at the KM site at present. Propane is more variable than is typically observed in cities, sometimes higher than ethane. Ethane is also somewhat higher than might be expected from a rural location. This unusual NMHC behaviour suggests a localised light alkane source, potentially from existing site extraction activities, or those nearby. This will be studied further and will be determined more accurately when there is a larger range of observations and wind directions.

Data gathered here and in the ongoing baseline will be compared to Auchencorth Moss, the only rural station that is part of the hydrocarbon monitoring network in the UK. Data from that station is only available from July 2015 so it is not possible to compare the hydrocarbons currently due to the seasonality difference that may occur.

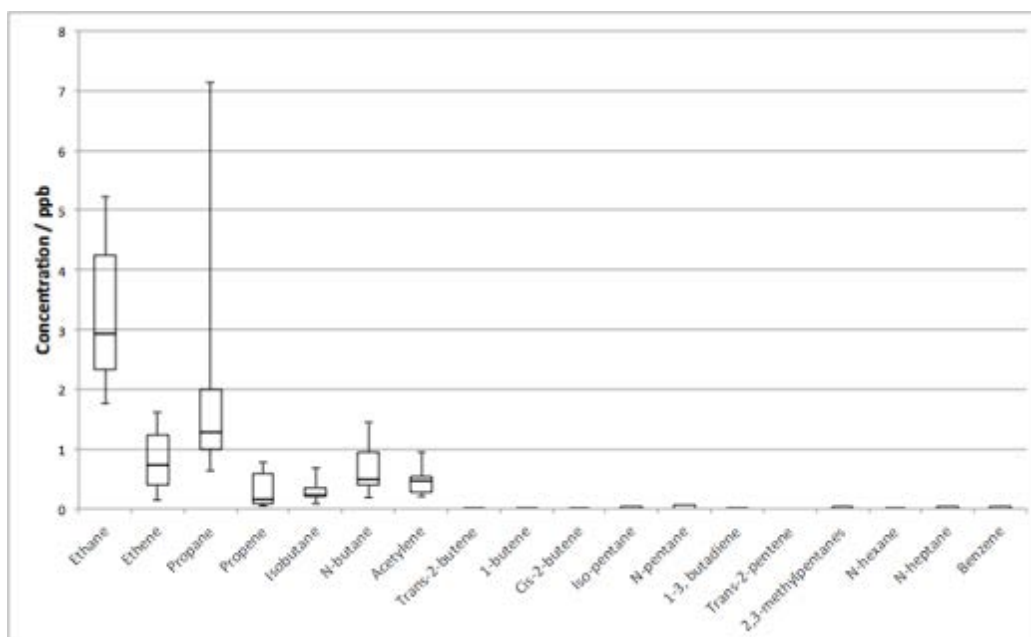


Figure 47. Box and whisker plot showing the variance in the NMHC measurements at KM. © Univ York, NCAS, 2016.

2.4.5.10 COMPARISON OF BOTH SITES

Comparing data from both measurement sites offers insight into the potential transferability of baseline datasets. In this section, we briefly compare the measurements made so far.

Greenhouse gases

Figure 48 illustrates greenhouse gas data collected for the period of simultaneous measurement thus far. It can be seen that there are many periods where CO_2 is simultaneously enhanced at both locations, especially in the period 8 Feb 2016 to 7 March 2016. However, there are notable times when this is not the case, or when one site appears to lag the other (e.g. 15 Jan 2016 to 18 Jan 2016). Such lag patterns reflect the advection of airmasses across the UK and also indicate that both sites often sample similarly polluted airmasses in terms of CO_2 . However, the picture is much more complicated for CH_4 (bottom panel of Figure 48). While many of the peaks in CH_4 are observed at similar times at both sites, the magnitude of the enhancement compared with the ~ 2 ppm background is markedly different, with LP seen to be much enhanced compared with KM. Many such periods (e.g. 11 Feb to 13 Feb) coincide with light easterly winds. It is interesting to note that LP is directly upwind of KM in this wind regime and that the enhancements seen at KM could be expected to represent sources of methane in the fetch between the two sites.

Figure 49 and Figure 50 illustrate the temporal cycles in greenhouse gas concentrations at both sites. It is interesting to note that even in this limited dataset, the diurnal cycles in both

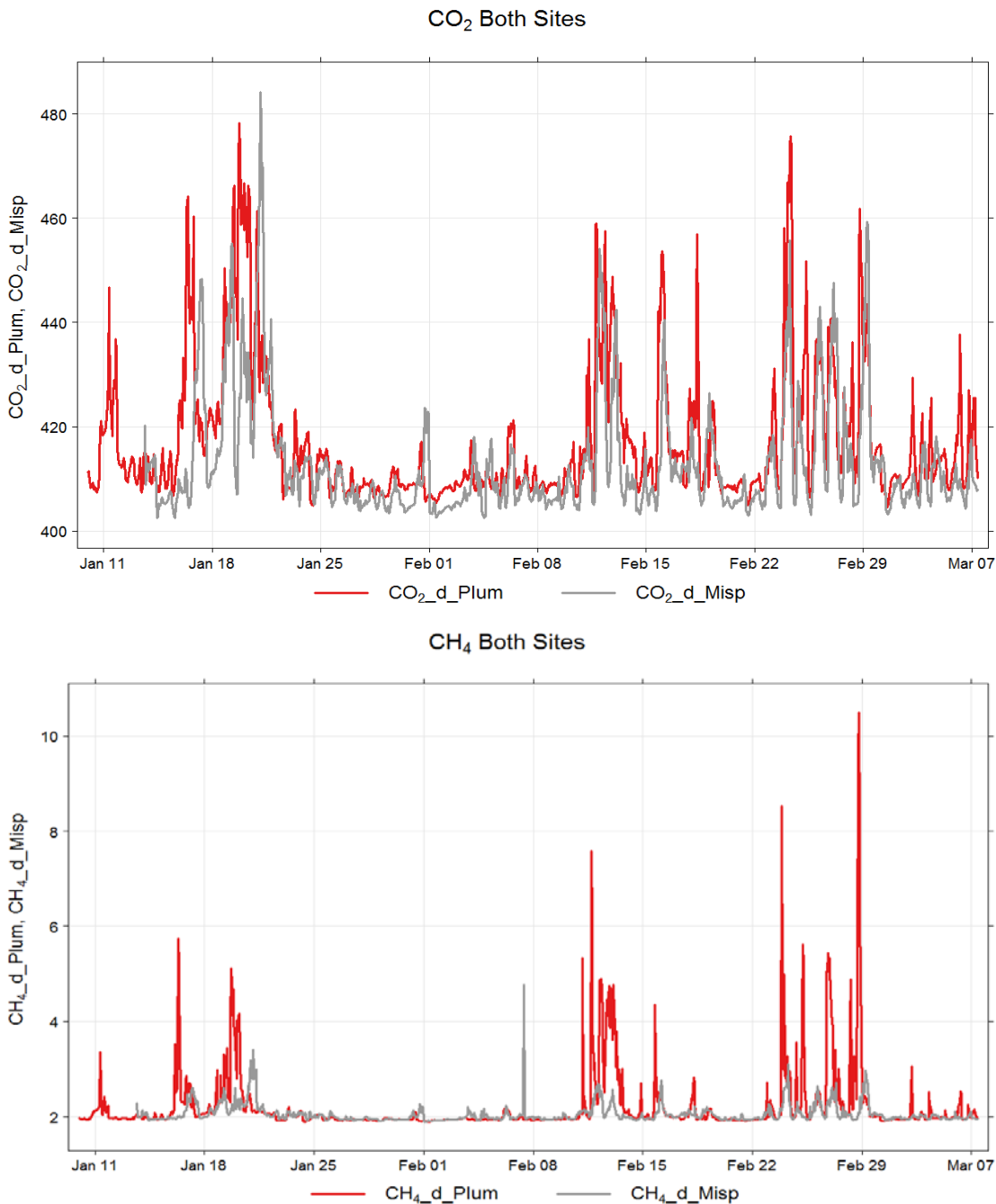


Figure 48. Carbon dioxide (top panel) and methane (bottom panel) concentrations at the LP site (red) and KM site (grey) for the period of simultaneous measurement between 10 Jan and 9 Mar 2016. © Univ Manchester, 2016.

CO₂ and CH₄ are broadly similar (see bottom left panels) with minima around midday in the KM wintertime dataset so far when compared with the longer term LP dataset. Very little significant difference between working day and weekend concentrations (or their range of variability) is observed. A broadly correlated seasonal cycle in both CO₂ and CH₄ is observed at the KM site, reflective of the relative activity of the Northern Hemispheric biosphere and summertime biogeochemical sinks, which typically outweigh emissions temporarily (seasonally). An apparent systematic difference in CH₄ concentration between KM and LP (bottom right panel of Figure 49) should not be over-interpreted at this stage, as this is expected to reflect the fact that data for LP represent a full year of data (and hence smooth the natural seasonal cycle), compared with KM, which represents a wintertime seasonal average only.

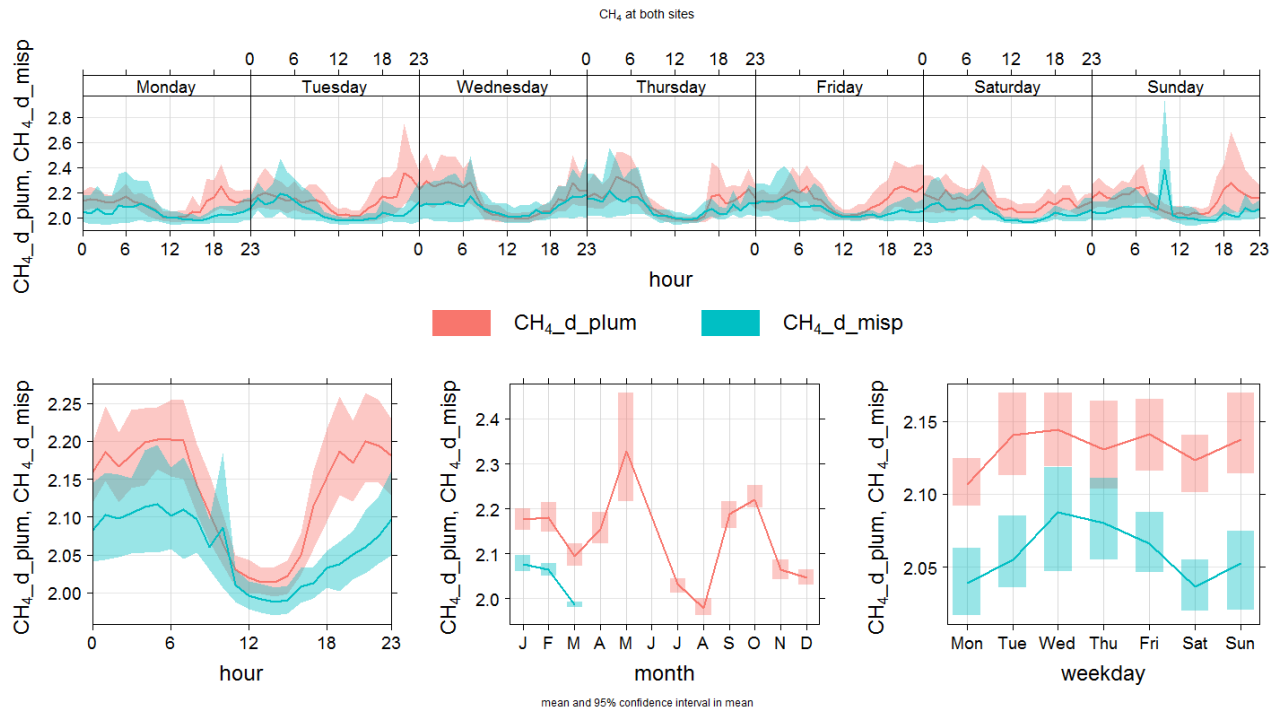


Figure 49. Methane temporal cycles at KM (blue) and LP (pink) by time of day and day of week (top panel), hour of day (bottom left), month of year (bottom centre), day of week (bottom right). In each case, the thick centre line denotes the mean concentration while the semi-transparent shadowed area represents the one standard deviation range of the mean. © Univ Manchester, 2016.

Air Quality

As with the greenhouse gas analyses it is difficult to draw firm conclusions on the differences between the sites with the limited data collected so far. Some initial observations are that:

- Both sites have elevated O₃ when the wind speed is at its highest and from the west.
- LP has a local pollution influence from the road beside it; this is not seen in the KM data
- KM has a localised source of propane, and to a lesser extent ethane, although the source is not yet firmly identified

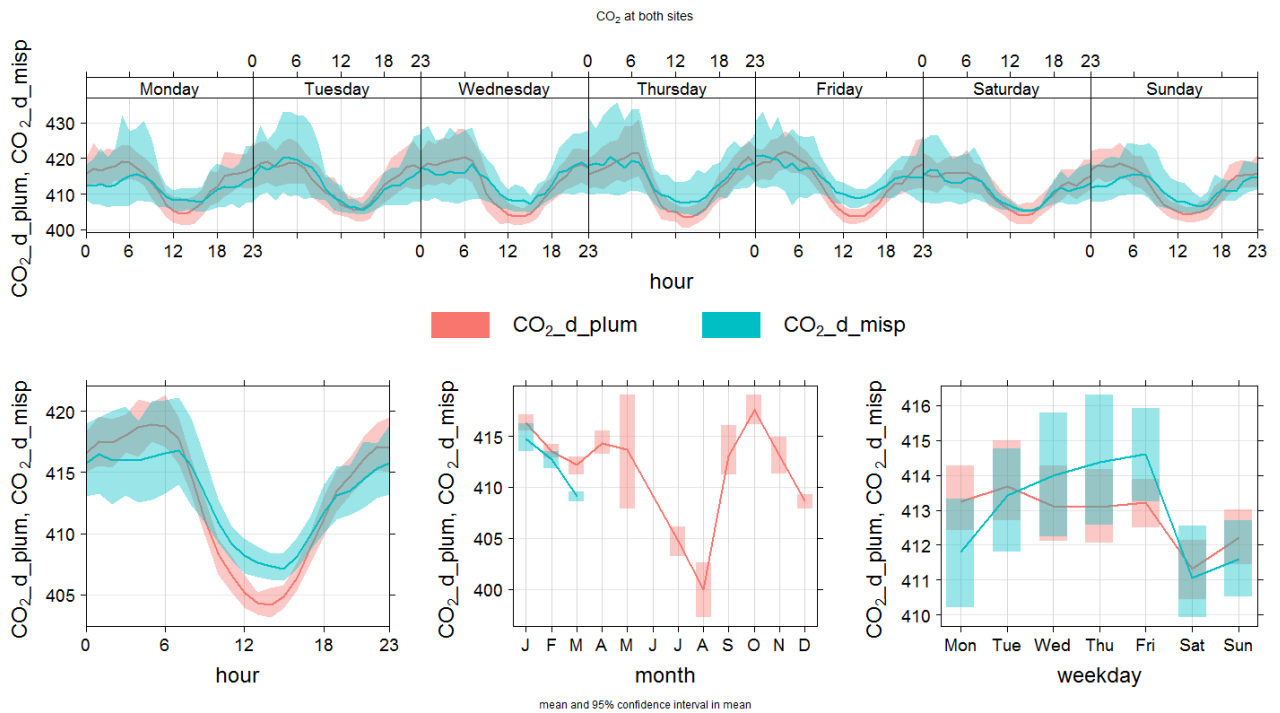


Figure 50. Carbon dioxide temporal cycles at KM (blue) and LP (pink) by time of day and day of week (top panel), hour of day (bottom left), month of year (bottom centre), day of week (bottom right). In each case, the thick centre line denotes the mean concentration while the semi-transparent shadowed area represents the one standard deviation range of the mean. © Univ Manchester, 2016.

2.4.5.11 COMPARISON WITH OTHER SITES

High Muffles

High Muffles (HM) is part of the Automatic Urban and Rural Network (AURN) and is classified a rural background site. It is situated on the North Yorkshire Moors, 16 km north of the KM site.

Table 10. Statistical air quality metrics for the HM, KM and LP measurement sites.

	HM 10 %	KM 10 %	LP 10 %	HM mean	KM mean	LP mean	HM 90 %	KM 90 %	LP 90 %
O ₃ (ppb)	12.16	13.36	11.37	29.14	28.92	33.32	37.18	38.44	41.21
NO (ppb)	0.12	-0.14	0.08	0.75	0.1	0.54	2.02	0.83	3.17
NO ₂ (ppb)	1.02	-0.03	-0.64	3.25	1.27	0.96	9.47	4.97	12.99
NO _x (ppb)	1.22	-0.19	0.38	4.06	1.41	1.60	11.56	5.51	17.36

Table 10 compares the data collected in the same period at HM to the KM and LP data. The wind rose for the site is shown in Figure 51 and like the other sites the wind direction is mainly from the western sectors. The mean O₃ and range of O₃ measurements at all 3 sites is similar. This can also be seen in Figure 52 where the HM site also shows enhanced O₃

from the west at highest wind speeds as KM and LP. The NO_x data does show distinct differences, KM shows the lowest concentrations of all 3 sites. Figure 30 shows HM having a large source of NO_x to the south of the south of the site. This is almost certainly an artefact arising from different measurement methods. At KM and LP a direct NO_2 measurement is made whereas the Defra site at HM using a molybdenum chemical conversion to NO. This results in other oxidised nitrogen species being reported as NO_2 and is a well-known technical issue at rural locations.

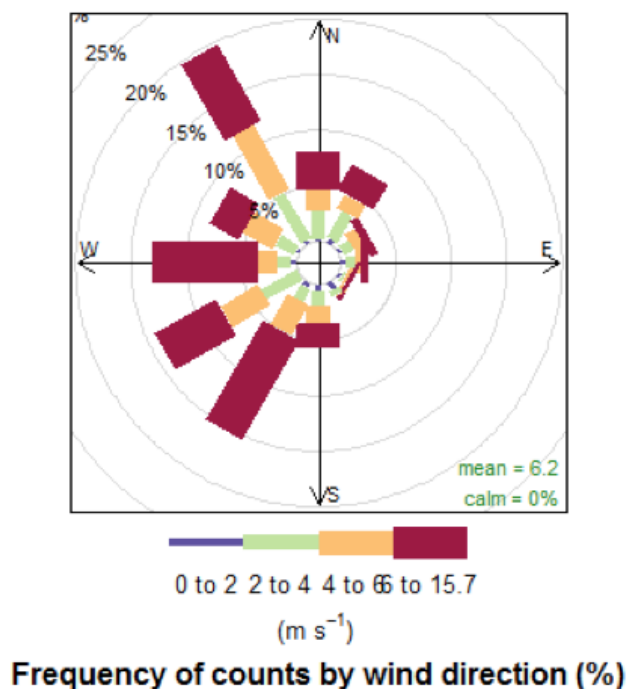


Figure 51. Wind rose for the High Muffles AURN site. © Univ Manchester, 2016.

2.4.6 Future work and baseline deliverable plan

The greenhouse gas analysis at LP begins our approach to final baseline deliverables. The local climatology of pollutants interpreted for wind direction and airmass history gives qualitative interpretation on the type (and magnitude) of pollution from upwind sources, both locally and regionally. Using correlations between different trace gases, and when analysed in the context of wind direction and airmass history (as diagnosed by back trajectories), we can interpret the proximity and relative impact of both nearby and far-field sources.

In our ongoing work, we will continue to augment this baseline, especially for air quality tracers, and provide final statistical analysis on a minimum 12-month dataset. We will use that analysis to qualitatively guide the utility of the baseline in representing a wider area and other sites. For example, the comparison of data so far for the two sites does indicate that far-field sources of greenhouse gases (e.g. Western Europe) are often common to both sites when the wind is from the east (albeit less frequently), as might be expected. And by comparing the difference between the two sites when the wind is in a direction that joins the two sites in the Lagrangian frame, we can interpret the addition of pollution in the path between the two sites (e.g. as air passes over the cities of Northern England). This networked approach begins to highlight the potential that a future monitoring network (complemented by the AURN network and DECC Tall Towers) could have as a powerful tool for interpreting sources of pollution within the mainland UK.

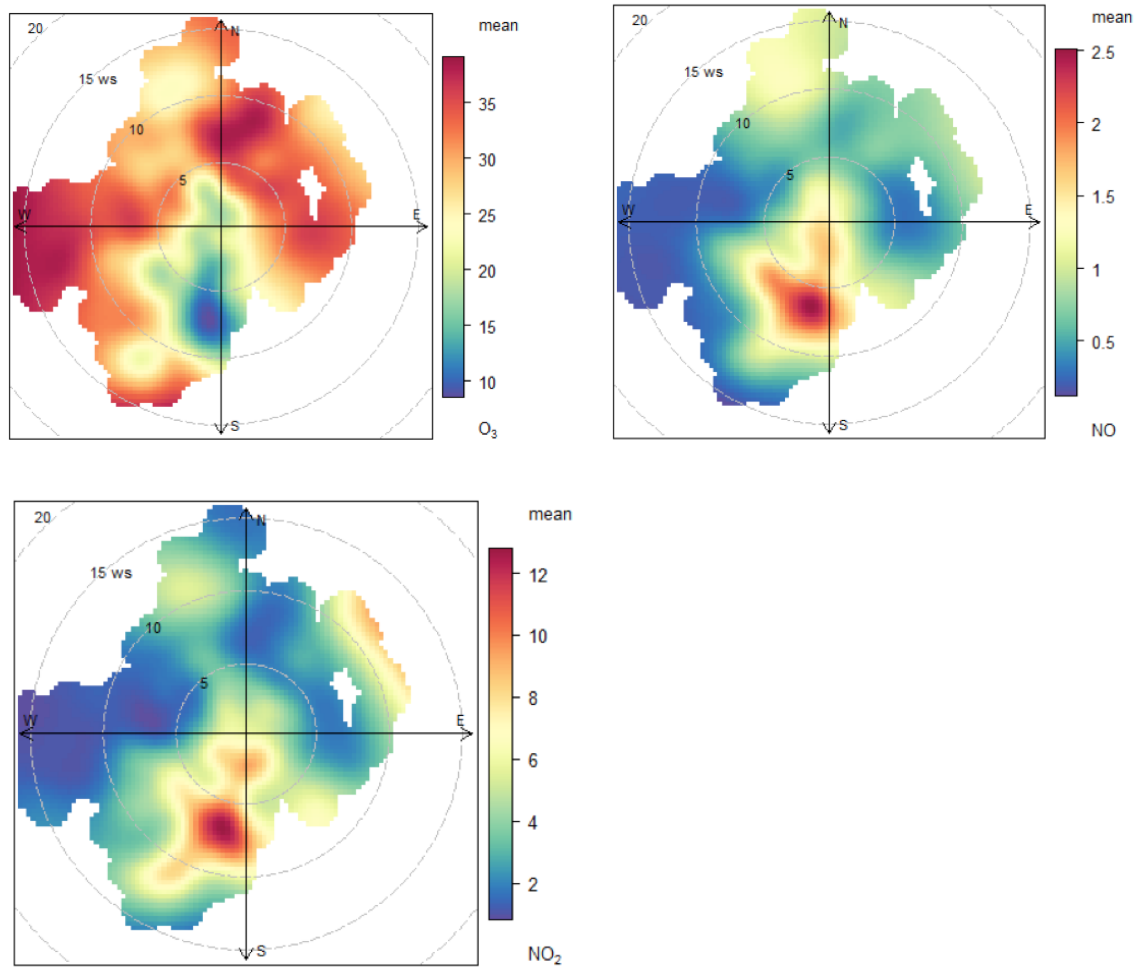


Figure 52. Polar plots for O₃, NO and NO₂ for the High Muffles AURN site. © Univ York, NCAS, 2016.

2.5 SOIL GASES

2.5.1 Original objectives

The objective of this work package was to collect baseline measurements of soil gas, soil gas flux to atmosphere and atmospheric gas in the area surrounding the KM8 site of proposed shale gas development. This was to include field measurement of methane, CO₂ (which could be produced from methane oxidation), O₂ (useful in helping determine the source of CH₄ and CO₂) and Rn (possible tracer of gas migration pathways). We also proposed collection of samples from a smaller number of sites of interest for subsequent laboratory analysis (both as a check of field measurements and for the determination of trace components) and mass spectrometry (for C isotopes in gaseous CH₄ and CO₂).

A mix of survey mode (single point and mobile) and continuous measurements at selected sites was planned. Surveying large areas for discrete surface gas outlets is best conducted with mobile equipment to identify locations of specific interest. However, due to dilution in air, sensitivity is reduced. Single-point measurements provide the highest sensitivity as the gas is extracted from the soil or soil surface where concentrations are highest, and a sufficient number of analyses over a site provide a good indication of the range of baseline conditions. Continuous measurements at a small number of sites provide information on temporal variations (e.g. diurnal or seasonal variations).

The study was to include:

- detailed coverage of near-ground atmospheric methane and CO₂ using mobile open path lasers.
- broad-scale grids of point measurements of soil gas (CO₂, CH₄, O₂, H₂, Rn) and flux (CO₂) in the field with subsequent analysis of selected gas samples in the laboratory;
- for specific sites and for a fixed time period, continuous measurement of atmospheric methane using a scanning open-path laser, plus CO₂ flux using accumulation chambers and eddy covariance techniques. Also at specific sites, for longer time periods, continuous measurements of soil gas CO₂ concentrations using buried probes.

Sites of interest include:

- a range of baseline measurements over superficial lacustrine deposits (e.g. differing lithologies, soil types, crop types, damper/drier ground, farmed/undisturbed);
- a range of baseline measurements over Corallian Limestone (different conditions as above);
- higher-density sampling around proposed exploration sites to provide more data in case of future 'borehole-related' anomalies;
- traverses across selected major faults in the area that are known to have conducted gas at depth in the geological past to reveal whether methane is naturally migrating to the surface.

In practice this work package was hampered by extremely wet conditions in the field during late 2015 and early 2016. This restricted the studies undertaken to point measurements of soil gas and flux, in November 2015. Some flux measurements were repeated in March 2016 but no soil gas could be obtained because of the saturated ground. Conditions were too wet for mobile vehicle-mounted surveys, although attempts were made. They also limited the value of installing continuous monitoring equipment although a BGS eddy covariance system was deployed in Lancashire as described below.

2.5.2 Sampling and measurement methods

Soil gas was monitored by hammering a small diameter steel tube into the ground to a depth of up to 1 m (Figure 53). Samples of gas were measured for CO₂, CH₄, O₂ and H₂S using a portable gas analyser. The steel tube was then removed from the ground. Flux was determined by placing a small metal chamber onto the ground surface and measuring the flow of the gas into the chamber. Both soil gas and flux measurements only took a few minutes and caused very little disturbance to the soil or vegetation. Eddy covariance was used to continuously measure CO₂ concentrations, along with 3D air movement and relative humidity. This technique allows CO₂ fluxes from the ground to be calculated over a larger footprint than the chamber method. The eddy covariance system was deployed at the Lancashire atmospheric monitoring site to provide an indication of CO₂ inputs to the atmosphere from the soil and comparative atmospheric measurements of CO₂. This site was preferred to the Vale of Pickering as atmospheric monitoring was already in place and logistics were simpler.



Figure 53 Soil gas measurement.

2.5.3 Results

2.5.3.1 SOIL GAS AND FLUX – VALE OF PICKERING

Initial soil gas surveys in the Vale of Pickering, North Yorkshire were carried out in the week of 2-6 November 2015. Measurements were made in an area to the east of Kirby Misperton (Figure 54). The superficial geology consists mainly of lake deposits with some alluvium in the river valleys and glacial material (diamicton) on bedrock highs around Kirby Misperton (Figure 54) (Ford et al, 2106). The underlying bedrock is predominantly mudstones of the Amphill Clay Formation and Kimmeridge Clay Formation (Undifferentiated) (Newell et al, 2016). A number of geological faults cut through the succession in the study area and the inferred surface trace of these is shown in Figure 54.

The sampling strategy provided a sufficient number of measurements for statistical analysis and included sites close to major faults, which might provide pathways for gas migration from depth, and near locations with higher than average methane concentrations in groundwater. Soil gas concentrations and fluxes were attempted at 142 sites, close to KM8 and groundwater monitoring sites and major faults.

Probability plots (for example Figure 55) can reveal different populations in datasets and thus be used to subdivide data, and highlight anomalies, before plotting it spatially. In this case the breaks indicated by the probability plots were sufficiently similar to those suggested by Jenks' Natural Breaks (in the ArcMap software used), so these were applied unmodified.

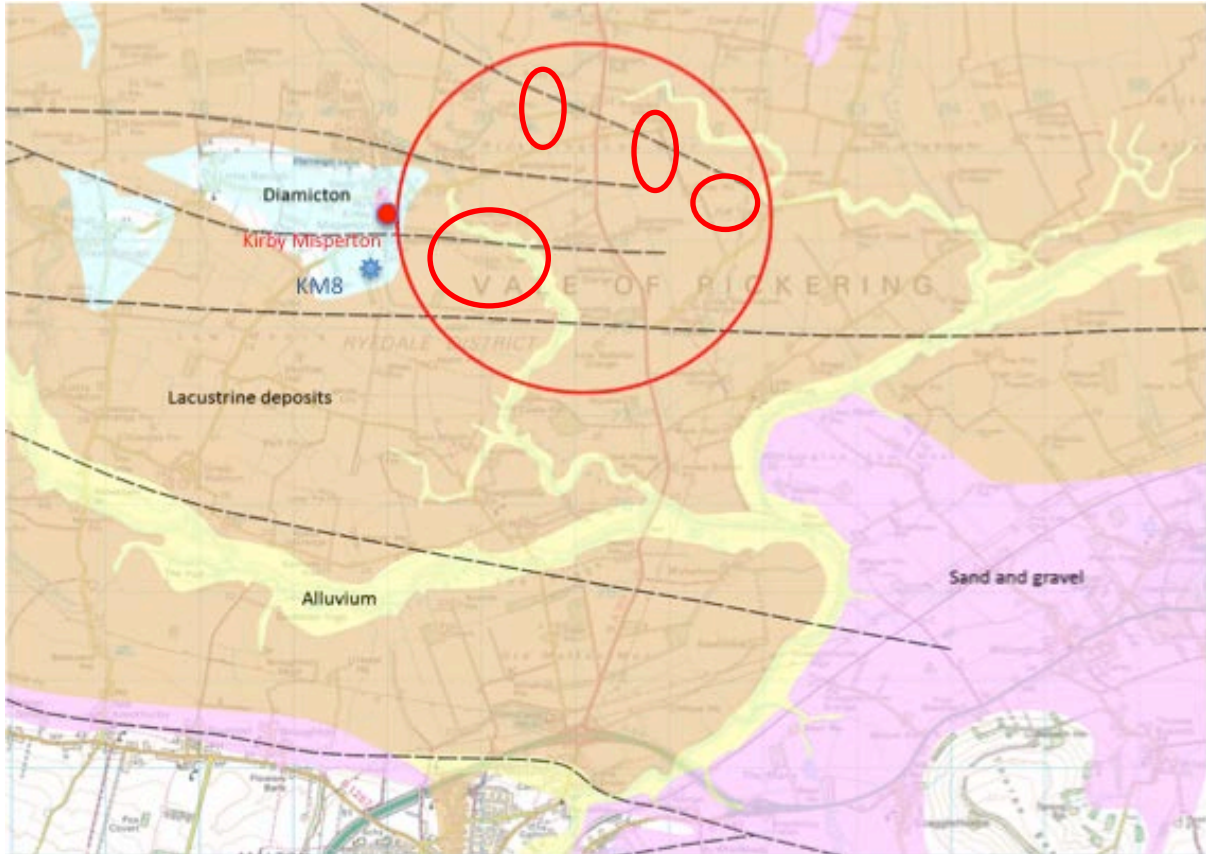


Figure 54 Soil gas study area to the east of Kirby Misperton within the red circle.

Plots of the soil gas and flux data (Figure 56 and Figure 57) show the spatial variability. There is no obvious correlation between higher values and proximity to geological faults, or to sites with higher groundwater methane concentrations, but the data are from a single survey under relatively wet soil conditions. This is likely to significantly inhibit upward migration of any gases and so result in an inability to detect anomalies as a result of this. Further sets of observations are needed under more optimal (drier) conditions to investigate the role of geological faults as pathways to the surface.

CO₂ in soil gas ranged from 0.07% to 10.0% (median 2.35%) and CO₂ flux ranged from 3.4 g m⁻² day⁻¹ to 34.7 g m⁻² day⁻¹ (median 12.2 g m⁻² day⁻¹). Because of saturated ground conditions no soil gas measurement was possible at 42 of the proposed measurement sites (Figure 56).

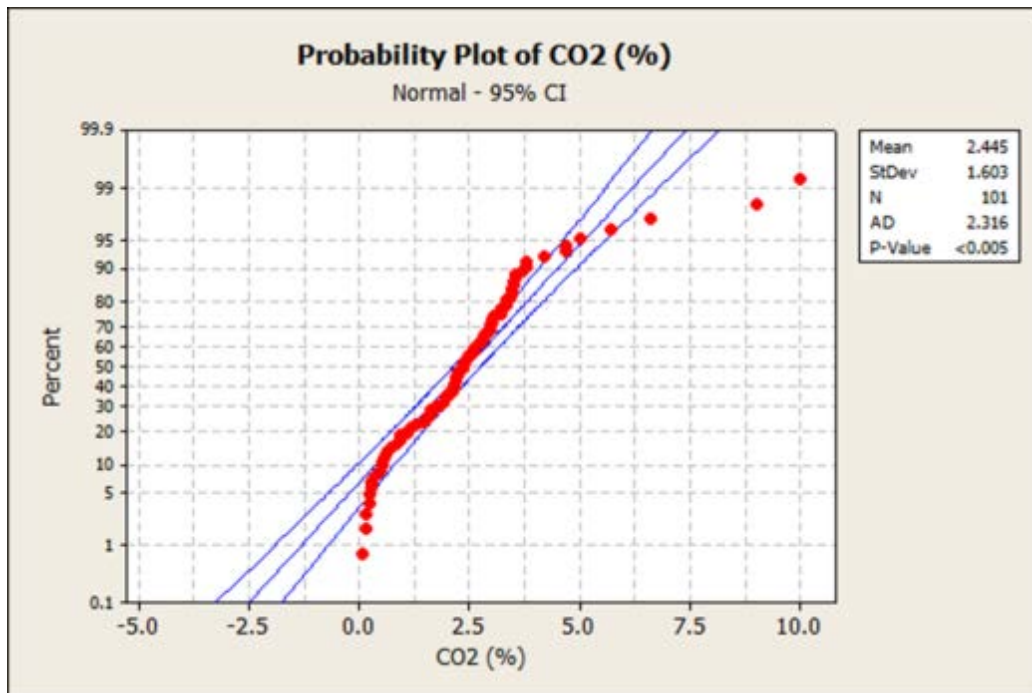


Figure 55. Normal probability plot of soil gas CO₂ data from the Vale of Pickering.

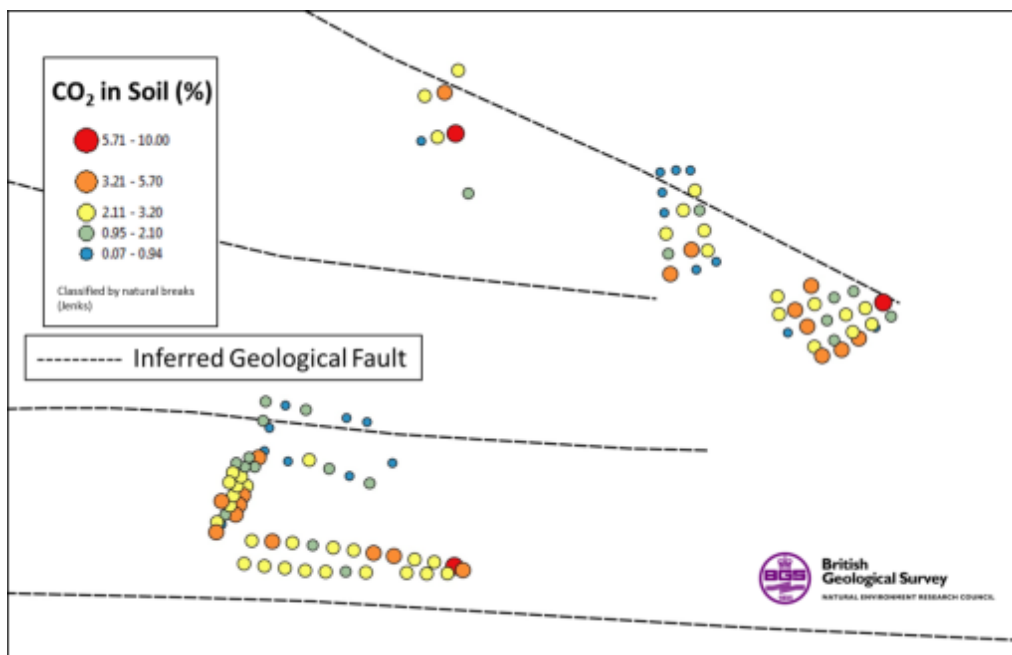


Figure 56. Plot of the concentration of CO₂ in soil gas in the Vale of Pickering, November 2015.

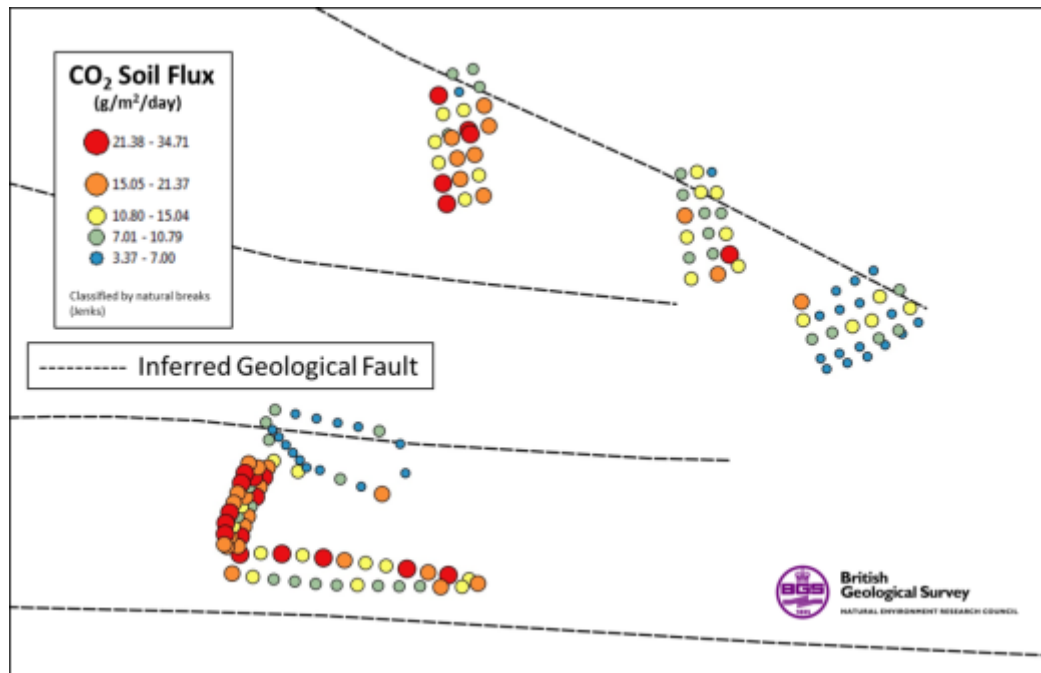


Figure 57. Plot of the flux of CO₂ from the soil in the Vale of Pickering, November 2015.

An appraisal of soil gas ratios is a powerful tool for identifying the origin of CO₂ in the soil gas. Deep leakage of CO₂ dilutes the existing gas so that O₂ and N₂ in the soil decrease to zero for 100% CO₂. In contrast CO₂ of shallow biological origin involves the removal of O₂ at an equal rate such that atmospheric levels of CO₂ (about 21%) are reduced to zero at about 21% CO₂. The oxidation of methane consumes oxygen at double this rate reducing it to zero for about 10.5% CO₂. N₂ is not involved in either of these reactions so remains constant. Dissolution of CO₂ in the porewater, and possible reaction with soil carbonate, decreases the free CO₂ in the soil gas moving it away from the ideal lines indicative of each mode of origin (Figure 58). Plots of gas ratios shows no evidence for deep CO₂ leakage (Figure 58 and Figure 59). Taken together the CO₂/O₂ (Figure 58) and CO₂/Balance (Figure 59) plots are indicative of shallow biologically produced CO₂ with modification of the ratios by dissolution of CO₂ in the soil pore water and possible reaction with soil carbonate. Whilst the CO₂/O₂ trend could suggest methane oxidation, when taken with the general tendency of balance (i.e. mostly N₂) towards higher than atmospheric levels with increasing CO₂, it is more consistent with CO₂ dissolution and reaction.

The higher CO₂ concentrations (around 10%) are likely to be caused by wet near surface conditions restricting the flux of gas out of the soil and allowing the build-up of CO₂.

Comparison of soil gas and flux measurements between the locations in the studied area showed little difference except for a tail of slightly higher flux values at location A (Figure 60). There were some differences related to land use, with lower values for both CO₂ and CO₂ flux on arable land at location A and for flux only at Farm B (Figure 61). These are probably the result of greater biological activity on established pasture at Farm A compared with recently planted arable land with only small seedlings emerging. Arable land at Farm B had a more developed growth of winter cover compared with that at Farm A.

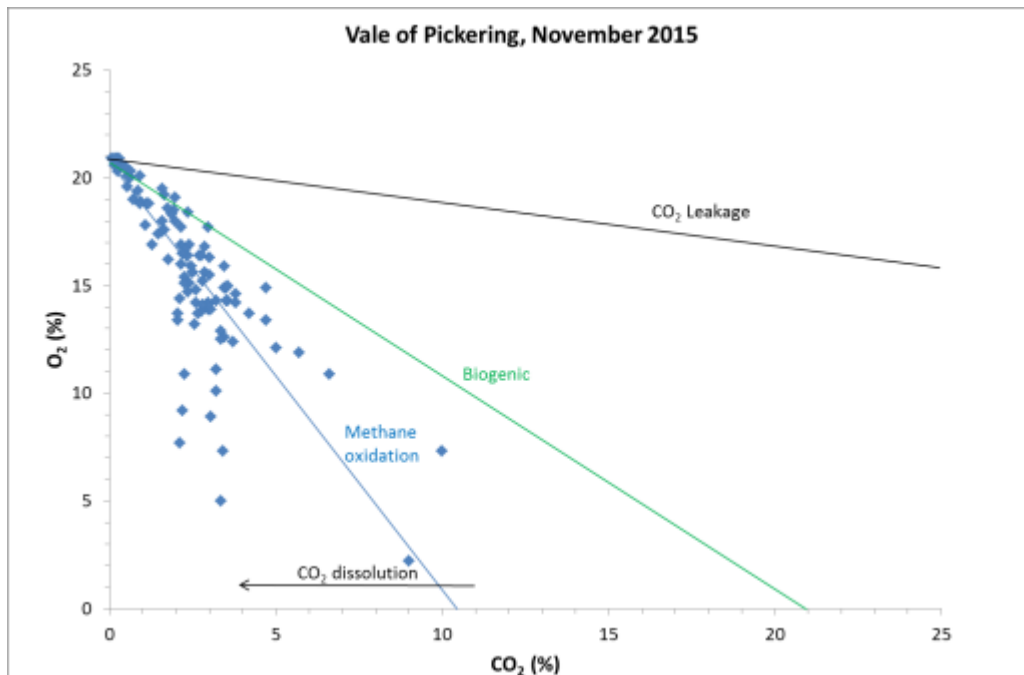


Figure 58. Plot of CO₂ versus O₂ for November 2015 soil gas data. Lines show the trends for deep leakage of CO₂, biogenic CO₂ (plant and microbial respiration) and CO₂ produced by methane oxidation. Dissolution of CO₂ in soil pore water, and reaction with any carbonate present moves points away from the trend lines in the direction of the arrow.

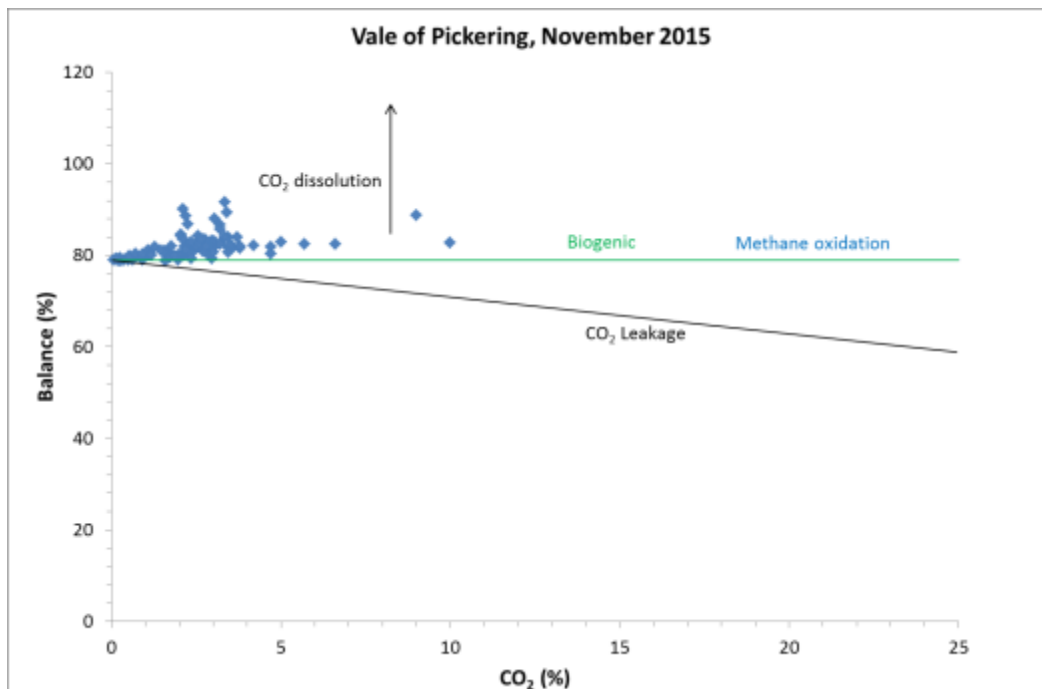


Figure 59. Plot of CO₂ versus Balance (mostly N₂ and some Ar) for November 2015 soil gas data. Lines show the trends for deep leakage of CO₂, biogenic CO₂ (plant and microbial respiration) and CO₂ produced by methane oxidation. Dissolution of CO₂ in soil pore water, and reaction with any carbonate present moves points away from the trend lines in the direction of the arrow.

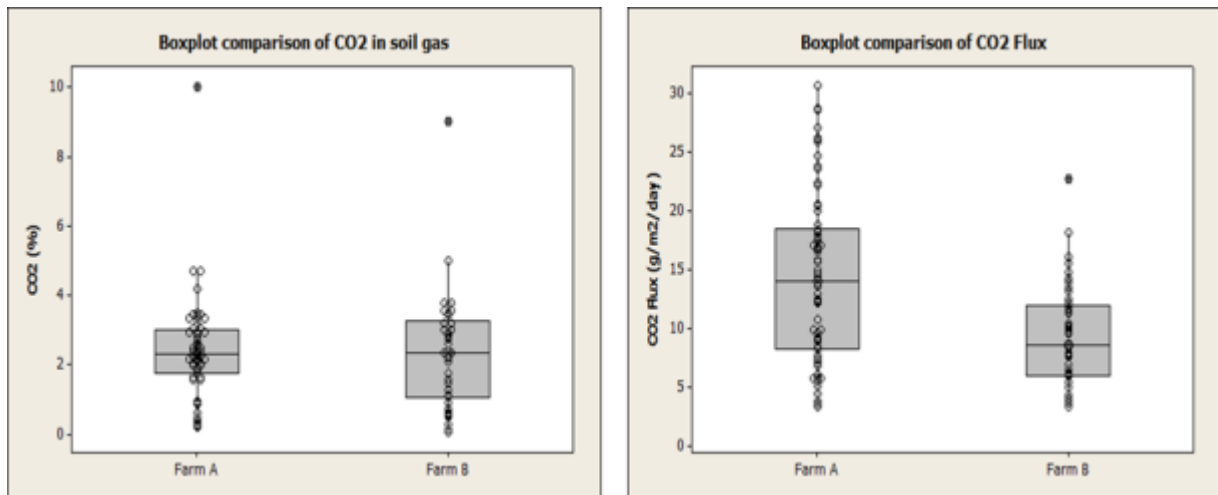


Figure 60. Comparative box and whisker plots for soil gas CO₂ and CO₂ flux between the two farms in the study area, November 2015.

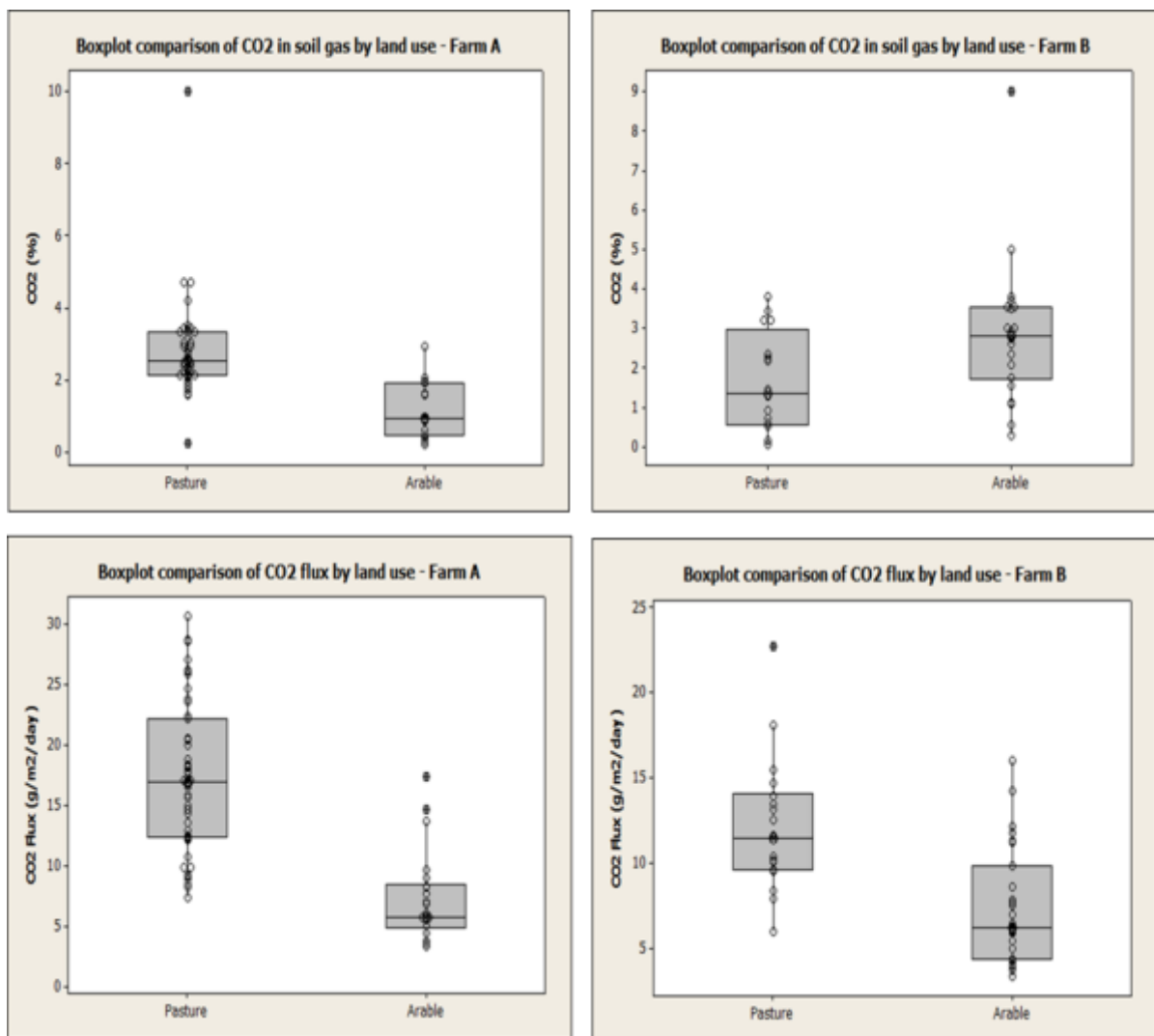


Figure 61. Comparative box and whisker plots for soil gas CO₂ and CO₂ flux with different land use for the two farms in the study area, November 2015.

A second field survey in the Vale of Pickering was carried out in the week of 7 March 2016. Flux measurements (CO₂ and CH₄; Figure 62a) were made at 21 out of 22 locations visited in the south of the studied area using a new survey flux meter capable of measuring both CO₂ and methane fluxes at low levels (the instrument used in November could only detect high methane fluxes). However, it was not possible to make soil gas concentration

measurements (for CO₂, CH₄, O₂, H₂S, Rn etc.) at any of these sites because of the continuing very wet ground conditions. There was standing water at several locations (e.g. Figure 62b) and even where the surface was drier there was insufficient free gas to obtain readings.



Figure 62. (a). Measurement of CO₂ and CH₄ flux and (b). Very wet ground conditions in March 2016.

The CO₂ flux measurements were generally lower than those obtained in November 2015 (Figure 64). They ranged from 2.2 to 24.9 g.m⁻².day⁻¹ with a median of 6.5 g.m⁻².day⁻¹. The CH₄ fluxes were uniformly very low (<0.01 g.m⁻².day⁻¹). The lower values in March probably result from a combination of lower biological activity and higher moisture content (with common waterlogging) of the soil.

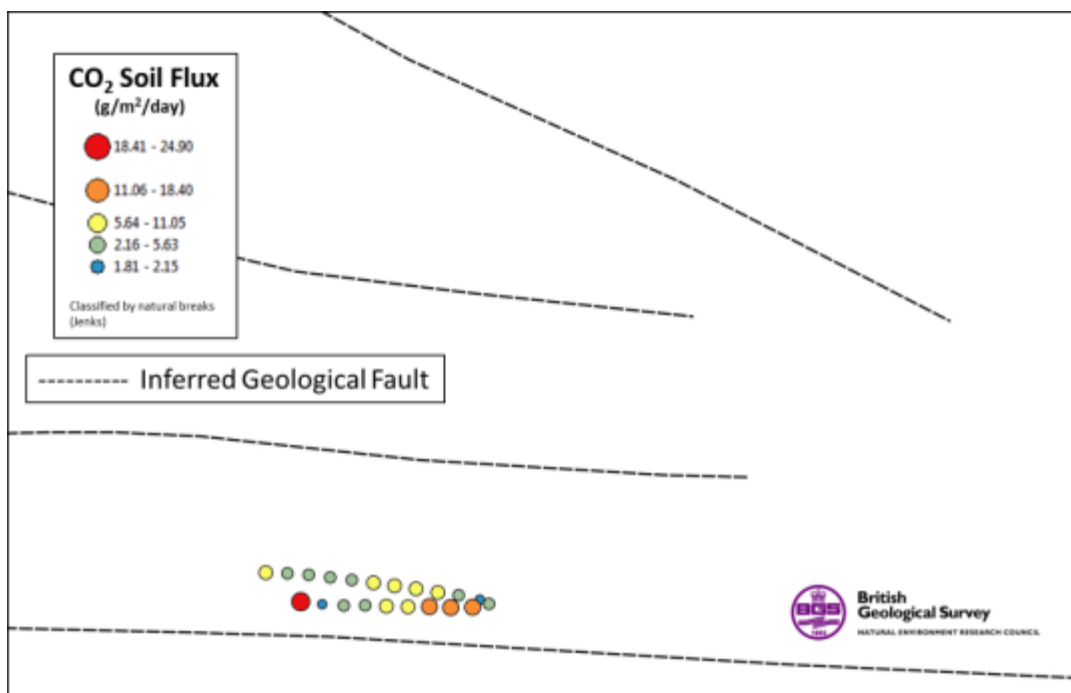


Figure 63. Plot of the flux of CO₂ from the soil in the Vale of Pickering, March 2016.

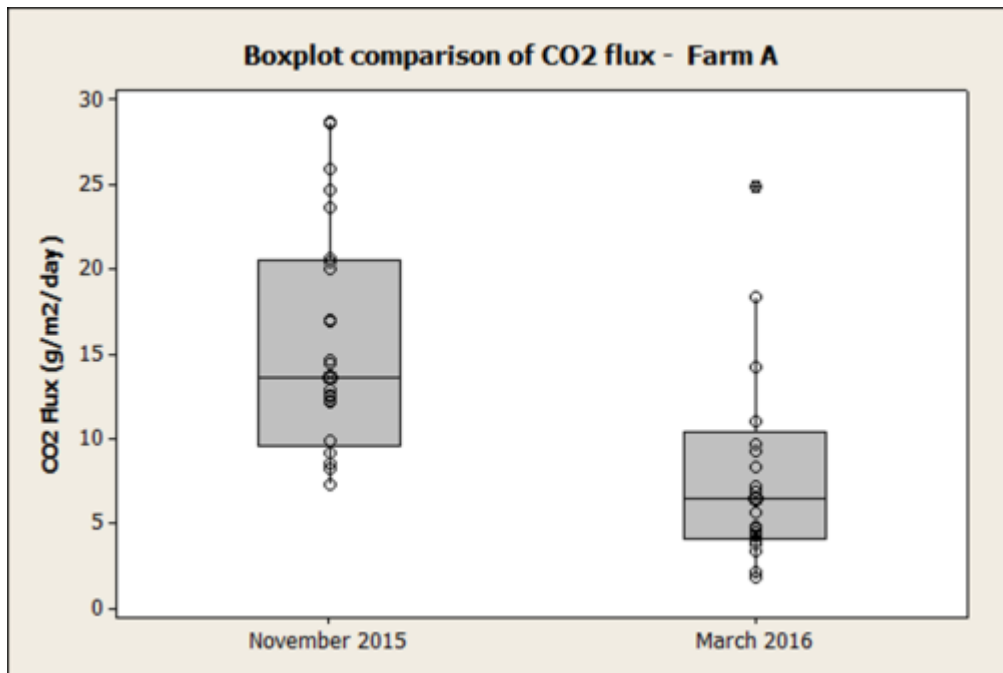


Figure 64. Comparative box and whisker plots of CO₂ flux at the same sites visited in November 2015 and March 2016.

2.5.3.2 EDDY COVARIANCE – LANCASHIRE

An eddy covariance system was installed at the Lancashire atmospheric monitoring site on 19th January 2016 to allow comparison with existing CO₂ sensors, to permit the calculation of local CO₂ fluxes into the atmosphere at the site and to provide additional high resolution meteorological data. The first batch of results (19th January to 5th February 2016) was downloaded and processed (Figure 65). Data acquisition is continuing.

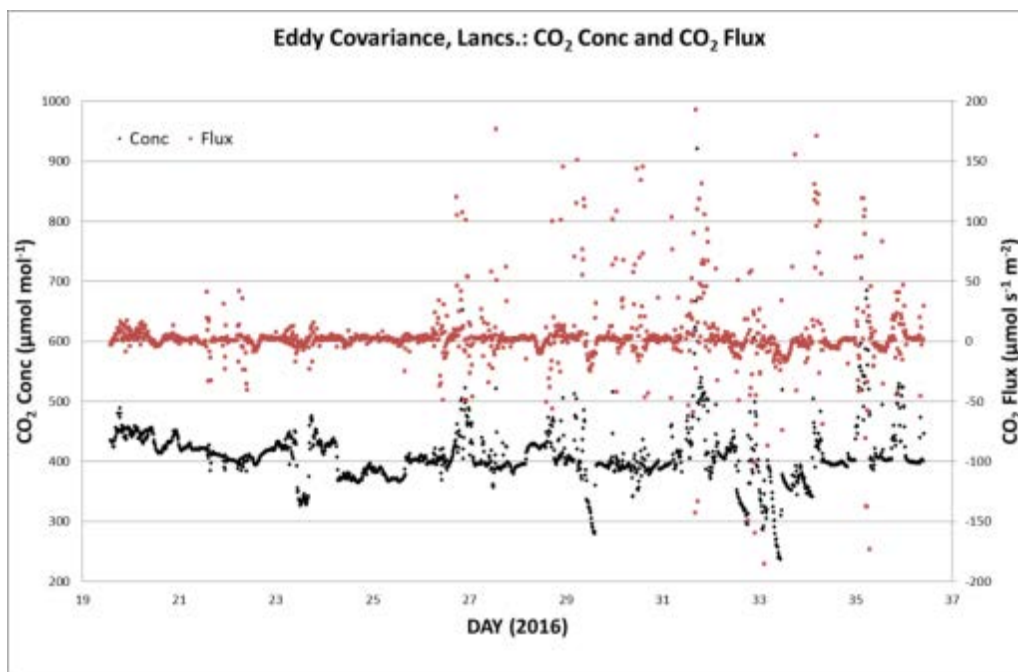


Figure 65. Preliminary calculated CO₂ concentrations and fluxes from initial Lancashire eddy covariance data (15 minute averaged processed data from original 10Hz observations).

Initial analysis reveals, as expected, that temperature has some correlation with CO₂ concentration (Figure 66). Increased temperatures tend to equate to reduced concentrations of CO₂ as levels of photosynthesis and hence CO₂ uptake in vegetation increase. There are

some exceptions where temperature is rapidly increased over a few hours and CO₂ follows suit. The cause of these events is unknown, but likely to be anthropogenically-induced. Figure 67 shows that the higher the wind speed, the lower the CO₂ concentration. Higher wind speeds tend to cause greater mixing of the atmospheric boundary layer, such that values become closer to the global baseline CO₂ mixing ratio (indicated by the blue line in Figure 67).

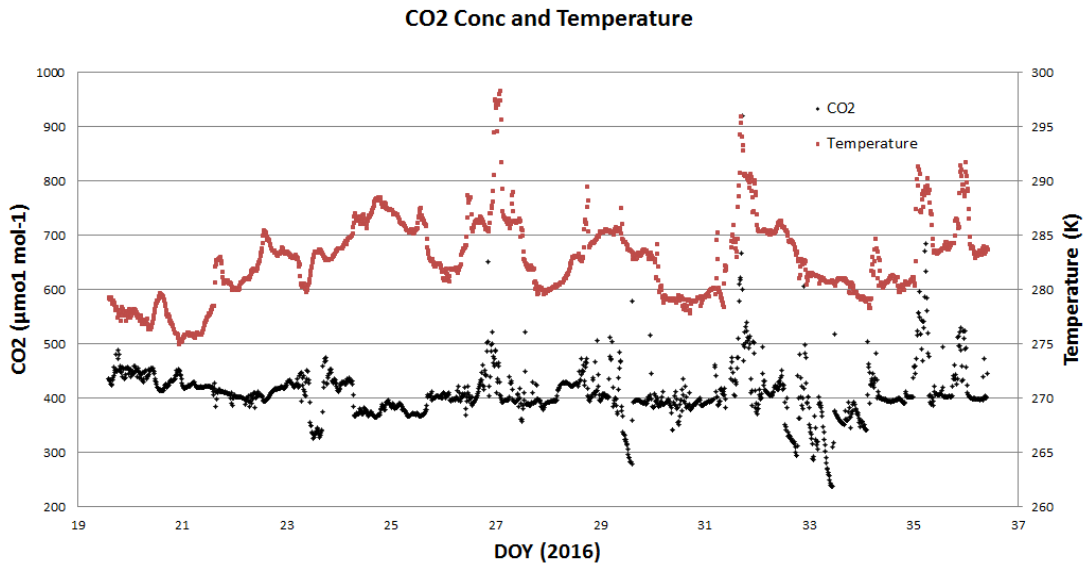


Figure 66. CO₂ concentrations plotted with temperature. Note that CO₂ concentrations tend to be inversely proportional to temperature, except during brief periods of rapid heating.

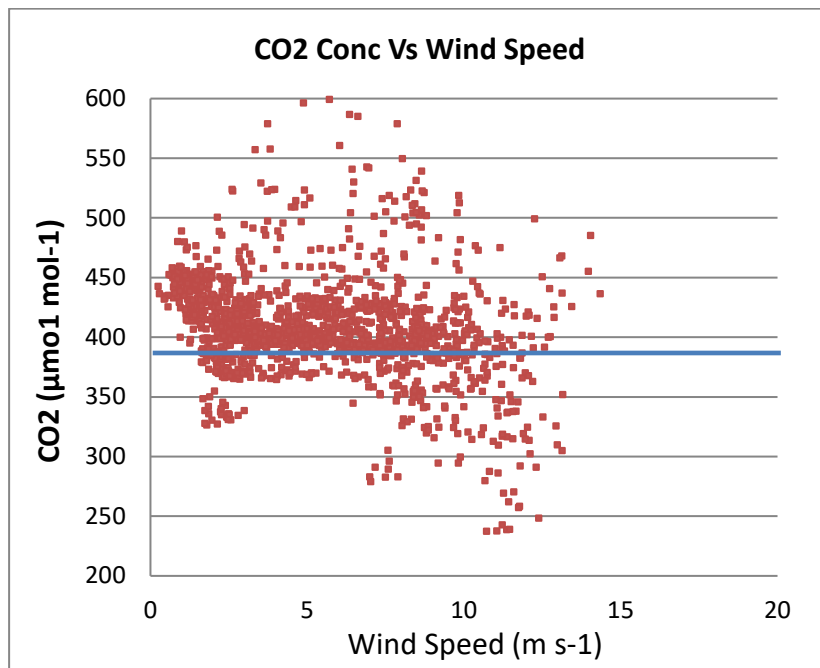


Figure 67. CO₂ concentrations plotted against wind speed. The tailing off of CO₂ concentration at higher wind speeds is indicative of the baseline mixing ratio of the boundary layer (blue line).

2.5.4 Recommendations for future work

A major drawback of the current study has been carrying out soil gas work in the autumn and winter, when the soil tends to become saturated. This can prevent the sampling and measurement of free gas and inhibit the flux from the soil. This has been compounded by unusually wet conditions in late 2015 and early 2016.

Because of the very wet autumn and winter in 2015/16 the amount of soil gas monitoring in the Vale of Pickering has been restricted. A fuller appraisal of baseline soil gas and flux would be possible under drier spring, summer and autumn conditions. More complete initial surveys would allow sites to be selected for sampling for supplementary laboratory analysis and for continuous monitoring to better define baseline variability. This would also have the potential to tie in more fully with groundwater and atmospheric monitoring.

The ideal time for soil gas and flux work is during the spring to early autumn when the upper layers of the soil tend to be drier, allowing soil gas sampling and the free flux of gas. However, it is important to assess the full temporal variability of soil gases and this requires multiple surveys under different seasonal (and year on year) conditions and continuous monitoring throughout the year.

Because of this we would recommend continuation of the project throughout 2016-17 to allow surveys under optimal conditions, and across the seasons, and collection of lengthy periods of continuous monitoring data. Longer term eddy covariance measurements in Lancashire should help to constrain the contribution of soil gas flux to the atmospheric measurements.

Continuation will allow us to deploy recently acquired survey equipment (e.g. a new flux meter that will measure low fluxes of both methane and CO₂) more extensively. There is also a possibility of additional new equipment becoming available, through other projects, during the coming year that would allow the field measurement of methane at ambient soil gas levels, rather than requiring subsequent laboratory analysis, and in situ determination of stable carbon isotopes.

2.6 RADON MONITORING

2.6.1 Introduction

The 2014 PHE report (PHE-CRCE-09, 2014) on the potential public health impact of shale gas in the UK identified that radon is likely to be present in shale gas and released to the environment as a result of its exploitation. A number of exposure pathways were identified as leading to potential limited radiation exposure and this has led to public concerns. The work outlined in this work package is aiming to establish the baseline for indoor and outdoor radon levels in air at various locations around the KM8 site ahead of on any hydraulic fracturing (if it is approved) and in control areas in other parts of the Vale of Pickering.

2.6.2 Outdoor radon monitoring

Outdoor radon levels are generally low in the UK. Measurements made in during a 1988 national survey established the average national value of 4 Bq m⁻³ (Wrixon et al,1988).

The outdoor radon monitoring in this project involved installation of passive radon detectors at three locations – one in close proximity to the proposed shale gas site (KM8), the second a suitable distance away to serve as a control but in an area with the same background radon potential, and a third site within close proximity to KM8 but within a natural radon Affected Area. In addition a fourth location in a similar area but remote to the Vale of Pickering was chosen as a second control.

Passive radon monitors very similar to those used routinely in homes by Public Health England (PHE) (<http://www.ukradon.org/information/measuringradon>), have been placed in small aluminium wrapped weather-proof plastic pots in discreet but open-air locations for 3 months or longer. The detectors were placed in suitable locations around the sites in accordance with best practice and replaced at pre-defined intervals during the lifetime of the project to characterise both spatial and temporal variability in radon.

2.6.2.1 OUTDOOR SITE SELECTION

Three sites have been selected for outdoor radon monitoring in the Vale of Pickering and one site in Oxfordshire:

- Area around Kirby Misperton at about 2 km from the KM8 site -15 sampling points
- Area around Yedingham at about 10 km from the KM8 site , control site - 8 sampling points
- Area around Pickering at about 10 km from the KM8 site - 6 sampling points
- Area around Chilton in the Vale of White Horse, Oxfordshire, control site - 8 sampling points

The locations of sampling points in the Vale of Pickering are given in Figure 68. Eight sampling points in the gardens of private homes in the OX11 and OX12 postcode areas in the Vale of White Horse, Oxfordshire were also used to act as a further control.

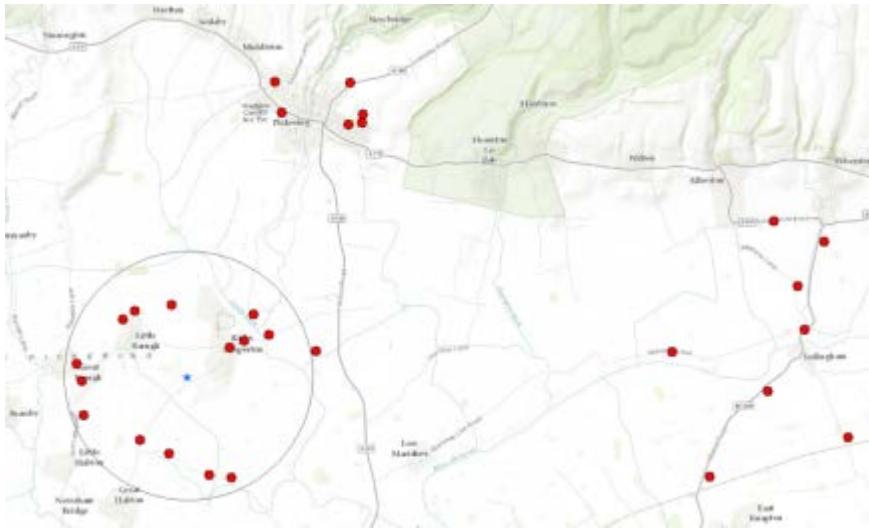


Figure 68. Outdoor radon sampling points in the Vale of Pickering. © PHE, 2016.

2.6.2.2 RESULTS FROM THE FIRST 3 MONTHS (OCTOBER 2015 TO JANUARY 2016)

Four 3-month passive detectors were used to record radon concentration at each sampling point. The estimated average radon concentrations at each sampling point in the area around Kirby Misperton, Yedingham and Pickering are presented in Figure 69. The average radon concentration at each sampling point in the area around the Vale of White Horse in Oxfordshire is shown in Figure 70.

The analysis of the detectors indicates that the average radon levels outdoors in the Vale of Pickering were:

- $7 \pm 3 \text{ Bq m}^{-3}$ for the area around Kirby Misperton
- $9 \pm 4 \text{ Bq m}^{-3}$ for the local control area of Yedingham
- $6 \pm 2 \text{ Bq m}^{-3}$ for the area of Pickering

The average radon levels in the outdoor air in the Vale of White Horse in Oxfordshire were found to be $11 \pm 4 \text{ Bq m}^{-3}$.

2.6.2.3 DISCUSSION OF THE 3-MONTH OUTDOOR RESULTS

The results from the first 3-month measurements indicated that the radon concentration in the outdoor air around the KM8 site is close to the UK average, 4 Bq m^{-3} . There is no indication of elevated radon concentrations in Pickering, a radon Affected Area to the north of the KM8 site. The analysis of results for Oxfordshire showed that the radon concentrations were similar to the ones for the Vale of Pickering.

It should be noted that passive detectors are operating at their limit of detection so the uncertainties on the results are large. The results from the 6-month measurements will give better estimates as these uncertainties will be reduced.

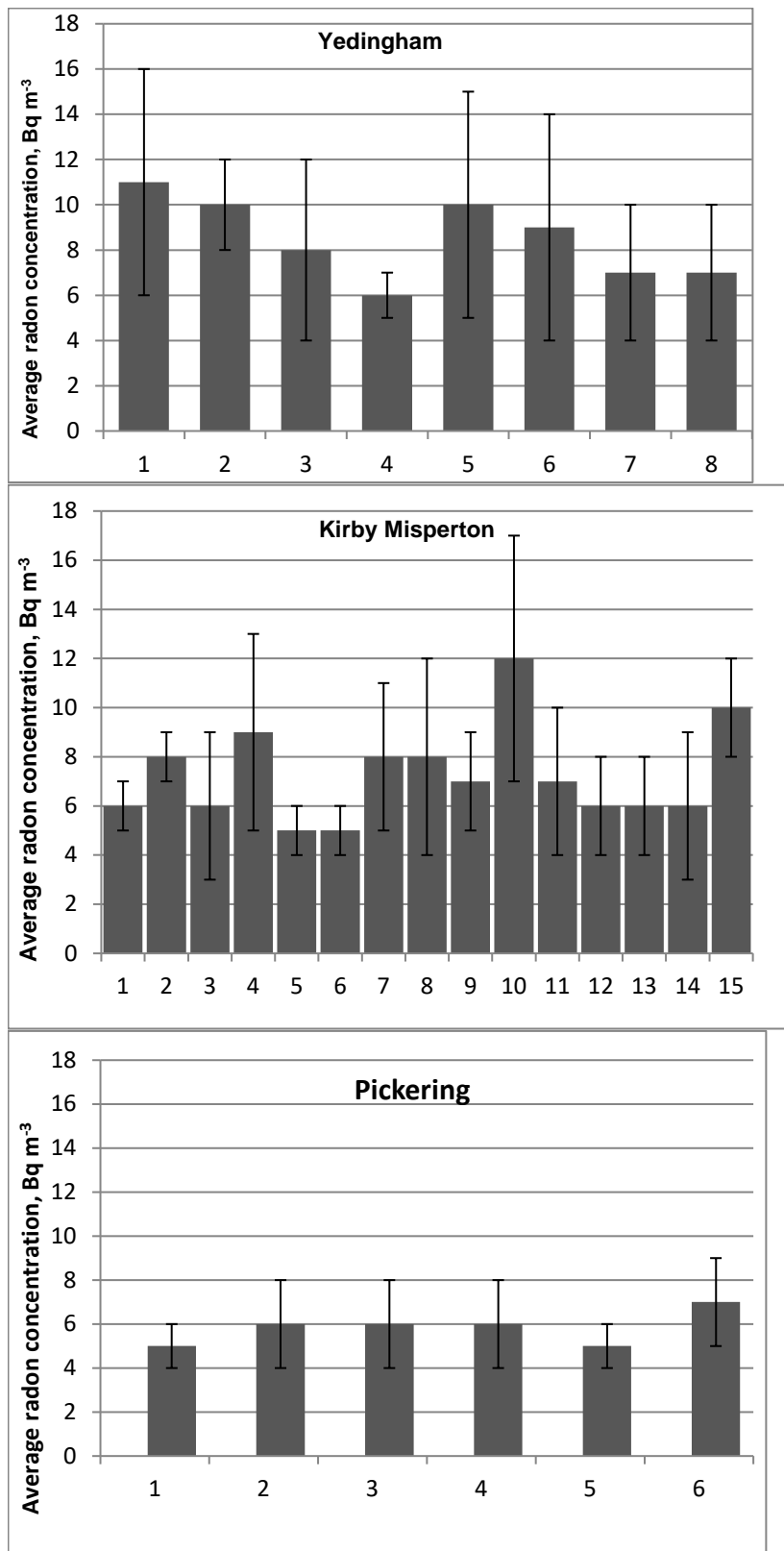


Figure 69. Average radon concentrations at the sampling points around Yedingham, Kirby Misperton and Pickering. © PHE, 2016.

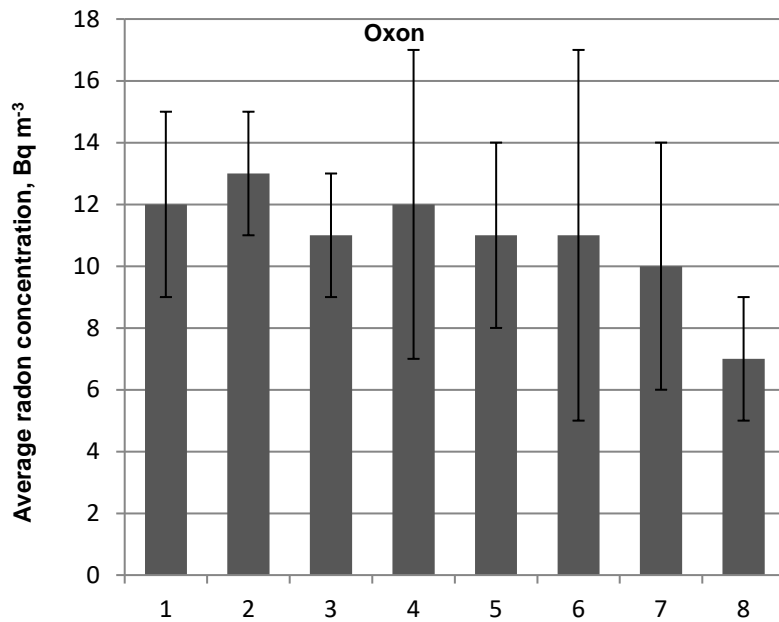


Figure 70. Average radon concentrations at the sampling points in the Vale of White Horse, Oxfordshire. © PHE, 2016.

2.6.3 Indoor radon monitoring

The results obtained in this study will establish the first estimate of the baseline indoor radon levels in over 100 homes near to the proposed shale gas site.

The main area of the Vale of Pickering is not a radon Affected Area so less than 1% of homes are expected to be above the UK Action Level, which is 200 Bq m⁻³. At around 5 to 8 km to the north and south of the KM8 site however there are areas of naturally elevated radon potential (see Figure 71). In these areas there is a higher probability for homes to have elevated radon levels.

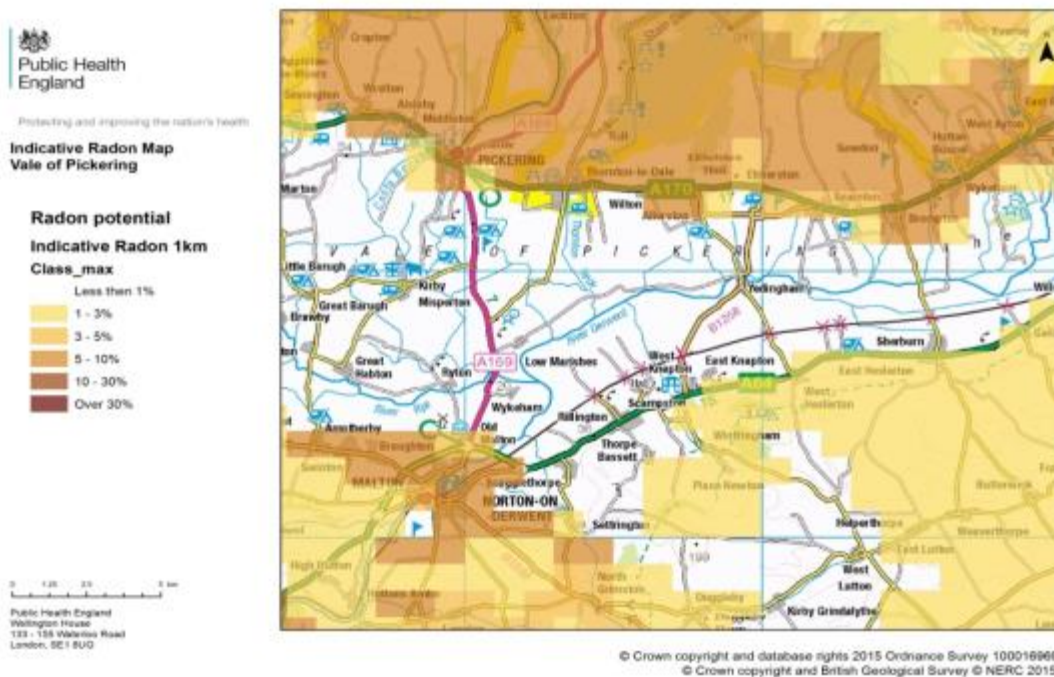


Figure 71. Radon potential in the Vale of Pickering. © PHE, 2016.

2.6.3.1 INDOOR SITE SELECTION

For the baseline survey areas were chosen in both radon Affected Areas and those with lower radon potential. The homes selected for measurement were chosen to avoid bias in the sample. We used the Royal Mail Post Code Address File[®] and selected a random sample in each of the study areas.

Volunteer householders were identified and radon detectors placed in each home following a standard procedure where householders were invited by letter to take part. The monitors were deployed for fixed periods in sufficient houses to give statistically valid data.

The numbers of recruited homes in the Vale of Pickering are given by area below:

- Kirby Misperton and Little Barugh: 36 homes
- Yedingham and surrounding area: 37 homes
- Pickering: 49 homes
- Malton: 23 homes

Detectors were sent in 3 batches for placement by the householder: one in late November 2015 and two in December 2015. The first batch of 3-month detectors was returned by householders for processing and analysis at the end of February 2016 beginning of March 2016. At the same time replacement 3 month detectors were sent out to householders.

The analysis of the results for 115 homes, (230 detectors) returned by 23rd March 2016, are included in this report. The result and advice on the need for action to reduce radon levels where appropriate will be reported to the individual householders following our standard procedures. The results for detectors returned later will be reported as detailed above and included in subsequent project reports.

2.6.3.2 RESULTS FROM THE FIRST 3 MONTHS (DECEMBER 2015 TO MARCH 2016)

The annual average radon concentration for each home has been estimated according to the UK Validation scheme (Howarth C B and Miles J C H, 2008). Weighted mean radon concentrations for each home for each 3-month period were calculated using a weighting factor of 0.45 for living room results and 0.55 for bedroom results (Wrixon et al, 1988). The annual mean radon concentration is calculated by multiplying the weighted mean radon concentration by an appropriate seasonal correction factor. The data without seasonal correction factors will be used for a seasonality study of the data once the results from the second 3-month tests are available.

Local radon distributions in the four selected areas in the Vale of Pickering -Kirby Misperton and Little Barugh, Yedingham and surrounding area, Pickering, and Malton are depicted in the Figure 72a, b, c and d, respectively. Indoor radon concentrations follow lognormal distribution (Miles, 1998). Although the statistics for some of the area like Malton is rather small it is evident from the plots that the distributions are skewed. Parameters of these distributions assuming radon log-normality are reported in Table 11.

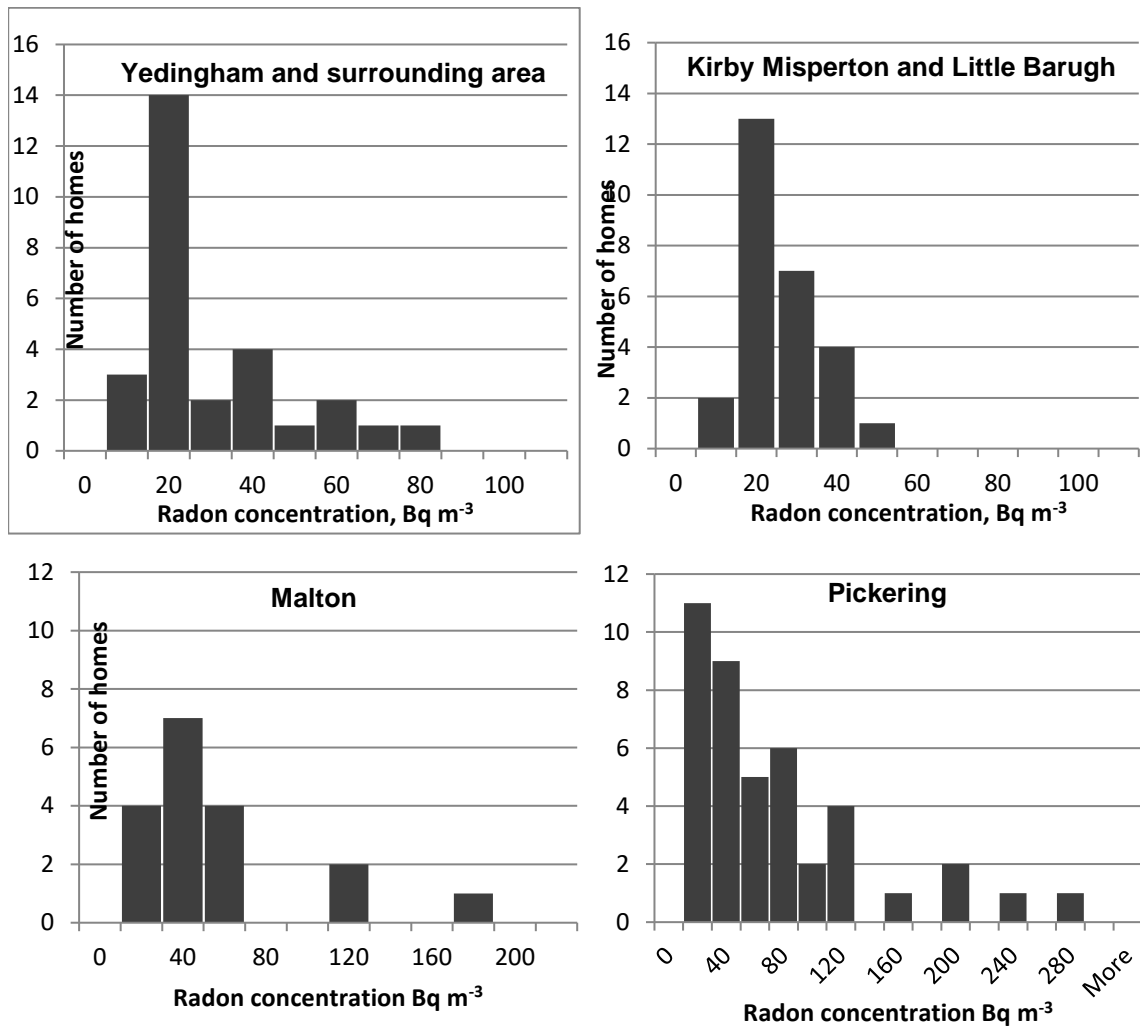


Figure 72. Indoor radon concentrations in the area of Kirby Misperton and Little Barugh. © PHE, 2016.

Results in Table 1 for the area of Kirby Misperton are consistent with its established status of not being a radon Affected Area. The measured arithmetic mean of indoor radon concentrations the area is the same as the average radon concentrations in the UK 20 Bq m⁻³, although we have to note that the statistics are quite limited.

The monitored area of Yedingham also confirms the prediction that is not an affected area. The range of radon concentrations is wider than in Kirby Misperton and the average radon concentrations are a little bit higher but broadly the two distributions are similar.

The area around Pickering has been previously identified as radon affected. That is supported by the indoor radon concentrations measured here which range from 6 to 266 Bq m⁻³ and the average radon concentrations of 63 Bq m⁻³.

In Malton, another Radon Affected area, we see radon concentrations from 12 - 174 Bq m⁻³. We cannot draw further conclusions however because the statistics of Malton are quite limited.

Table 11. Range and distribution of indoor radon measurements.

Area	Radon concentration range Bq m ⁻³	Arithmetic mean Bq m ⁻³	Geometric mean Bq m ⁻³	Geometric standard deviation
Kirby Misperton and Little Barugh (27 homes)	9 - 14	20	18	1.5
Yedingham and surrounding area (28 homes)	9 - 72	26	21	1.9
Pickering (42 homes)	6 - 266	63	40	2.7
Malton (18 homes)	12-174	48	36	2.1

2.6.3.3 DISCUSSION OF THE 3-MONTH INDOOR RESULTS

Two homes were found where radon levels exceeded the radon Action Level of 200 Bq m⁻³. Both homes were located in the Pickering area where such results might be expected given that they in a radon Affected Area.

2.6.4 Conclusions and suggestions for further work

The results from the first 3-month measurements of outdoor air around KM8 site indicated that the radon concentrations are close to the UK average, 4 Bq m⁻³. There is no indication of elevated radon concentrations in Pickering, a radon Affected Area in close proximity of the KM8 site. The analysis of results for another control site in Oxfordshire showed that the radon concentrations were similar to those for the Vale of Pickering.

The analysis of the first 3-month results for 115 homes (79 % of the total recruited) showed that the distributions of indoor radon concentrations are skewed, consistent with the usual log-normal distribution for indoor radon. The Kirby Misperton and Little Barugh areas are not radon affected, and the observed distribution conforms with UK average radon concentrations. The monitored area of Yedingham is also not radon affected and the distribution of radon concentrations is similar. On the other hand both Pickering and Malton confirm our assessment as being radon Affected Areas with radon concentrations spread over a wider range from about 10 to nearly 300 Bq m⁻³.

The numbers of homes in each of the areas where the radon concentrations were found to be at or above the Action Level followed the predicted numbers in each case.

The continuation of the current programme will allow an assessment of the annual average baseline radon concentration in each home and in each area to be established more accurately. It will also enable the direct measurement of the local distributions without the need for seasonality adjustments.

2.6.5 References

Howarth C B and Miles J C H (2008) Validation scheme for organisations making measurements of radon in dwellings: 2008 revision. Chilton, HPA-RPD-047.

Miles J C H (1998) Mapping radon- prone areas by lognormal modelling of house radon data. Health Physics 74(3), 370-378.

PHE-CRCE-009: Review of the Potential Public Health Impacts of Exposures to Chemical and Radioactive Pollutants as a Result of the Shale Gas Extraction Process, © Crown copyright 2014.

Wrixon A D, Green B M R, Lomas P R, Miles J C H, Cliff K D, Francis E A, Driscoll C M H, James A C, O’Riordan M C (1988) Natural radiation exposure in UK dwellings. London: Her Majesty’s Stationery Office, Report NRPB-R190.